



MASTER'S THESIS

# RESUMMATION PREDICTIONS FOR ASSOCIATED PRODUCTION OF SQUARKS AND ELECTROWEAKINOS AT THE LHC

Alexander Puck Neuwirth

Institut für Theoretische Physik Münster

Supervisor & first examiner: Prof. Dr. Michael Klasen  
Second examiner: Prof. Dr. Anna Kulesza

October 14, 2021

## Kurzfassung

In dieser Arbeit wird die assoziierte Produktion eines Squarks zusammen mit einem Elektroweakino, also Neutralino oder Chargino, am Large Hadron Collider untersucht. Da diese supersymmetrischen Teilchen noch nicht nachgewiesen wurden, müssen sie eine hohe Masse haben. Um sie nachweisen zu können, müssen sowohl das Experiment als auch die Theorie eine hohe Präzision aufweisen. Daher haben wir die Berechnungen der reellen und virtuellen Korrekturen, die zusammen die nächsthöhere Ordnung ergeben, für den genannten Prozess, durchgeführt. Die Anwendung des Catani-Seymour-Formalismus spielt dabei eine wichtige Rolle. Diese Korrekturen sind Voraussetzungen für die Erzielung einer höheren Präzision durch Resummation von Logarithmen nächsthöherer Ordnung. Wir zeigen verschiedene Möglichkeiten auf, um die Korrektheit der Berechnungen zu überprüfen. Sowohl die vorgestellten Korrekturrechnungen als auch die Prüfroutinen haben wir in dem frei verfügbaren Programm Resummino implementiert.

## Abstract

In this thesis, the associated production of a squark together with an electroweakino, i.e. neutralino or chargino, is studied at the Large Hadron Collider. Since these supersymmetric particles have not yet been detected, they must have high masses. In order to detect them, both experiment and theory must have a high precision. Therefore, we have performed the calculations of the real and virtual corrections, which together give the next-to-leading order. The application of the Catani-Seymour formalism plays an important role. These corrections are preconditions for obtaining a higher precision by resumming next-to-leading logarithms. We show different possibilities to check the correctness of the calculations. We have implemented both the presented higher order calculations and the test routines in the freely available program Resummino.

# Contents

<b>1. Introduction</b>	<b>1</b>
<b>2. The Minimal Supersymmetric Standard Model</b>	<b>2</b>
2.1. Supersymmetry . . . . .	2
2.2. Soft breaking . . . . .	2
2.3. Squarks . . . . .	5
2.4. Electroweakinos . . . . .	6
2.4.1. Charginos . . . . .	6
2.4.2. Neutralinos . . . . .	7
2.5. Gluino . . . . .	7
<b>3. Leading order</b>	<b>8</b>
3.1. Feynman diagrams . . . . .	8
3.2. Averaged matrix element . . . . .	9
<b>4. Formalisms</b>	<b>11</b>
4.1. The Catani-Seymour formalism . . . . .	11
4.1.1. The Method . . . . .	11
4.1.2. Notations . . . . .	12
4.1.3. Dipoles . . . . .	13
4.2. Regularization and Reduction . . . . .	14
4.2.1. Dimensional regularization schemes . . . . .	14
4.2.2. Passarino-Veltman reduction . . . . .	15
4.3. Renormalization . . . . .	17
4.3.1. Quarks . . . . .	18
4.3.2. Squarks . . . . .	19
4.3.3. Gluon . . . . .	20
4.4. Threshold Resummation . . . . .	21
<b>5. Next-to-leading order</b>	<b>22</b>
5.1. Real corrections . . . . .	22
5.1.1. Quark gluon initiated corrections . . . . .	22
5.1.2. Gluon gluon initiated corrections . . . . .	26
5.1.3. Quark antiquark initiated corrections . . . . .	28
5.1.4. Quark quark initiated correction . . . . .	29
5.2. Virtual corrections . . . . .	30
5.2.1. Self energies . . . . .	30
5.2.2. Vertex corrections . . . . .	33
5.2.3. Boxes . . . . .	36
5.2.4. Vertex counterterms . . . . .	37
5.2.5. Integrated dipoles . . . . .	37
<b>6. Numerical tests</b>	<b>39</b>
6.1. Leading Order . . . . .	39
6.1.1. Polarized matrix element . . . . .	39

6.1.2. MadGraph . . . . .	40
6.2. Real corrections . . . . .	40
6.2.1. Dipole subtraction . . . . .	40
6.2.2. On-shell subtraction . . . . .	42
6.2.3. Total Reals . . . . .	42
6.3. Virtuals . . . . .	43
6.3.1. Madgraph . . . . .	43
6.3.2. Pole cancellation . . . . .	45
<b>7. Results</b>	<b>46</b>
<b>8. Conclusion</b>	<b>49</b>
<b>9. Outlook</b>	<b>49</b>
<b>10. References</b>	<b>50</b>
<b>A. Feynman rules</b>	<b>55</b>
A.1. Standard model . . . . .	55
A.1.1. Propagators . . . . .	55
A.1.2. Vertices . . . . .	55
A.2. Minimal supersymmetric standard model . . . . .	56
A.2.1. Propagators . . . . .	56
A.2.2. Vertices . . . . .	56
<b>B. Polarized Born matrix element</b>	<b>57</b>
B.1. SS case . . . . .	57
B.2. UU case . . . . .	58
B.3. SU case . . . . .	59
<b>C. Virtual corrections</b>	<b>60</b>
C.1. Self energies . . . . .	60
C.1.1. Quark self energies . . . . .	60
C.1.2. Squark self energies . . . . .	62
C.1.3. Gluon self energies . . . . .	65
C.2. Vertex corrections . . . . .	70
C.2.1. Quark-quark-gluon vertex . . . . .	70
C.2.2. Squark-squark-gluon vertex . . . . .	74
C.2.3. Quark-squark-gaugino vertex . . . . .	83
C.2.4. Gluino-gaugino-gluon vertex . . . . .	85
C.3. Boxes . . . . .	88
C.3.1. Gluon-quark-quark-squark box . . . . .	90
C.3.2. Gluino-squark-squark-quark box . . . . .	90
C.3.3. Quark-gluon-gluon-squark box . . . . .	91
C.3.4. Squark-gluino-gluino-quark box . . . . .	92
C.3.5. Quark-gluon-squark-squark box . . . . .	93
C.3.6. Squark-gluino-quark-quark box . . . . .	93

C.3.7. Quark-gluon-squark box . . . . .	94
C.4. FeynCalc implementation . . . . .	94
<b>D. Real corrections</b>	<b>96</b>
D.1. Polarized dipole kinematics and connection matrix . . . . .	96
D.1.1. Initial state emitter and final state spectator . . . . .	96
D.1.2. Initial state emitter and final state spectator . . . . .	98
<b>E. Relations</b>	<b>102</b>
E.1. Colour . . . . .	102
E.1.1. Definitions . . . . .	102
E.1.2. Fierz identity . . . . .	102
E.2. Gamma Matrix . . . . .	103
E.2.1. Gamma trace relations . . . . .	103
E.2.2. $D$ -dimensional Gamma Matrix . . . . .	103
E.3. Passarino-Veltman . . . . .	103
E.3.1. Reduction . . . . .	103
E.3.2. Divergences . . . . .	104
<b>F. Implementation into Resummino</b>	<b>104</b>

# 1. Introduction

The Standard Model (SM) has proven to be an extremely successful description of particle physics over the past decades. Nevertheless, there are still open questions both on small and large scales. Prominent examples are the deviation of the measurement of the Muon  $g - 2$  experiment from the SM predictions [1], the origin and scale of neutrino masses [2] and the unknown dark matter [3]. A potential solution to these problems is provided by the extension of the SM to the Supersymmetric (SUSY) SM.

Within the Minimal Supersymmetric Standard Model (MSSM), each particle is given a superpartner that differs only by  $\frac{1}{2}$  in spin. Two scalar squarks are assigned to each quark and each gluon, Higgs boson, W boson and B boson is assigned a fermionic gluino, Higgsino, Wino and Bino, respectively, as superpartners. In analogy to the mixing of mass and interaction eigenstates in neutrinos, the neutral and charged interaction states of higgsinos, binos and winos mix to form neutralinos and charginos. Since such particles have not yet been discovered, it can be assumed that the supersymmetry is softly broken, giving the superpartners much higher masses. The lightest supersymmetric particle (LSP) has all the properties of a dark matter candidate. The parameter space of the MSSM is constrained from LHC data at 13 TeV [4] and XENON1T [5]. A combination of these two and several more is found in [6].

The expansion of the Large Hadron Collider (LHC) into the High-Luminosity LHC (HL-LHC) is planned for the next few years and should enable the search for even more massive particles [7]. While the production of supersymmetric dark matter particles will most likely be dominated by strong interactions [8], e.g. squark or gluino pair production, more insights beyond the masses of new particles can be found in the weakly interacting sector [9]. In the last decade the precise investigation beyond next-to-leading order (NLO) of gluino pair [10], slepton pair [11] and gaugino-gluino [12] production was accomplished.

In this work we will focus on production of a squark and electroweakino in a hadron collider like the LHC. The process will appear as missing transverse energy from the electroweakinos and a hard jet from the squark. Such monojets are a well-studied signature of dark matter [13]. From the CMS collaboration chargino and neutralino masses between 300 GeV and 1450 GeV [14] and a top squark mass below 1300 GeV [15] are excluded at 95% confidence level, though a dependence on the model remains. At leading order (LO) the process involves weak  $\alpha_{\text{EM}}$  and strong  $\alpha_s$  interactions and is already known in detail [9][16][17][18]. However, only precise theoretical predictions will allow the comparison between theory and experiment. For this purpose, the NLO corrections proportional to  $\alpha_{\text{EM}}\alpha_s^2$ , composed of virtual and real corrections, are needed.

The goal of this thesis is to precisely compute the production of squarks and electroweakinos at NLO and implement them into **Resummino** [19] First, in section 2 we establish the necessary basics of SUSY and the MSSM. Next, section 3 will introduce how we compute a cross section at leading order. Then we review the methods of computing at higher orders in section 4. The actual computation follows in section 5. In section 6 we present the consistency checks, comparisons and tests performed. Finally, section 7 contains our NLO and preliminary resummation results. This thesis is concluded in section 8 and section 9 gives an outlook on the continuation of the project.

## 2. The Minimal Supersymmetric Standard Model

### 2.1. Supersymmetry

Much of the success of the Standard Model (SM) can be attributed to symmetries. In particular, external space-time symmetries and internal gauge symmetries make precise prediction possible. Supersymmetry (SUSY) integrates another through relating fermionic and bosonic degrees of freedom. Only after the development of SUSY it became clear, that it provides potentials solutions to remaining shortcomings of the Standard Model. For a deeper insight into Supersymmetry, we refer the reader to our sources for this chapter and their references [20][21][22][23] [24].

The extension of the Standard Model turns out to be not so simple, since the Coleman-Mandula theorem [25] restricts the extension of the Poincaré group. To maximize the symmetry of the SM beyond trivial extensions the Haag-Lopuszanski-Sohnius theorem [26] establishes the inclusion of anticommutation relations. The transformation from fermionic to bosonic states and vice versa is carried out by an anti-commuting spinor operator  $Q$ . For realistic theories they satisfy

$$\{Q, Q^\dagger\} = P^\mu, \quad (2.1)$$

$$\{Q, Q\} = \{Q^\dagger, Q^\dagger\} = 0, \quad (2.2)$$

$$[P^\mu, Q] = [P^\mu, Q^\dagger] = 0, \quad (2.3)$$

where  $P^\mu$  generates space-time translations. From the last relation (eq. (2.3)) we directly see that the masses of superpartners are equal, since they have the same eigenvalues  $P^2$ . This obviously contradicts experimental observation and has the consequence that SUSY must be softly broken, which leads to higher masses.

### 2.2. Soft breaking

The Minimal Supersymmetric Standard Model (MSSM) is the simplest direct supersymmetrisation of the SM. It is minimal in the sense that it uses the fewest new particles to obtain a supersymmetric field theory. In table 1 we list all the supermultiplets of the MSSM. The supersymmetric particles solely differ in spin by  $\frac{1}{2}$  (before mass generation) and get marked by a tilde.

The scalar spin 0 particles do not have a helicity, the indices  $L$  and  $R$  therefore refer to the superpartner. The only exception to the direct definitions of superpartners is in the definition of the Higgsinos. In the MSSM there are two Higgs supermultiplets  $H_D$  and  $H_U$  to cancel chiral anomalies and generate the masses of the up- and down-type particles. The neutral Standard Model Higgs is then obtained from the combination of  $H_u^0$  and  $H_d^0$ .

The procedure to describe the Lagrangian in superspace is to use a holomorphic superpotential

$$W_{\text{MSSM}}(\Phi) = U_R \mathbf{y}^u Q_L H_U - D_R \mathbf{y}^d Q_L H_D - E_R \mathbf{y}^e L_L H_D + \mu H_U H_D, \quad (2.4)$$

where the  $\mathbf{y}$  are  $3 \times 3$  Yukawa matrices of each family and  $\mu$  is a generalized Higgs mass term. Following [27] we arrive at the expanded MSSM Lagrangian that still conserves

Table 1: Supermultiplets in the Minimal Supersymmetric Standard Model.  $S$  denotes the spin. The transformation properties under the Standard Model gauge group  $SU(3)_C \times SU(2)_L \times U(1)_Y$  are presented in the last column.

Multiplet	Name		$S = 0$	$S = \frac{1}{2}$	$S = 1$	SM group
chiral	s-/quarks	$Q_L$	$(\tilde{u}_L, \tilde{d}_L)$	$(u_L, d_L)$	-	$(\mathbf{3}, \mathbf{2}, \frac{1}{6})$
	(3 generations)	$U_R$	$\tilde{u}_R^c$	$u_R^\dagger$	-	$(\bar{\mathbf{3}}, \mathbf{1}, -\frac{2}{3})$
		$D_R$	$\tilde{d}_R^c$	$d_R^\dagger$	-	$(\bar{\mathbf{3}}, \mathbf{1}, \frac{1}{3})$
	s-/leptons	$L_L$	$(\tilde{\nu}, \tilde{e}_L)$	$(\nu, e_L)$	-	$(\mathbf{1}, \mathbf{2}, -\frac{1}{2})$
	(3 generations)	$E_R$	$\tilde{e}_R^c$	$e_R^\dagger$	-	$(\mathbf{1}, \mathbf{1}, 1)$
	higgs/-inos	$H_U$	$(H_u^+, H_u^0)$	$(\tilde{H}_u^+, \tilde{H}_u^0)$	-	$(\mathbf{1}, \mathbf{2}, +\frac{1}{2})$
	(1 generation)	$H_D$	$(H_d^0, H_d^-)$	$(\tilde{H}_d^0, \tilde{H}_d^-)$	-	$(\mathbf{1}, \mathbf{2}, -\frac{1}{2})$
	gluon/-ino	$V_G$	-	$\tilde{g}$	$g$	$(\mathbf{8}, \mathbf{1}, 0)$
	W boson/Wino	$V_W$	-	$(\tilde{W}^\pm, \tilde{W}^0)$	$(W^\pm, W^0)$	$(\mathbf{1}, \mathbf{3}, 0)$
	B boson/Bino	$V_B$	-	$\tilde{B}^0$	$B^0$	$(\mathbf{1}, \mathbf{1}, 0)$

Supersymmetry [24]

$$\begin{aligned}
\mathcal{L}_{\text{MSSM}}^{\text{SUSY}} = & \sum_i \left[ D_\mu \phi_i^\dagger D^\mu \phi^i + \frac{i}{2} \left( \psi^i \sigma^\mu D^\mu \bar{\psi}_i - D^\mu \psi^i \sigma^\mu \bar{\psi}_i \right) \right] \\
& + \sum_k \left[ -\frac{1}{4} V_k^{\mu\nu} V_k^{\mu\nu} + \frac{i}{2} \left( \tilde{V}_k \sigma^\mu D^\mu \tilde{\bar{V}}_k - D^\mu \tilde{V}_k \sigma^\mu \tilde{\bar{V}}_k \right) \right] \\
& - \frac{1}{2} \sum_{i,j} \left[ \frac{\partial^2 W_{\text{MSSM}}(\phi)}{\partial \phi^i \partial \phi^j} \psi^i \cdot \psi^j + \text{h.c.} \right] - \sum_i \frac{\partial W_{\text{MSSM}}(\phi)}{\partial \phi^i} \frac{W_{\text{MSSM}}^*(\phi^\dagger)}{\partial \phi_i^\dagger} \\
& - \frac{1}{2} \sum_k \left[ \left( g_k \sum_j [\phi_j^\dagger T^k \phi^j] \right) \left( g_k \sum_i [\phi_i^\dagger T^k \phi^i] \right) - i 2\sqrt{2} \sum_i \left( g_k \tilde{V}^k \cdot \bar{\psi}_i T_k \phi^i + \text{h.c.} \right) \right].
\end{aligned} \tag{2.5}$$

We write  $\psi$  or  $\tilde{V}$  for left-handed and  $\bar{\psi}$  and  $\tilde{\bar{V}}$  for right-handed spinors.  $\sigma_\mu = (1, \sigma^i)$  are constructed from the Pauli matrices and  $D_\mu$  are covariant derivatives. The index  $k$  indicates the MSSM gauge group such that couplings  $g_k$  and generators  $T_k$  are generic. Indices  $i$  and  $j$  refer to the members of scalar  $\phi$  or fermionic  $\psi$  supermultiplet members.

The first two lines are the typical kinetic terms for fermions and bosons in two-component Weyl fermion notation. The second derivative of the superpotential leaves us with the Yukawa interactions. From the last term in the fourth line we get interactions between gauginos scalars and fermions. They appear by requesting supersymmetry to hold after transitioning from ordinary to gauge-covariant derivatives [20]. The remaining terms include the scalar potential.



For phenomenological studies the breaking mechanism must not be known in detail. Instead, it will get parametrized into an extra term  $\mathcal{L}^{\text{soft}}$  which gets added to the  $\mathcal{L}^{\text{SUSY}}$ . A general approach to the soft Lagrangian is

$$\begin{aligned} \mathcal{L}_{\text{MSSM}}^{\text{soft}} = & -\frac{1}{2} \left[ M_1 \tilde{B} \cdot \tilde{B} + M_2 \tilde{W} \cdot \tilde{W} + M_3 \tilde{g} \cdot \tilde{g} + \text{h.c.} \right] \\ & - \tilde{Q}_L^\dagger \mathbf{m}_{\tilde{\mathbf{Q}}}^2 \tilde{Q}_L - \tilde{u}_R^\dagger \mathbf{m}_{\tilde{\mathbf{U}}}^2 \tilde{u}_R - \tilde{d}_R^\dagger \mathbf{m}_{\tilde{\mathbf{D}}}^2 \tilde{d}_R - \tilde{L}_L^\dagger \mathbf{m}_{\tilde{\mathbf{L}}}^2 \tilde{L}_L - \tilde{e}_R^\dagger \mathbf{m}_{\tilde{\mathbf{E}}}^2 \tilde{e}_R \\ & - m_{H_u}^2 H_u^\dagger H_u - m_{H_d}^2 H_d^\dagger H_d \\ & - \left[ \tilde{u}_R^\dagger \mathbf{T}^u \tilde{Q}_L \cdot H_u - \tilde{d}_R^\dagger \mathbf{T}^d \tilde{Q}_L \cdot H_d - \tilde{e}_R^\dagger \mathbf{T}^e \tilde{L}_L \cdot H_d + b H_u \cdot H_d + \text{h.c.} \right] \end{aligned} \quad (2.6)$$

where  $M_k$  denotes the mass of the fermionic gauginos: bino, winos and gluino. Next there are  $3 \times 3$  matrices  $\mathbf{m}$  for both squarks and sleptons and  $m_H$  masses for the two Higgs doublets. Then the  $3 \times 3$  matrices  $\mathbf{T}$  parametrize trilinear soft multiscalar interactions and the supersymmetry-breaking term of the Higgs potentials is  $b$ .

In total the MSSM contains 124 real parameters, including 19 of the SM, but not all the parameters are completely independent. On the basis of experiments, this arbitrariness in the MSSM can be reduced by additional assumptions on the soft breaking. Thus, many phenomenological versions of the MSSM, abbreviated as pMSSM, include fewer parameters. Now that we have established the MSSM we can discuss some of its intriguing properties.

First, by including additional particles in loops, unification of all three gauge couplings at the Grand Unified Theory (GUT) scale becomes possible. This is observed through evolving the couplings by solving the renormalization group equations up to the GUT scale  $M_{\text{GUT}} \approx 10^{16} \text{GeV}$ .

Second, loop correction to the Higgs boson's mass exhibit quadratic divergences. In SUSY these are however cancelled from the sign arising in loops due to the different statistics of superpartners. By assuming a cut-off  $\Lambda_{\text{UV}}$  at the Planck scale in combination with natural couplings  $\lambda \sim 1$  the smallest mass related to the soft breaking  $m_{\text{soft}}$  must be in the order of  $\mathcal{O}(1)$  TeV to reproduce the observed light Higgs mass without fine-tuning.

The open question on dark matter could be resolved through imposing the conserved  $R$ -Parity

$$R_p = (-1)^{3(B-L)+2S}. \quad (2.7)$$

In the definition of the superpotential eq. (2.4) we did not include lepton  $L$  or baryon  $B$  number violating terms. Including such terms is heavily constrained from e.g. proton decays  $p \rightarrow e^+ + \pi^0$ . Only squarks and quarks have  $|B| = \frac{1}{3}$  and the sleptons and leptons carry  $|L| = 1$ . From  $\Delta S = \frac{1}{2}$  between superpartners it follows that  $R_p = +1$  for SM and  $R_p = -1$  for SUSY particles. Then only an even number of sparticles are allowed at each vertex, prohibiting the lightest supersymmetric particle (LSP) from decaying. All remaining particles with a higher mass must decay into the LSP. Another consequence is that sparticles will only be produced in pairs at collider experiments.

Next, we will take a closer look at the supersymmetric particles of interest for our process at leading order namely squarks and electroweakinos. At next-to-leading order we will also encounter gluinos. While we give equations for the mixing and masses of these particles, in practice the mass spectra are generated by dedicated tools following the SUSY Les Houches Accord (SLHA) conventions [28]. We are going to use the Feynman rules from [29] in the same format as in [22] (cf. appendix A).

### 2.3. Squarks

We will investigate the mixing of left- and right-handed squarks. The MSSM Lagrangian mass term written in gauge eigenstates  $\tilde{q} = \begin{pmatrix} \tilde{q}_L \\ \tilde{q}_R \end{pmatrix}$  for squarks reads

$$\mathcal{L}_{\text{mass}}^{\tilde{q}} = - \sum_{\tilde{q}} \tilde{q}^\dagger \mathcal{M}_{\tilde{q}}^2 \tilde{q} \quad \text{with} \quad \mathcal{M}_{\tilde{q}}^2 = \begin{pmatrix} \mathcal{M}_{\tilde{q},LL}^2 & \mathcal{M}_{\tilde{q},LR}^2 \\ \mathcal{M}_{\tilde{q},LR}^{2*} & \mathcal{M}_{\tilde{q},RR}^2 \end{pmatrix} \quad (2.8)$$

where the squark mass matrix is

$$\mathcal{M}_{\tilde{q}}^2 = \begin{pmatrix} M_{\tilde{q}}^2 + m_Z^2 \cos(2\beta)(I_3 - e_q \sin^2 \theta_W) + m_q^2 & m_q(A_q^* - \mu \tan(\beta)^{-2I_3}) \\ m_q(A_q - \mu^* \tan(\beta)^{-2I_3}) & M_{\tilde{q}'}^2 + m_Z^2 \cos(2\beta)e_q \sin^2 \theta_W + m_q^2 \end{pmatrix}. \quad (2.9)$$

The parameters entering are the quark mass  $m_q$ , electric charge  $e_q$ , third weak isospin  $I_3$ , Z-boson mass  $m_Z$  and the Weinberg angle  $\theta_W$ . From the MSSM we have the trilinear Higgs-squark-squark coupling  $A_q$ , higgsino mass parameter  $\mu$  and mixing angle  $\tan \beta = \frac{v_2}{v_1}$ , defined by the ratio of the Higgs vacuum expectation values  $v_1$  and  $v_2$ . The mass terms  $M_{\tilde{q}}^2$  and  $M_{\tilde{q}'}^2$  parametrize the soft SUSY breaking with respect to left- and right-handed squarks.

Since we want to investigate mass eigenstates, we need to diagonalize this matrix. For the first two generations of squarks we can neglect the mixing between left- and right-handed states because the off-diagonal components are proportional to the corresponding quark mass which become negligible in high-energy computation. The mixing in the third generation of  $\tilde{t}$  will not be dropped. The diagonalization of a mass eigenstate from an interaction eigenstate is analogous to the prominent case of neutrino masses. A unitary squark mixing matrix  $S^{\tilde{q}}$  should satisfy

$$S^{\tilde{q}} \mathcal{M}_{\tilde{q}}^2 S^{\tilde{q}\dagger} = \begin{pmatrix} m_{\tilde{q}_1}^2 & 0 \\ 0 & m_{\tilde{q}_2}^2 \end{pmatrix} \quad \text{and} \quad \begin{pmatrix} \tilde{q}_1 \\ \tilde{q}_2 \end{pmatrix} = S^{\tilde{q}} \begin{pmatrix} \tilde{q}_L \\ \tilde{q}_R \end{pmatrix}. \quad (2.10)$$

The eigenvalues of  $\mathcal{M}_{\tilde{q}}^2$  are

$$m_{\tilde{q}_{1,2}}^2 = \frac{1}{2} \left[ \mathcal{M}_{\tilde{q},LL}^2 + \mathcal{M}_{\tilde{q},RR}^2 \mp \sqrt{(\mathcal{M}_{\tilde{q},LL}^2 - \mathcal{M}_{\tilde{q},RR}^2)^2 + 4|\mathcal{M}_{\tilde{q},LR}^2|^2} \right] \quad (2.11)$$

with the ordering  $m_{\tilde{q}_1}^2 < m_{\tilde{q}_2}^2$ . The squark mixing matrix can be expressed as a rotation by a mixing angle  $\theta_{\tilde{q}}$

$$\begin{pmatrix} S_{ii}^{\tilde{q}} & S_{i(i+3)}^{\tilde{q}} \\ S_{(i+3)i}^{\tilde{q}} & S_{(i+3)(i+3)}^{\tilde{q}} \end{pmatrix} = \begin{pmatrix} \cos \theta_{\tilde{q}} & \sin \theta_{\tilde{q}} \\ -\sin \theta_{\tilde{q}} & \cos \theta_{\tilde{q}} \end{pmatrix} \quad \text{where} \quad \tan 2\theta_{\tilde{q}} = \frac{2\mathcal{M}_{\tilde{q},LR}^2}{\mathcal{M}_{\tilde{q},LL}^2 - \mathcal{M}_{\tilde{q},RR}^2}, \quad (2.12)$$

where we added an index  $i$  for each generation resulting in a  $6 \times 6$  matrix. Then the coupling of a gluino to a quark  $I$  and an antiquark  $j$  is given by

$$\begin{aligned}\mathcal{R}'_{Ij} &= \mathcal{L}^*_{Ij} = \sqrt{2}S^{\tilde{q}}_{j(I+3)} \\ \mathcal{L}'_{Ij} &= \mathcal{R}^*_{Ij} = -\sqrt{2}S^{\tilde{q}}_{jI}.\end{aligned}\tag{2.13}$$

The restriction to minimal squark mixing results in

$$\begin{aligned}S^{\tilde{q}*}_{j(I+3)}S^{\tilde{q}}_{jJ} &= 0 = \mathcal{L}\mathcal{L}' \\ S^{\tilde{q}*}_{jI}S^{\tilde{q}}_{j(I+3)} &= 0 = \mathcal{R}\mathcal{R}',\end{aligned}\tag{2.14}$$

since one of the elements of  $S$  is an off-diagonal element which are zero.

## 2.4. Electroweakinos

The neutralinos and charginos are mixtures of higgsinos and electroweak gauginos. This mixing is an effect of electroweak symmetry breaking. We will occasionally refer to them loosely as gauginos, although we do not mean to include the gluino.

### 2.4.1. Charginos

As only fields with the same quantum numbers mix, the charginos will consist of charged higgsinos ( $\tilde{H}_u^+$  and  $\tilde{H}_d^-$ ) and winos ( $\tilde{W}^+$  and  $\tilde{W}^-$ ) and carry a charge of  $\pm 1$ . The relevant Lagrangian in two-component Weyl spinors is

$$\mathcal{L}_{\text{mass}}^n = -(\psi^-)^T \mathcal{M}^c \psi^+ + \text{h.c.}\tag{2.15}$$

with

$$\mathcal{M}^c = \begin{pmatrix} M_2 & \sqrt{2}M_W \sin \beta \\ \sqrt{2}M_W \cos \beta & \mu \end{pmatrix}, \quad \psi^+ = \begin{pmatrix} i\tilde{W}^+ \\ \tilde{H}_u^+ \end{pmatrix} \quad \text{and} \quad \psi^- = \begin{pmatrix} i\tilde{W}^- \\ \tilde{H}_d^- \end{pmatrix}.\tag{2.16}$$

Mass eigenstates follow from diagonalization with two unitary matrices  $U$  and  $V$ .

$$\begin{pmatrix} \tilde{\chi}_1^+ \\ \tilde{\chi}_2^+ \end{pmatrix} = V \begin{pmatrix} i\tilde{W}^+ \\ \tilde{H}_u^+ \end{pmatrix} \qquad \begin{pmatrix} \tilde{\chi}_1^- \\ \tilde{\chi}_2^- \end{pmatrix} = U \begin{pmatrix} i\tilde{W}^- \\ \tilde{H}_d^- \end{pmatrix}\tag{2.17}$$

The masses are again ordered  $M_{\tilde{\chi}_1^\pm} < M_{\tilde{\chi}_2^\pm}$

$$M_{\tilde{\chi}_{1,2}^\pm} = \frac{1}{2} \left( |M_2|^2 + |\mu|^2 + 2m_W^2 \mp \sqrt{(|M_2|^2 + |\mu|^2 + 2m_W^2)^2 - 4|m_W^2 \sin 2\beta - \mu M_2|^2} \right).\tag{2.18}$$

### 2.4.2. Neutralinos

The neutralino has no charge and is a Majorana particle. In contrast to charginos the mixing also includes binos  $\tilde{B}$ . The Lagrangian in gauge eigenstates  $\psi^0$  is

$$\mathcal{L}_{\text{mass}}^c = -\frac{1}{2}(\psi^0)^T \mathcal{M}^n \psi^0 + \text{h.c.}, \quad (2.19)$$

where the mass matrix is

$$\mathcal{M}^n = \begin{pmatrix} M_1 & 0 & -M_Z c_\beta s_W & M_Z s_\beta s_W \\ 0 & M_2 & M_Z c_\beta c_W & -M_Z s_\beta c_W \\ -M_Z c_\beta s_W & M_Z c_\beta c_W & 0 & -\mu \\ M_Z s_\beta s_W & -M_Z s_\beta c_W & -\mu & 0 \end{pmatrix}, \quad \text{and} \quad (\psi^0)^T = \begin{pmatrix} i\tilde{B} \\ i\tilde{W}^0 \\ \tilde{H}_d^0 \\ \tilde{H}_u^0 \end{pmatrix} \quad (2.20)$$

with abbreviated sin and cos for the Weinberg angle  $\theta_W$  and the relation between the two Higgs vacuum expectation values  $\beta$ . The unitary matrix  $N$  transforms the gauge eigenstates to a mass diagonal form via  $N^* \mathcal{M}^n N^{-1}$  and the mass eigenstates are

$$\begin{pmatrix} \tilde{\chi}_1^0 \\ \tilde{\chi}_2^0 \\ \tilde{\chi}_3^0 \\ \tilde{\chi}_4^0 \end{pmatrix} = N \begin{pmatrix} i\tilde{B} \\ i\tilde{W}^0 \\ \tilde{H}_d^0 \\ \tilde{H}_u^0 \end{pmatrix}. \quad (2.21)$$

From the usual ordering  $|M_{\tilde{\chi}_1^0}| < |M_{\tilde{\chi}_2^0}| < |M_{\tilde{\chi}_3^0}| < |M_{\tilde{\chi}_4^0}|$  the  $\tilde{\chi}_1^0$  could emerge as the lightest supersymmetric particle (LSP) and dark matter (DM) candidate.

## 2.5. Gluino

In the MSSM there is no other colour octet fermion that could mix with the gluino. The gluino mass enters as the parameter  $M_3$  in the MSSM and as it is electrically neutral it is a Majorana fermion. In most scenarios the gluino is much heavier than the charginos and neutralinos. This is a consequence of requesting unification at the GUT scale and at higher orders the gluino mass is no longer  $M_3$ [20].

### 3. Leading order

Now we are interested in comparing the MSSM against reality. One way to test a theory is by investigating the scattering process of various particles. Historically, a successful method of finding new particles as well as verifying associated theories are particle collisions at the LHC. If we want to compute a cross section we must account for the fact that we collide protons which consist of partons, namely quarks and gluons.

Given that in a hadron  $h$  the number density of a parton  $i$  with a momentum fraction  $x_i$  can be written as  $f_{i/h}(x_i)$ , the hadronic cross section  $\sigma^h$  is a convolution and sum of partonic cross sections  $\sigma_{ab}$

$$\sigma^h(P_A, P_B) = \sum_{a,b} \int_0^1 \int_0^1 dx_a dx_b f_{a/A}(x_a) f_{b/B}(x_b) \sigma_{ab}(x_a P_A, x_b P_B), \quad (3.1)$$

where  $P_A$  and  $P_B$  refer to the momenta of the hadrons. To calculate the partonic cross section we must integrate our averaged squared matrix element  $\langle \mathcal{M} \rangle^2$  over the 2-particle phase space of our final state particles and include a Flux factor of  $\frac{1}{8\pi^2 s}$ . We can already limit the partonic processes from charge conservation to

$$q_{u,d} g \rightarrow \tilde{q}_{u,d} \tilde{\chi}_k^0 \quad (3.2)$$

$$q_{u,d} g \rightarrow \tilde{q}_{d,u} \tilde{\chi}_k^\mp, \quad (3.3)$$

where  $k$  identifies the neutralino or chargino, respectively. In this section we will explain the construction of the squared matrix element from Feynman diagrams at leading order.

#### 3.1. Feynman diagrams

The diagrams derive their name from the Mandelstam variables

$$s = (p_a + p_b)^2 \quad t = (p_a - p_1)^2 \quad u = (p_a - p_2)^2 \quad (3.4)$$

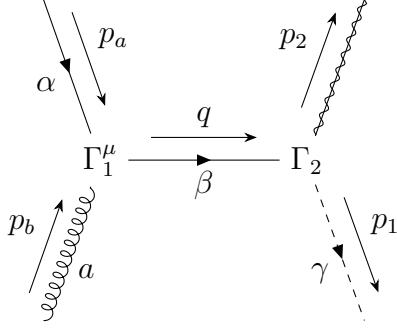
which give for our process

$$s + t + u = m_q^2 + m_\chi^2 \quad (3.5)$$

from four-momentum conservation and external particles being on-shell ( $p^2 = m^2$ ).

##### s-channel

To construct the matrix element from the Feynman diagram we follow the well established standard model procedure. The non-standard-model squark is a scalar and its inclusion is straight forward. For the majorana neutralinos however the fermion flow needs to be fixed [30][31]. We choose it to follow the charge flow of the quarks and get  $\bar{u}(p_2)$  as well as in the chargino case. Using the Feynman rules from appendix A we get:



$$\Gamma_1^\mu = -ig_s \gamma^\mu T_{\beta\alpha}^a \quad (3.6)$$

$$\Gamma_2 = i(L'P_L + R'P_R)\delta_{\gamma\beta} \quad (3.7)$$

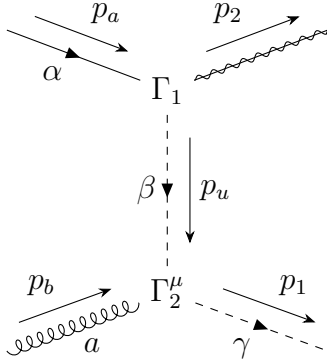
$$i\mathcal{M}_s = \bar{u}(p_2)\Gamma_2 \frac{i\not{q}}{q^2} \Gamma_1^\mu u(p_a)\epsilon^\mu \quad (3.8)$$

$$-i\mathcal{M}_s^\dagger = \bar{u}(p_a)\bar{\Gamma}_1^\mu \frac{-i\not{q}}{q^2} \bar{\Gamma}_2 u(p_2)\epsilon^{*\nu} \quad (3.9)$$

The definition  $\bar{\Gamma} = \gamma_0 \Gamma^\dagger \gamma_0$  comes from conjugation and insertions of  $\gamma_0^2 = 1$  in between the various  $\gamma$ .

### u-channel

In contrast to previous channel we have a massive intermediate squark now. In a strict manner we would have to distinguish between the squark propagator in the normal  $\mathcal{M}_u$  and conjugated  $\mathcal{M}_u^\dagger$  matrix elements, but since we know that the gluon coupling to a squark only has an effect on the colour (and kinematics) the squark stays the same and we get following amplitudes: <sup>1</sup>



$$\Gamma_1 = i(L'P_L + R'P_R)\delta_{\alpha\beta} \quad (3.10)$$

$$\Gamma_2^\mu = -ig_s(p_u + p_1)^\mu T_{\gamma\beta}^a \quad (3.11)$$

$$i\mathcal{M}_u = \bar{u}(p_2)\Gamma_1 u(p_a) \frac{i}{p_u^2 - m_{\tilde{q}}^2} \Gamma_2^\mu \epsilon^\mu \quad (3.12)$$

$$-i\mathcal{M}_u^\dagger = \bar{u}(p_a)\bar{\Gamma}_1 u(p_2) \frac{-i}{p_u^2 - m_{\tilde{q}}^2} \bar{\Gamma}_2^\nu \epsilon^{*\nu} \quad (3.13)$$

From these amplitudes we can construct the averaged matrix element.

## 3.2. Averaged matrix element

We average over incoming quark spin and colour ( $\frac{1}{2 \cdot 3}$ ) and gluon polarization and colour ( $\frac{1}{2 \cdot 8}$ ). Spin and colour of the final state particles are not averaged but summed. Here we use the Feynman gauge for the gluon polarization sum. Squaring the s channel diagram gives

$$\langle \mathcal{M}_s \rangle^2 = -g_{\mu\nu} \frac{1}{2 \cdot 3 \cdot 2 \cdot 8} \text{Tr} \left[ \Gamma_2 \frac{i\not{q}}{q^2} \Gamma_1^\mu \not{p}_a \bar{\Gamma}_3^\nu \frac{-i\not{q}}{q^2} \bar{\Gamma}_4 (\not{p}_2 + m_{\tilde{\chi}}) \right] \quad (3.14)$$

$$= \frac{g_s^2 C_A C_F}{96q^4} 8(|R|^2 + |L|^2)(D-2)(p_a p_b)(p_2 p_b) \quad (3.15)$$

$$= \frac{g_s^2 C_A C_F}{96q^2} 2(|R|^2 + |L|^2)(D-2)(m_{\tilde{q}}^2 - t), \quad (3.16)$$

<sup>1</sup>Please note that  $p_1$  and  $p_2$  are swapped for readability in the final state ( $u$  diagram looks like a  $t$  diagram).

where the  $D$  dimensional gamma matrices relation  $\gamma^\mu \not{q} \gamma^\mu = (2 - D)\not{q}$  is inserted. We use the anticommutation property of the  $\gamma^5$  matrices contained in  $P_{L,R}$  to get a trace of only 4-vector  $\gamma$ 's (more on this in section 4.2.1). The evaluation of the resulting trace is possible with appendix E.2 or tools like `Form`[32], `Tracer`[33] and `FeynCalc`[34]. We will not need this  $D$  dependent result and use 4 instead. The u-channel squared evaluates to

$$\langle \mathcal{M}_u \rangle^2 = -g_{\mu\nu} \frac{1}{2 \cdot 3 \cdot 2 \cdot 8} \text{Tr} \left[ \Gamma_1 \not{p}_a \bar{\Gamma}_3 (\not{p}_2 + m_\chi) \right] \Gamma_2^\mu \bar{\Gamma}_4^\nu \frac{i}{p_u^2 - m_{\bar{q}}^2} \frac{-i}{p_u^2 - m_{\bar{q}}^2} \quad (3.17)$$

$$= -\frac{g_s^2 C_A C_F}{96(u - m_{\bar{q}}^2)^2} 2(|R|^2 + |L|^2)(m_\chi^2 - u)(m_{\bar{q}}^2 + u), \quad (3.18)$$

and the interference terms is

$$2 \text{Re}[\mathcal{M}_s \mathcal{M}_u^\dagger] = -2g_{\mu\nu} \frac{1}{96} \text{Tr} \left[ \Gamma_2 \frac{i\not{q}}{q} \Gamma_1 \not{p}_a \bar{\Gamma}_3 (\not{p}_2 + m_\chi) \right] \frac{-i}{p_u^2 - m_{\bar{q}}^2} \bar{\Gamma}_4 \quad (3.19)$$

$$= 2 \frac{g_s^2 C_A C_F}{96s(u - m_{\bar{q}}^2)} (|R|^2 + |L|^2) \\ \left( 2(m_\chi^4 - m_{\bar{q}}^4) + m_{\bar{q}}^2(2u - 3s) - 2m_\chi^2(2m_{\bar{q}} + u) - su \right). \quad (3.20)$$

## 4. Formalisms

The Next-to-Leading-Order (NLO) cross section is defined as

$$\sigma_{\text{NLO}} = \int_3 d\sigma^{\text{R}} + \int_2 d\sigma^{\text{V}}. \quad (4.1)$$

The integration over the 3-particle phase space of the real corrections  $d\sigma^{\text{R}}$  turns out to be problematic due to **infrared (IR)** divergences, meaning very small momenta in denominators. From the Kinoshita-Lee-Nauenberg (KLN) theorem [35][36] it is known that these soft and/or collinear divergences cancel against the IR divergences from the virtual corrections  $d\sigma^{\text{V}}$ . When we compute the virtual corrections, will encounter integration over unconstrained loop momenta. They will give rise to **ultraviolet (UV)** divergences, meaning very large momenta. UV divergences will be absorbed into counterterms during renormalization. In the end a measurable inclusive quantity will have no more divergences.

To calculate the next-to-leading order we must introduce several methods and formalisms. We start with introducing the Catani-Seymour formalism in section 4.1. Then in section 4.2 we explain the regularization of divergences. Followed by a description of the on-shell renormalization in section 4.3.

### 4.1. The Catani-Seymour formalism

The Catani-Seymour dipole formalism provides a convenient way of handling infrared divergences. A full explanation of this method can be found in [37] for massless and in [38] for massive particles. The regularization scheme dependence of the dipoles is available here [39] and in even more generality in the references of section 4.2. First we introduce the general method. Then before going into more detail, we cover some notations from mentioned papers.

#### 4.1.1. The Method

One consequence of the IR divergences is that a Monte-Carlo integration over the 3-particle phase space will not give reliable results. The solution of the formalism can be written in a short equation

$$\sigma^{\text{NLO}} = \int_3 [d\sigma^{\text{R}} - d\sigma^{\text{A}}]_{\epsilon=0} + \int_2 \left[ d\sigma^{\text{V}} + \int_1 d\sigma^{\text{A}} \right]_{\epsilon=0}. \quad (4.2)$$

An auxiliary function  $\sigma^{\text{A}}$  is subtracted from the real corrections and added to the virtuals. It will be chosen in such a way that it cancels all the soft and collinear divergences arising in  $\sigma^{\text{R}}$ . The method derives its name from the construction of  $\sigma^{\text{A}}$  by summing over different dipoles

$$d\sigma^{\text{A}} = \sum_{\text{dipoles}} d\sigma^{\text{B}} \otimes dV_{\text{dipole}} \quad (4.3)$$



correlated with spins and colours of the leading order  $\sigma^B$ . The contribution to the virtuals corrections can then be rewritten

$$\int_1 d\sigma^A = d\sigma^B \otimes \sum_{\text{dipoles}} \int_1 dV_{\text{dipole}} = d\sigma^B \otimes \mathbf{I}, \quad (4.4)$$

where an insertion operator  $\mathbf{I}$  is introduced. As a consequence of the KLN theorem, it will cancel the infrared divergences in the virtual corrections. In hadron collisions there will be extra contributions from the collinear remainder  $\mathbf{P}$  and  $\mathbf{K}$ :

$$\sigma^{\text{NLO}} = \int_3 [d\sigma^R - d\sigma^A]_{\epsilon=0} + \int_2 \left[ d\sigma^V + \int_1 d\sigma^A \right]_{\epsilon=0} + \int_0^1 dx \int_2 [d\sigma^B(xp) \otimes (\mathbf{P} + \mathbf{K})(x)]_{\epsilon=0} \quad (4.5)$$

We will focus on the dipoles, but before that we introduce some notations.

#### 4.1.2. Notations

The following notations define a very convenient to express the unintegrated and integrated dipoles.

**Matrix elements:** A basis for colour  $c$  and helicity  $s$  space is introduced such that an amplitude of  $m$  particles is written as

$$\mathcal{M}_m^{c_1, \dots, c_m; s_1, \dots, s_m}(p_1, \dots, p_m) := (\langle c_1, \dots, c_m | \otimes \langle s_1, \dots, s_m |) |1, \dots, m\rangle_m \quad (4.6)$$

and the squared matrix element is

$$|\mathcal{M}_m|^2 = {}_m\langle 1, \dots, m | 1, \dots, m \rangle_m. \quad (4.7)$$

**Colour structure:** We use  $\mathbf{T}_i$  to represent the emission of a gluon from parton  $i$

$$\langle c_1, \dots, c_m | \mathbf{T}_i | c'_1, \dots, c'_m \rangle_m = \delta_{c_1 c'_1} \dots \mathcal{T}_{c_i c'_i} \dots \delta_{c_m c'_m}, \quad (4.8)$$

where

$$\mathcal{T}_{cb}^a := \begin{cases} if_{cab} & \text{adjoint representation (} i \text{ gluon or gluino)} \\ \pm T_{cb}^a & \text{fundamental representation (} i \text{ quark or squark)} \end{cases}. \quad (4.9)$$

The  $(-)$  case is for antiparticles. Since  $|1, \dots, m\rangle_m$  is a colour-singlet state, colour conservation can be written as

$$\sum_i^m \mathbf{T}_i |1, \dots, m\rangle_m = 0. \quad (4.10)$$

Lastly, the colour charge algebra commutes unless it is a quadratic Casimir operator

$$[\mathbf{T}_i, \mathbf{T}_j] = 0 \quad \mathbf{T}_i^2 = C_i = \begin{cases} C_F = \frac{4}{3} & i \text{ fundamental} \\ C_A = 3 & i \text{ adjoint} \end{cases} \quad (4.11)$$

Using these conventions we write the colour-correlated squared amplitude as

$${}_2\langle \dots, j; k, \dots | \mathbf{T}_j \mathbf{T}_k | \dots, j; k, \dots \rangle_2 = \mathcal{M}_{\text{LO}}^{\dots, b_j, b_k, \dots *} \mathcal{T}_{b_j a_j}^n \mathcal{T}_{b_k a_k}^n \mathcal{M}_{\text{LO}}^{\dots, a_j, a_k, \dots}. \quad (4.12)$$

### 4.1.3. Dipoles

The dipole factorization formula reads

$$|\mathcal{M}_{2 \rightarrow 3}^{\text{DIP}}|^2 = \sum_{i,j} \sum_{k \neq i,j} \mathcal{D}_{ij,k} + \sum_{i,j} \sum_a \mathcal{D}_{ij}^a + \sum_{a,i} \sum_{j \neq i} \mathcal{D}_j^{ai} + \sum_{a,i} \sum_{b \neq a} \mathcal{D}^{ai,b},$$

where the sums mean that we include all possible dipoles associated with our real correction Feynman diagrams. The definition of the dipoles will cancel the singular regions of our real correction  $2 \rightarrow 3$  matrix element. Each dipole  $\mathcal{D}$  comes from a different emitter-spectator case. Both emitter and spectator are coloured particles. In fig. 1 four cases are shown.

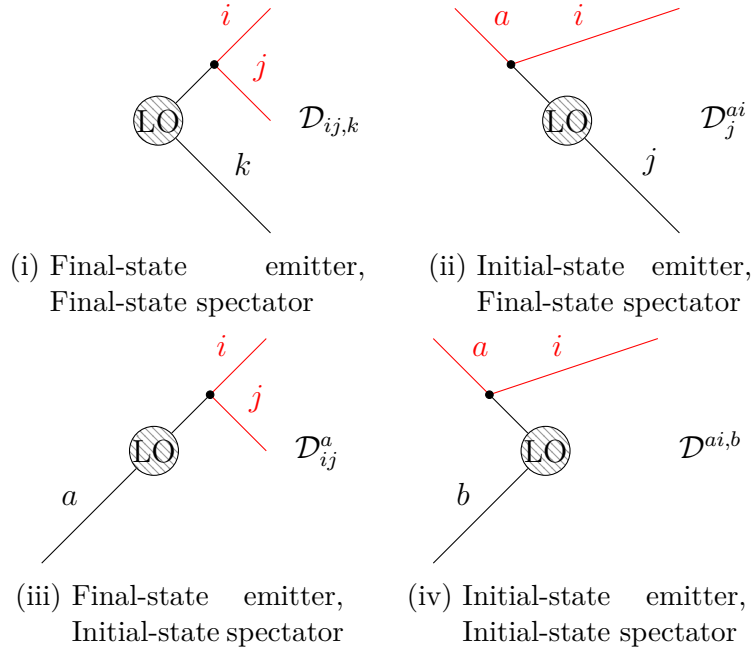


Figure 1: Dipole diagrams for various emitter-spectator cases.

The general structure of all these dipoles is

$$\mathcal{D}_j^{ai}(p_1, p_2, p_3; p_a, p_b) \propto \frac{1}{p^2} {}_2\langle \dots, j, \dots; ai, \dots | \frac{\mathbf{T}_{\text{spectator}} \mathbf{T}_{\text{interm.}}}{\mathbf{T}_{\text{interm.}}^2} \mathbf{V} | \dots, j, \dots; ai, \dots \rangle_2, \quad (4.13)$$

where the division by  $p^2$  can constitute a divergence. The Casimir operator  $\mathbf{T}_{\text{interm.}}^2$  is linked to the particle that enters the leading order process and is connected to two external particles (red). The kernel  $\mathbf{V}$  will depend on the momenta and is closely related to the Altarelli-Paris splitting functions [40]. In order to match the divergence of the real corrections the colour correlation needs to be taken into account through  $\mathbf{T}_{\text{spectator}} \mathbf{T}_{\text{interm.}}$ . The 3-particle phase space needs to be mapped to a 2-particle phase space such that the limiting behaviour is correct and momentum conservation holds.

By integrating out the soft emitted particle of the dipoles, the insertion operator  $\mathbf{I}$  can be determined. We refer to [37] for more detailed equations where these derivations are explained in detail.

## 4.2. Regularization and Reduction

A proper treatment of the divergences requires them to be regularized. The following methods are motivated by the fact that changing the number of dimensions affects the divergence of an integral

$$\int_a^\Lambda \frac{1}{r^2} d^3r \sim \mathcal{O}(\Lambda) \quad \int_a^\Lambda \frac{1}{r^2} d^2r \sim \mathcal{O}(\ln \Lambda) \quad \int_a^\Lambda \frac{1}{r^2} d^1r \sim \mathcal{O}(1) \quad (4.14)$$

for a large cut-off scale  $\Lambda$ . Transitioning to a  $D = 4 - 2\epsilon$  dimensional momentum integral

$$\int d^4l \rightarrow \mu^{4-D} \int d^Dl \quad (4.15)$$

regularizes the divergence through poles in  $\epsilon$  with a renormalization scale  $\mu_R$  to conserve mass-dimensions.

### 4.2.1. Dimensional regularization schemes

We will look briefly at the schemes encountered in this thesis. They differ in their treatment of the vector field regularization (i.e. gluon). Since these schemes use different spaces, we list them here:

- 4-dimensional Minkowski space ( $\mathbf{S}_{[4]}$ )
- quasi- $d$ -dimensional space ( $\mathbf{QS}_{[d]}$ ) is infinite dimensional and as a consequence it is a superspace of  $\mathbf{S}_{[4]} \subset \mathbf{QS}_{[d]}$ .
- quasi-4-dimensional space ( $\mathbf{QS}_{[d_s]}$ ) is closely related to  $\mathbf{S}_{[4]}$  but  $\mathbf{QS}_{[d]} \subset \mathbf{QS}_{[d_s]} = \mathbf{QS}_{[d_s]} \otimes \mathbf{QS}_{[n_\epsilon]}$  must hold to sustain gauge invariance. Thereby,  $d_s \equiv d + n_\epsilon = 4 - 2\epsilon + n_\epsilon$ .

The index in brackets  $[d]$  refers to the dimension of the space. From here we can look at the consequences for the metric tensors and gamma matrices:

$$g_{[d_s]}^{\mu\nu} = g_{[d]}^{\mu\nu} + g_{[n_\epsilon]}^{\mu\nu} \quad g_{[\text{dim}]}^{\mu\mu} = \text{dim} \quad g_{[d]}^{\mu\nu} g_{[n_\epsilon]}^{\nu\rho} = 0 \quad (4.16)$$

$$\gamma_{[d_s]}^\mu = \gamma_{[d]}^\mu + \gamma_{[n_\epsilon]}^\mu \quad \{\gamma_{[\text{dim}]}^\mu, \gamma_{[\text{dim}]}^\nu\} = 2g_{[\text{dim}]}^{\mu\nu} \quad \{\gamma_{[d]}^\mu, \gamma_{[n_\epsilon]}^\nu\} = 0 \quad (4.17)$$

The ordering of these spaces implies the projections relations to be

$$g_{[d_s]}^{\mu\nu} g_{[d]}^{\nu\rho} = g_{[d]}^{\mu\rho} \quad g_{[d_s]}^{\mu\nu} g_{[4]}^{\nu\rho} = g_{[4]}^{\mu\rho} \quad g_{[d]}^{\mu\nu} g_{[4]}^{\nu\rho} = g_{[4]}^{\mu\rho} \quad (4.18)$$

meaning that we take the subspace upon contractions with a different space.

After settling these formalities, we move on to the regularization. Regardless of the scheme the momentum integration is done in  $d$  dimensions. We will call singular gluons **internal**, meaning those in collinear/soft emissions or loops, and the remaining gluons **external**. Divergences only appear with internal ones so regularization of external gluons is optional. Four prominent regularization schemes are:

- **Conventional Dimensional Regularization (CDR)**: Both internal and external gluons are treated  $d$ -dimensional. This makes this scheme appealing for automatized calculations.
- **'t Hooft Veltman (HV)**: The internal gluons are  $d$ -dimensional but the external ones are 4-dimensional.
- **Dimensional Reduction (DRED)**: Both internal and external gluons are quasi-4-dimensional.
- **Four Helicity Dimension (FHD)**: The internal gluons are quasi-4-dimensional but the external ones are 4-dimensional. This scheme is used in **MadGraph**[41] since it allows using a helicity formalism through **HELAS**[42].

For DRED and FHD  $d_s$  is usually 4 or equivalently  $n_\epsilon = 2\epsilon$ .

The HV and CDR scheme introduce a mismatch between the  $(d - 2)$  gluon and the 2 gluino degrees of freedom. Their regularization then breaks supersymmetry. This problem does not happen in the DRED or FHD scheme. Luckily, it is possible to include SUSY restoring counterterms for the gaugino-squark-quark  $\hat{g}$  and gluino-squark-quark  $\hat{g}_s$  vertices

$$\hat{g}_s = g_s \left[ 1 + \frac{\alpha_s}{3\pi} \right] \quad \hat{g} = g \left[ 1 - \frac{\alpha_s}{8\pi} C_F \right]. \quad (4.19)$$

Methods for converting different schemes can be found in [43][44][45] and more details and examples are available in [46][47][48][49]. The application of  $\gamma^5$  in  $D$  dimensions must also be reconsidered. We will stick to the naive handling by keeping its anticommutation relation  $\{\gamma_5, \gamma_\mu\} = 0$  and dropping the trace relation  $\text{Tr}[\gamma^\mu \gamma^\nu \gamma^\rho \gamma^\sigma \gamma_5] = i4\epsilon^{\mu\nu\rho\sigma}$  [50]. By convention the trace is evaluated to  $\text{Tr}[\mathbb{1}] = 4$ .

#### 4.2.2. Passarino-Veltman reduction

To evaluate a divergent loop integral in  $D - 2\epsilon$  dimensions the Passarino-Veltman reduction is very useful. A general  $N$ -loop integral is depicted in fig. 2 written in the following in an algebraic form

$$T_{\mu_1, \dots, \mu_M}^N(p_1, \dots, p_M, m_1, \dots, m_M) = \frac{\mu^{4-D}}{i\pi^{D/2} r_\Gamma} \int d^D l \frac{l_{\mu_1} \dots l_{\mu_M}}{\mathcal{D}_1 \dots \mathcal{D}_N} \quad (4.20)$$

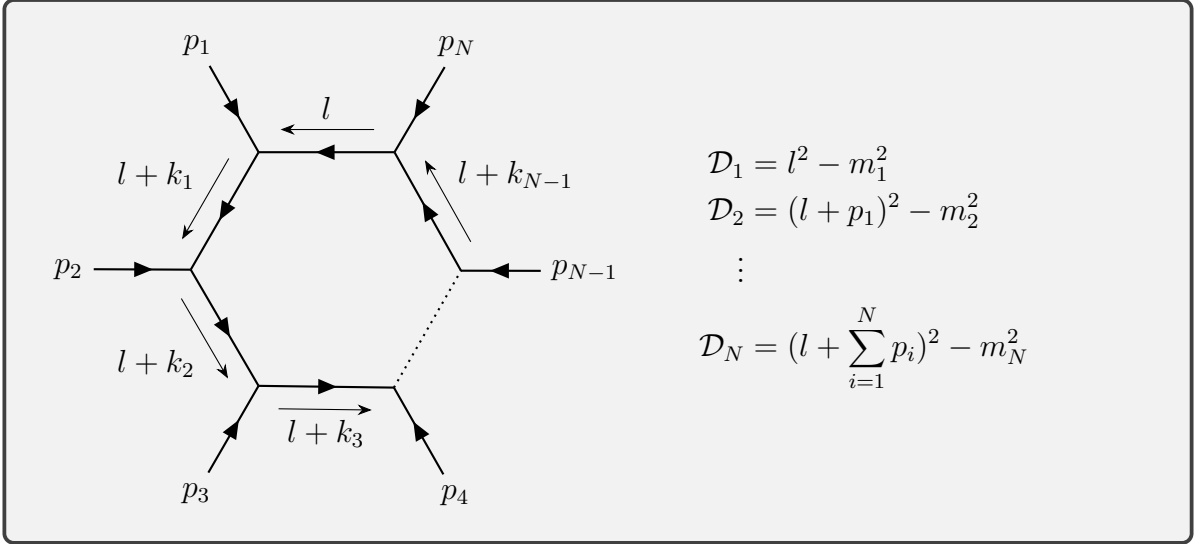
with the prefactor

$$r_\Gamma = \frac{\Gamma(1 - \epsilon)^2 \Gamma(1 + \epsilon)}{\Gamma(1 - 2\epsilon)} = 1 - \gamma_E \epsilon + \left( \frac{\gamma_E^2}{2} - \frac{\pi^2}{12} \right) \epsilon^2 + \mathcal{O}(\epsilon^3). \quad (4.21)$$

Alternative definitions factorize  $1/\Gamma(1 + \epsilon)$  giving differences of order  $\mathcal{O}(\epsilon)$

$$\frac{\Gamma(1 + \epsilon)}{\Gamma(1 - \epsilon)^2 \frac{\Gamma(1 + \epsilon)}{\Gamma(1 - 2\epsilon)}} = 1 + \frac{\pi^2}{6} \epsilon^2 + \mathcal{O}(\epsilon^3) \quad (4.22)$$

resulting in shifted finite ( $\epsilon^0$ ) contributions when double poles ( $\epsilon^{-2}$ ) appear.

Figure 2: Momentum conventions for general  $N$ -loop diagrams.

In accordance with `LoopTools`[51] conventions we introduce the notation

$$\Delta = \frac{1}{\epsilon} - \gamma_E + \ln 4\pi \quad (4.23)$$

and use the definition of the momenta

$$k_n = \sum_{i=1}^n p_i. \quad (4.24)$$

Of special importance are the scalar integrals ( $M = 0$ ). We will need them with up to four particles in the loop:

$$T^1 = A_0(m_1^2) = \frac{\mu^{4-D}}{i\pi^{D/2}r_\Gamma} \int d^D l \frac{1}{\mathcal{D}_1} =: \int_l \frac{1}{\mathcal{D}_1} \quad (4.25)$$

$$T^2 = B_0(p_1^2, m_1^2, m_2^2) = \int_l \frac{1}{\mathcal{D}_1 \mathcal{D}_2} \quad (4.26)$$

$$T^3 = C_0(p_1^2, p_2^2, (p_1 + p_2)^2, m_1^2, m_2^2, m_3^2) = \int_l \frac{1}{\mathcal{D}_1 \mathcal{D}_2 \mathcal{D}_3} \quad (4.27)$$

$$T^4 = D_0(p_1^2, p_2^2, p_3^2, p_4^2, (p_1 + p_2)^2, (p_2 + p_3)^2, m_1^2, m_2^2, m_3^2, m_4^2) = \int_l \frac{1}{\mathcal{D}_1 \mathcal{D}_2 \mathcal{D}_3 \mathcal{D}_4}. \quad (4.28)$$

They were first calculated by 't Hooft and Veltman in [52]. The tensor reduction proposed by Passarino and Veltman avoids solving more complicated integrals by recycling the scalar integrals [53]. Exemplary,  $B^\mu = p_1^\mu B_1$  must have that form since  $p_1^\mu$  is the only available Lorentz-structure and

$$2p_1^2 B_1 = 2p_1^\mu B^\mu = \int_l \frac{2pl}{\mathcal{D}_1 \mathcal{D}_2} = \underbrace{\int_l \frac{(l + p_1)^2 - m_1^2}{\mathcal{D}_1 \mathcal{D}_2}}_{A_0(m_1^2)} - \underbrace{\int_l \frac{l^2 - m_1^2}{\mathcal{D}_1 \mathcal{D}_2}}_{A_0(m_2^2)} - (p_1^2 - m_2^2 + m_1^2) \underbrace{\int_l \frac{1}{\mathcal{D}_1 \mathcal{D}_2}}_{B_0} \quad (4.29)$$

gives  $B^\mu$  in terms of scalar integrals. Some other tensor decompositions give:

$$\begin{aligned} B^{\mu\nu} &= g^{\mu\nu} B_{00} + k_1^\mu k_1^\nu B_{11} \\ C^\mu &= k_1^\mu C_1 + k_2^\mu C_2 \\ C^{\mu\nu} &= g^{\mu\nu} C_{00} + k_1^\mu k_1^\nu C_{11} + (k_1^\mu k_2^\nu + k_2^\mu k_1^\nu) C_{12} + k_2^\mu k_2^\nu C_{22} \\ &\vdots \end{aligned} \tag{4.30}$$

Their derivations can be found in [54] [55] or the original papers. We will use various results from these summarized in appendix E.3.

Now that we have a practical machinery to handle divergences, we work out the necessary renormalization of our fields in the next chapter.

### 4.3. Renormalization

In order to absorb the UV-divergences appearing at one-loop level we replace the bare bosonic fields  $\Phi_0$  with renormalized fields  $\Phi$

$$\Phi_0 = \sqrt{Z_0} \Phi_0 \rightarrow \sqrt{Z_\Phi} \Phi = \sqrt{1 + \delta Z_\Phi} \Phi = (1 + \frac{1}{2} \delta Z_\Phi) \Phi. \tag{4.31}$$

Left- and right-handed fermionic fields are treated separately

$$\Psi_0 = \sqrt{Z_0} \Psi_0 \rightarrow (1 + \frac{1}{2} \delta Z_\Psi^L P_L + \frac{1}{2} \delta Z_\Psi^R P_R) \Psi, \tag{4.32}$$

where we introduce the chirality projectors  $P_{L,R} = \frac{1}{2}(1 \mp \gamma_5)$  since we are operating in the mass-eigenstates now. The  $L, R$  index notation is used to separate the two cases in analogy to the  $\pm$  notation.

Similarly, couplings  $\lambda$  and masses  $m$  get corrections:

$$\lambda_0 \rightarrow Z_\lambda \lambda = \lambda + \delta Z_\lambda \lambda \tag{4.33}$$

$$m_0 \rightarrow Z_m m = m + \delta Z_m m \tag{4.34}$$

The advantage of using a renormalization constant  $\delta Z$  shifted from the bare coupling 1 instead of the whole multiplicative renormalization constants  $Z$  is that we reproduce our original bare Lagrangian with new counterterms

$$\mathcal{L}_0 \rightarrow \mathcal{L} + \mathcal{L}_\times. \tag{4.35}$$

The counterterms will then be chosen to explicitly cancel the UV-divergences encountered at one-loop level in the bare Lagrangian.

In the on-shell (OS) renormalization scheme the renormalized masses correspond to the physical masses and the real part of the propagator's residue is normalized to 1. This differs from the modified minimal subtraction scheme, where one includes extra counterterms to account for the proper normalization of the residue [56]. Another advantage of the OS renormalization is that we do not have to compute loops at the legs of our Feynman diagrams. Furthermore, the cancellation of UV divergences between various vertices and wave-function renormalization functions is checked explicitly.

Since we only encounter squarks and quarks as intermediate particle at leading order in our process, we look at their renormalization first. To determine the running of the coupling we will also renormalize the gluon propagator. The electroweakinos do not need any treatment, since the goal of our perturbative calculation is an improvement by  $\mathcal{O}(\alpha_s)$ .

#### 4.3.1. Quarks

The kinetic and mass terms of the bare Lagrangian for quarks reads

$$\mathcal{L}_0 = i\bar{\psi}_0^L \not{\partial} \psi_0^L - m_0 \bar{\psi}_0^R \psi_0^L + (L \leftrightarrow R). \quad (4.36)$$

Here the upper indices refer to whether a quark is left- or right-handed. Replacing the bare quantities

$$\psi_0^{L,R} \rightarrow \sqrt{Z_\psi^{L,R}} \psi_{L,R} = (1 + \frac{1}{2} \delta Z_\psi^{L,R}) \psi_{L,R} \quad (4.37)$$

$$m_0 \rightarrow Z_m m = (1 + \delta Z_m) m \quad (4.38)$$

in the bare Lagrangian  $\mathcal{L}_0$  yields

$$\mathcal{L} = \underbrace{i\bar{\psi}^L \not{\partial} \psi^L - m \bar{\psi}^R \psi^L}_{\mathcal{L}_0} \quad (4.39)$$

$$+ \underbrace{i \operatorname{Re}[\delta Z_\psi^L] \bar{\psi}^L \not{\partial} \psi^L - m \left( \delta Z_m + \frac{1}{2} (\delta Z_\psi^{R*} + \delta Z_\psi^L) \right) \bar{\psi}^R \psi^L}_{\mathcal{L}_\times} + (L \leftrightarrow R) \quad (4.40)$$

without higher order terms in  $\delta Z$ . The bare Lagrangian  $\mathcal{L}_0$  gives the typical two-point Green's function by replacing the derivatives with the momenta  $-ip$ , formally a Fourier transformation into momentum space, and dropping the fields  $\psi$

$$-i\Sigma_0 = i(\not{p} - m) \quad (4.41)$$

where we apply  $P_L + P_R = 1$ , after using  $\bar{\psi}_R \psi_L = \bar{\psi} P_L \psi$  and  $\bar{\psi}_L \gamma^\mu \psi_L = \bar{\psi} \gamma^\mu P_L \psi$ . Following the same steps, the new two-point Green's function for the counterterms is obtained

$$-i\Sigma_\times = i \left( \not{p} \operatorname{Re}[\delta Z_\psi^L] - m \left( \delta Z_m + \frac{1}{2} (\delta Z_\psi^{R*} + \delta Z_\psi^L) \right) \right) P_L + (L \leftrightarrow R). \quad (4.42)$$

The NLO propagator  $\Pi_\psi^{\text{NLO}}$  then consists of additional self energies and counterterms

$$\Pi_\psi^{\text{NLO}} = \Pi_\psi^{\text{LO}} + \Pi_\psi^{\text{LO}} (-i\Sigma) \Pi_\psi^{\text{LO}} + \Pi_\psi^{\text{LO}} (-i\Sigma_\times) \Pi_\psi^{\text{LO}} \quad (4.43)$$

$$= \Pi_\psi^{\text{LO}} (1 + (-i\hat{\Sigma}) \Pi_\psi^{\text{LO}}) \quad (4.44)$$

where  $\Sigma$  are the bare self energy loop contributions. Combining the counterterms and self energies then gives the renormalized self energy  $\hat{\Sigma}$ . Splitting up the vectorial  $\Sigma_V$  and scalar  $\Sigma_S$  part allows us to rewrite

$$\hat{\Sigma} = \left( \underbrace{\not{p} (\Sigma_V - \operatorname{Re}[\delta Z_\psi^L])}_{\hat{\Sigma}_V^L} + m \underbrace{\left( \delta Z_m + \frac{1}{2} (\delta Z_\psi^{R*} + \delta Z_\psi^L) + \frac{\Sigma_S^L}{m} \right)}_{\hat{\Sigma}_S^L} \right) P_L + (L \leftrightarrow R). \quad (4.45)$$

To realize on-shell renormalization the following two conditions must be satisfied [57] [58]. First, the real part of the propagator's pole must be the physical mass, that is

$$\text{Re} \left[ \frac{1}{\Pi_{\psi}^{\text{NLO}}(m^2)} \right] u(p, m) = 0 \quad \xrightarrow{4.44} \quad \text{Re}[\hat{\Sigma}(p^2 = m^2)]u(p, m) = 0 \quad (4.46)$$

And second, the real part of the propagator's residue should be normalized to 1, translating to

$$\lim_{p^2 \rightarrow m^2} \text{Re}[-i(\not{p} - m)\Pi_{\psi}^{\text{NLO}}]u(p, m) = u(p, m) \quad \xrightarrow{4.44} \quad \lim_{p^2 \rightarrow m^2} \frac{\not{p} + m}{p^2 - m^2} \text{Re}[\hat{\Sigma}]u(p, m) = 0. \quad (4.47)$$

These conditions define how we get the on-shell renormalization constants  $\delta Z$  from the bare self energies  $\Sigma$

$$\delta Z_m = -\frac{1}{2} \text{Re} \left[ \Sigma_V^L + \Sigma_V^R + \frac{\Sigma_S^L + \Sigma_S^R}{m} \right]_{p^2=m^2} \quad (4.48)$$

$$\delta Z_{\psi}^{L,R} = \text{Re} \left[ \Sigma_V^{L,R} + m^2(\dot{\Sigma}_V^{L,R} + \dot{\Sigma}_V^{R,L} + \frac{\dot{\Sigma}_S^{L,R} + \dot{\Sigma}_S^{R,L}}{m}) \right]_{p^2=m^2}, \quad (4.49)$$

where  $\dot{\Sigma}$  is the derivative in  $p^2$ . However, we will see in the following sections that no corrections to the quark mass are necessary, since the only particle we treat as massive is the top, which we assume to be negligible in the proton initial state.

### 4.3.2. Squarks

We start from a typical bare Lagrangian for scalars

$$\mathcal{L}_0 = \sum_{i=1}^2 (\partial_{\mu} \tilde{q}_{0,i}^{\dagger} \partial_{\mu} \tilde{q}_{0,i} - m_{0,i}^2 \tilde{q}_{0,i}^{\dagger} \tilde{q}_{0,i}), \quad (4.50)$$

but include a sum over the mass eigenstates  $i$ . Our renormalization constants are

$$\tilde{q}_{0,i} \rightarrow \sqrt{Z_{ij}} \tilde{q}_j = (\delta_{ij} + \frac{1}{2} \delta Z_{ij}) \tilde{q}_j \quad (4.51)$$

$$m_{0,i}^2 \rightarrow Z_{m_i}^2 m_i^2 = (\delta_{ij} + \delta Z_{m_i}^2) m_i^2 \quad (4.52)$$

where the sum over  $j$  allows for the inclusion of mixing between eigenstates in loop corrections. Replacing the bare fields gives the new Lagrangian

$$\begin{aligned} \mathcal{L} = & \underbrace{\sum_{i=1}^2 (\partial_{\mu} \tilde{q}_i^{\dagger} \partial_{\mu} \tilde{q}_i - m_i^2 \tilde{q}_i^{\dagger} \tilde{q}_i)}_{\mathcal{L}_0} \\ & + \underbrace{\sum_{i=1}^2 \sum_{j=1}^2 \left( \frac{1}{2} (\delta Z_{ji}^* + \delta Z_{ij}) \partial_{\mu} \tilde{q}_i^{\dagger} \partial_{\mu} \tilde{q}_j - (\delta_{ij} \delta Z_{m_i}^2 + \frac{1}{2} (\delta Z_{ji} m_j^2 + \delta Z_{ij} m_i^2)) \tilde{q}_i^{\dagger} \tilde{q}_j \right)}_{\mathcal{L}_x}. \end{aligned} \quad (4.53)$$



Repeating the same steps as for the quarks, we get a two-point function from the Lagrangian for the counterterms.

$$-i\Sigma_{\times,ij} = i \left( \frac{1}{2}(\delta Z_{ij} + \delta Z_{ji}^*)p^2 - \frac{1}{2}(m_i^2 \delta Z_{ij} + m_j^2 \delta Z_{ji}^*) - m_i^2 \delta Z_{m_i}^2 \delta_{ij} \right) \quad (4.54)$$

Combining bare self energy and counterterms

$$\hat{\Sigma}_{ij} = \Sigma_{ij} + \Sigma_{\times,ij} \quad (4.55)$$

we get the renormalized self energy. Again using the on-shell conditions we obtain our renormalization constants. Requiring the propagator pole to be the physical mass in the case of  $i = j$  leads to

$$\text{Re}[\hat{\Sigma}_{ii}(m_i^2)] = 0 \implies \delta Z_{m_i}^2 = -\frac{\text{Re}[\Sigma_{ii}(m_i^2)]}{m_i^2} \quad (4.56)$$

and the fact that the real part of the residue of the propagator must be one results in

$$\delta Z_{ii} = \text{Re}[\dot{\Sigma}_{ii}(m_i^2)]. \quad (4.57)$$

For  $i \neq j$  the mass counterterm does not appear, since we want no transition from type  $i$  to  $j$ . Thus, we write

$$\text{Re}[\hat{\Sigma}_{12}(m_1^2)] = 0 \qquad \text{Re}[\hat{\Sigma}_{12}(m_2^2)] = 0 \quad (4.58)$$

leading to

$$\delta Z_{12} = -2 \frac{\text{Re}[\Sigma_{12}(m_2^2)]}{m_1^2 - m_2^2} \qquad \delta Z_{21} = +2 \frac{\text{Re}[\Sigma_{21}(m_1^2)]}{m_1^2 - m_2^2}. \quad (4.59)$$

### 4.3.3. Gluon

The renormalization of the gluon is determined in a similar procedure to the previous squark case. But a difference lies in the vanishing longitudinal propagator due to gauge invariance

$$-i\Pi_{\mu\nu}^{ab}(p^2) = -i\delta^{ab} \left( (g^{\mu\nu} - \frac{p^\mu p^\nu}{p^2})\Pi_t(p^2) + \frac{p^\mu p^\nu}{p^2}\Pi_l(p^2) \right). \quad (4.60)$$

Since the gluon is massless, its renormalization constant is solely determined by the on-shell condition

$$\delta Z_g = -\text{Re} \left[ \frac{d\Pi_t(p^2)}{dp^2} \right]_{p^2=0}. \quad (4.61)$$

## 4.4. Threshold Resummation

Covering the whole topic of resummation would go far beyond the scope of this thesis. We will sketch the key concepts related to resummation and refer the interested reader to [19] and its references. First, we should ask ourselves why resummation is interesting and important for our process? We are looking at the production of heavy particles therefore we are close to the limits of the phase space. For massless virtual particles (e.g. gluon) we integrate over the full loop momentum. This is in contrast to the particles in real emissions, since their integration is constrained. And as a consequence there are large logarithmic remainders

$$\alpha_s^n(\mu_R^2) \left[ \frac{\ln^m(1-z)}{1-z} \right]_+, \quad (4.62)$$

where  $z = M^2/s$  is the fraction of the invariant masses of final and initial state and  $m \leq 2n - 1$ . For soft particles  $z \rightarrow 1$  the arising divergences prohibit us from using normal perturbation theory and the logarithmic terms need to be resummed up to all order [22] [59].

To calculate the soft emission up to all orders, dynamical and kinematical factorization are fundamental. **Dynamical factorization** is possible by the eikonal approximation, that is simplified Feynman rules dropping insignificant terms for small momenta. One approach to **kinematical factorization** is by transforming into Mellin space such that the phase space factorizes

$$\int dz z^{N-1} d\phi_{2+n}(z) \approx d\phi_2 \times d\phi_n(N) \quad (4.63)$$

where  $N$  is our new Mellin momentum of  $z$ .

Due to the factorization theorem we can split an IR sensitive quantity  $\mathcal{R}$  into a hard scattering  $\mathcal{H}$  and long distance  $\mathcal{S}$  behaviour, where only the later two depend on the factorization scale  $\mu_F$ . Exploiting the independence of the factorization scale in  $\mathcal{R}$  and setting it to  $\mu_F = M$  yields

$$\mathcal{R}(M^2, m^2) = \mathcal{H}(1)\mathcal{S}(1) \exp \left( - \int_{m^2}^{M^2} \frac{dk^2}{k^2} \gamma_s(k^2) \right) \quad (4.64)$$

where the scale dependence is in the exponent, named Sudakov form factor, consisting of the **soft anomalous dimension**  $\gamma_s$ . Furthermore, the **hard matching coefficient** will be needed for matching the resummation to our NLO calculation where one must avoid double counting in the soft region.

Our resummed results are, however, preliminary, since we use the already in **Resummino** included computations of the hard matching coefficient and soft anomalous dimension for squark-gaugino production.

## 5. Next-to-leading order

In previous section we went through the necessary methods to compute a NLO cross section. Now we will apply them to the production of a squark and electroweakino. First, section 5.1 will explain the computation of the real corrections. The second puzzle piece, the virtuals, are presented in section 5.2.

### 5.1. Real corrections

The real corrections consist of the additional emission of a massless coloured particle. Here, this is either a gluon or an (anti-)quark. The corresponding diagrams are shown below.

$$i\mathcal{M}^{\text{NLO}} = \text{[Four diagrams showing real corrections with gluon emission]} + \dots$$

We can already see that the first two and the last two diagrams are related by crossing relations. Therefore, in total only two  $2 \rightarrow 3$  matrix elements need to be calculated. An exemplary demonstration of the dipole subtraction is given in section 5.1.1. Followed by working out the subtraction of on-shell resonances section 5.1.2.

#### 5.1.1. Quark gluon initiated corrections

We use QGRAF[60] to generate the Feynman diagrams contributing to the  $2 \rightarrow 3$  corrections with one quark and one gluon in the initial state.

$$\text{[Diagrammatic equation (5.1) showing 11 Feynman diagrams for quark gluon initiated corrections]} \quad (5.1)$$

Since we use the Feynman gauge for gluons, we need to eliminate the unphysical longitudinal polarization from the gauge-fixing. These are cancelled by including (anti-)ghost diagrams (dashed without arrows). The squared matrix element is then constructed as

$$\langle |\mathcal{M}|^2 \rangle = \sum_i \langle |\mathcal{M}_i|^2 \rangle + 2 \sum_i \sum_{j < i} \text{Re} [\langle \mathcal{M}_i^* \mathcal{M}_j \rangle] . \quad (5.2)$$

The straight up application of Feynman rules and interference of all these amplitudes is best handled in an automated symbolic calculation. For this purpose we use FORM[32], which also handles  $\gamma$  matrices. The steps in our computation are, completely analogous to analytic calculation,

1. Contract colour structures
2. Apply completeness relations for spinors and polarization sums
3. Evaluate spinor traces for each closed fermion line
4. Simplify momenta and factorize out common prefactors

Then the resulting matrix-element can be embedded in a Monte-Carlo integrator. In the red coloured (1-5, 11) diagrams of eq. (5.1) we encounter soft and/or collinear divergences from a gluon emission and a naive integration over the 3-particle phase space will fail. We also notice that if we remove the red particles from our Feynman diagrams we restore either the s- or u-channel Born-diagram. If we look at a propagator of an intermediate particle connected to the red particles, we see a divergence towards low transverse momenta in the eikonal limit

$$\frac{i}{(p-k)^2 - m^2} \xrightarrow{k \rightarrow 0} \frac{-i}{2p \cdot k} \sim \frac{1}{k_t^2}. \quad (5.3)$$

Here  $k$  belongs to the emitted massless particle (here gluon) and  $p$  to the emitter with mass  $p^2 = m^2$ .

The previously presented dipole formalism gives us extra terms to include in our integration over the 3-particle phase space such that these divergences vanish. Next, we will apply this procedure exemplary to the last diagram of eq. (5.1).

### Applying the dipole formalism

Looking at fig. 3 we can see two potential spectators coloured in blue. One case is classified as an initial-final and the other as an initial-initial dipole. As the spectator is used for colour correlations, colourless particles vanish with  $\mathbf{T} = 0$ .



Figure 3: Dipole identification of diagram 11 in eq. (5.1).

We will focus on the initial-emitter final-spectator case depicted on the right in fig. 3. The corresponding equation for the dipole

$$\mathcal{D}_j^{ai}(p_1, p_2, p_3; p_a, p_b) = -\frac{1}{2p_a p_i} \frac{1}{x_{ij,a}} {}_2 \langle \dots, j, \dots; ai, \dots | \frac{\mathbf{T}_j \mathbf{T}_{ai}}{\mathbf{T}_{ai}^2} \mathbf{V}_j^{ai} | \dots, j, \dots; ai, \dots \rangle_2 \quad (5.4)$$

is associated with both diagrams where a quark emits a gluon (4, 11 in eq. (5.1)) and the spectator  $j$  is a final state particle.

Since we want to reuse our Born matrix element which includes a different colour correlation, we define our colour rescale factor as

$$c = \langle \mathbf{T}_j \mathbf{T}_{ai} \rangle_3 := \frac{{}_2\langle \dots, j, \dots; ai, \dots | \mathbf{T}_j \mathbf{T}_{ai} | \dots, j, \dots; ai, \dots \rangle_2}{{}_2\langle \dots, j, \dots; ai, \dots | \mathbb{1} | \dots, j, \dots; ai, \dots \rangle_2} = -\frac{T_{\beta\gamma}^a T_{\gamma\rho}^b T_{\delta\beta}^b T_{\rho\delta}^a}{T_{\beta'\alpha'}^c T_{\alpha'\beta'}^c} = \frac{T_R}{C_A}. \quad (5.5)$$

This is possible because both leading order diagrams have the same colour structure. In a more general approach one can show that for 3 partons the colour algebra factorizes by application of the colour conservation eq. (4.10) [37, Appendix A]:

$$0 = (\mathbf{T}_1 + \mathbf{T}_2 + \mathbf{T}_3) |1, 2, 3\rangle \quad (5.6)$$

$$(2\mathbf{T}_1 \mathbf{T}_2) |1, 2, 3\rangle = (\mathbf{T}_1 \mathbf{T}_2 + \mathbf{T}_2 \mathbf{T}_1) |1, 2, 3\rangle \quad (5.7)$$

$$= (\mathbf{T}_1(-\mathbf{T}_1 - \mathbf{T}_3) + \mathbf{T}_2(-\mathbf{T}_2 - \mathbf{T}_3)) |1, 2, 3\rangle \quad (5.8)$$

$$= (\mathbf{T}_3^2 - \mathbf{T}_1^2 - \mathbf{T}_2^2) |1, 2, 3\rangle \quad (5.9)$$

$$\implies c = \langle \mathbf{T}_1 \mathbf{T}_2 \rangle_3 = T_R(C_3 - C_1 - C_2) \quad (5.10)$$

And we get the same colour factor  $c = T_R(C_A - C_F - C_F) = \frac{T_R}{C_A}$ . Since we only have one adjoint (gluon) and two fundamental (quark and squark) particles at leading order, the only other possible combination of Casimir operators is  $T_R(C_F - C_A - C_F) = -T_R C_A$ . In the aforementioned dipole formula the kernel  $\mathbf{V}$  is diagonal in the spin  $s$

$$\langle s | \mathbf{V}_j^{qg} | s' \rangle = 8\pi\mu^{2\epsilon}\alpha_s C_F \left\{ \frac{2}{2 - x_{ij,a} - \tilde{z}_j} - 1 - x_{ij,a} - \epsilon(1 - x_{ij,a}) \right\} \delta_{ss'} \quad (5.11)$$

and the last ingredient is the transition from a three  $\{i, ai, j\}$  to a two  $\{ai, j\}$  particle phase space. This transformation must respect momenta conservation and the on-shell particles should keep their masses

$$p_i^\mu + p_j^\mu + p_{ai}^\mu = \tilde{p}_{ai}^\mu + \tilde{p}_j^\mu \quad (5.12)$$

$$p_a^2 = p_i^2 = \tilde{p}_{ai}^2 = 0 \quad (5.13)$$

$$p_j^2 = \tilde{p}_j^2 = m_j^2. \quad (5.14)$$

An approach similar to the parton distribution functions is to rescale the momentum of a particle by  $x$  after an emission

$$\tilde{p}_{ai}^\mu := x_{ij,a} p_a^\mu \quad (5.15)$$

$$\tilde{p}_j^\mu := p_i^\mu + p_j^\mu - (1 - x_{ij,a}) p_a^\mu, \quad (5.16)$$

which consequently can be determined to be

$$x_{ij,a} = \frac{p_a p_i + p_a p_j - p_i p_j}{p_a p_i + p_a p_j}. \quad (5.17)$$

The remaining dipole cases follow the same steps but use different functions from [38]. In table 4 we list the dipoles with their only undetermined quantity the colour rescale factor and the Casimir operator  $\mathbf{T}^2$  of the intermediate particle.

Table 2: List of dipoles for quark-gluon initial state.

Diagrams	dipole type	emitter	spectator	emitted	colour $c$	Casimir $\mathbf{T}_{\text{interm.}}^2$
4, 11	initial-final	quark	squark	gluon	$\frac{T_R}{C_A}$	$C_F$
4, 11	initial-initial	quark	gluon	gluon	$-T_R C_A$	$C_F$
3, 5	final-initial	squark	quark	gluon	$\frac{T_R}{C_A}$	$C_F$
3, 5	final-initial	squark	gluon	gluon	$-T_R C_A$	$C_F$
1, 2	initial-final	gluon	squark	gluon	$-T_R C_A$	$C_A$
1, 2	initial-initial	gluon	quark	gluon	$-T_R C_A$	$C_A$

The case where a gluon emits another gluon is a bit more involved since the kernel will depend on the helicity of the external gluon.

$$\begin{aligned}
\langle \mu | \mathbf{V}_j^{gg} | \nu \rangle = & 16\pi\mu^{2\epsilon}\alpha_s C_A \left\{ -g^{\mu\nu} \left[ \frac{1}{2 - x_{ij,a} - \tilde{z}_j} - 1 + x_{ij,a}(1 - x_{ij,a}) \right] \right. \\
& \left. + (1 - \epsilon) \frac{1 - x_{ij,a}}{x_{ij,a}} \frac{\tilde{z}_i \tilde{z}_j}{p_i p_j} \left( \frac{p_i^\mu}{\tilde{z}_i} - \frac{p_j^\mu}{\tilde{z}_j} \right) \left( \frac{p_i^\nu}{\tilde{z}_i} - \frac{p_j^\nu}{\tilde{z}_j} \right) \right\} \quad (5.18)
\end{aligned}$$

It's Lorentz-structure consists of four tensors  $g^{\mu\nu}$ ,  $p_i^\mu p_i^\nu$ ,  $p_j^\mu p_j^\nu$ ,  $p_i^\mu p_j^\nu + p_i^\nu p_j^\mu$ . We notice that they all are symmetric in  $\mu \leftrightarrow \nu$  and any contraction with an antisymmetric tensor will vanish. If we look at our polarized Born matrix element we identify seven variants  $g^{\mu\nu}$ ,  $p_a^\mu p_a^\nu$ ,  $q^\mu q^\nu$ ,  $p_2^\mu p_2^\nu$ ,  $p_a^\mu q^\nu + q^\mu p_a^\nu$ ,  $p_a^\mu p_2^\nu + p_2^\mu p_a^\nu$ ,  $q^\mu p_2^\nu + p_2^\mu q^\nu$  (appendix B). From these we compute a  $7 \times 4$  matrix with all possible contractions of the kernel with our Born matrix element. We write the prefactors to the kernel as a 4 dimensional vector and the prefactors of the polarized matrix element in a 7 dimensional vector. To get a scalar result we just need to sandwich the matrix between the vectors.

We already show results from the complete computation in table 3. The computation of the  $7 \times 4$  matrix for both initial-initial and initial-final can be found in appendix D.1.

Table 3: List of Lorentz-structure tensor prefactors from the Born process. A global factor of  $2g_s^2(L^2 + R^2)C_A C_F$  as well as the corresponding propagator denominators are omitted. The calculation is in appendix B.

Tensor structure	SS	UU	SU
$g^{\mu\nu}$	$-q^2 p_2 p_b$	0	0
$p_a^\mu p_a^\nu$	0	$p_2 p_a$	$2p_2 q$
$q^\mu q^\nu$	0	$p_2 p_a$	$q^2 - 2p_a p_2$
$p_1^\mu p_1^\nu$	0	$4p_2 p_a$	$4p_a q$
$p_a^\mu q^\nu + p_a^\nu q^\mu$	$m_2^2 - m_1^2$	$-p_2 p_a$	$(-p_2 q) + (-p_a q + p_2 p_a)$
$p_a^\mu p_1^\nu + p_a^\nu p_1^\mu$	$q^2$	$2p_2 p_a$	$2p_2 q + p_a q$
$q^\mu p_1^\nu + q^\nu p_1^\mu$	0	$-2p_2 p_a$	$2(-p_a q + p_2 p_a) - p_a q$

### 5.1.2. Gluon gluon initiated corrections

To get the gluon-gluon initial diagram we cross the final state gluon and initial quark of our previous calculation. This means we swap  $p_a \leftrightarrow -p_3$ , collect a factor of  $(-1)$  from Fermi statistics and adjust the averaging over initial particles by  $\frac{N_c}{N_c^2 - 1}$ .

(5.19)

The only subtlety arising with the dipoles is that they must be included twice but with different kinematics.

Table 4: List of dipoles for gluon-gluon initial state. Each dipole appear twice, but with different kinematics.

Diagrams	dipole type	emitter	spectator	emitted	colour $c$	$\mathbf{T}_{\text{interm.}}^2$
4, 5, 10, 11	initial-final	gluon	squark	(anti-)quark	$\frac{T_R}{C_A}$	$C_F$
4, 5, 10, 11	initial-initial	gluon	gluon	(anti-)quark	$-T_R C_A$	$C_F$

There is however the complication that some squark propagators can go on-shell.

### On-shell resonance subtraction

First, we must understand what these resonances mean and why we must subtract them. The resonances appear when the particle's momentum gets close to its mass  $p_{\text{res}}^2 \rightarrow m_{\tilde{q}}^2$ . Then the process of diagram 3 in eq. (5.19) splits into a leading order process with a subsequent decay. Schematically,

(5.20)

This process is only possible if the squark has a higher mass than the gaugino to allow a decay in its own reference frame. We do not want this contribution in our computation since it is already a part of the prediction of producing two squarks at leading order.

In a first step we regularize the on-shell divergence by introducing a finite width  $\Gamma_{\tilde{q}}$  to the propagator such that

$$\frac{1}{p_{\text{res}}^2 - m_{\tilde{q}}^2} \rightarrow \frac{1}{p_{\text{res}}^2 - m_{\tilde{q}}^2 + im_{\tilde{q}}\Gamma_{\tilde{q}}}.$$
(5.21)

This width will act purely as a regulator and does not need to be the physical width. If two amplitudes are combined and each has a resonant propagator we get a double resonant propagator (note the conjugation of one propagator)

$$\frac{1}{(p_{\text{res}}^2 - m_{\tilde{q}}^2)^2} \rightarrow \frac{1}{(p_{\text{res}}^2 - m_{\tilde{q}}^2)^2 + m_{\tilde{q}}^2\Gamma_{\tilde{q}}^2}.$$
(5.22)

Our total matrix-element splits into three pieces

$$|\mathcal{M}_{\text{tot}}|^2 = |\mathcal{M}_{nr}|^2 + 2\text{Re}[\mathcal{M}_r\mathcal{M}_{nr}^*] + |\mathcal{M}_r|^2.$$
(5.23)

The non-resonant diagrams (2, 4, 5, 8, 9, 10, 11) are part of  $\mathcal{M}_{nr}$  and the remaining resonant diagrams (1, 3, 6, 7, 9) are included in  $\mathcal{M}_r$ .

The simplest method to exclude the large contributions is **Diagram Removal (DR)**, where double resonance  $|\mathcal{M}_r|^2$  and the interference  $2\text{Re}[\mathcal{M}_r\mathcal{M}_{nr}^*]$  are not considered (**DR-I**). It is also possible to only exclude the double resonant part and keep the interference (**DR-II**)[61]. The price one pays for such a simple method is the apparent loss of gauge invariance.

Therefore, we will instead apply **Diagram Subtraction (DS)**. DS keeps both the single (interference) and double resonant pieces and only locally subtracts the contribution from the leading order process followed by the decay (lhs. eq. (5.20)). The advantage of this method is that it respects gauge invariance for vanishing width  $\Gamma_{\tilde{q}}$ . Consequently, we do not just integrate  $|\mathcal{M}_{\text{tot}}|^2$  over a 3-particle phase space  $d\phi_3$  but instead include a point wise subtraction



$$\left( |\mathcal{M}_{\text{tot}}|^2 - |\mathcal{M}_r(\tilde{\phi}_3)|^2 \underbrace{\frac{m_{\tilde{q}}^2 \Gamma_{\tilde{q}}^2}{(p_{\text{res}}^2 - m_{\tilde{q}}^2)^2 + m_{\tilde{q}}^2 \Gamma_{\tilde{q}}^2}}_{\text{Breit-Wigner}} \underbrace{\Theta(\sqrt{s} - m_{\tilde{q}} - m_{\tilde{q}^*})}_{\tilde{q}\tilde{q}^*\text{-production}} \underbrace{\Theta(m_{\tilde{q}} - m_{\tilde{\chi}})}_{\text{decay}} \frac{d\tilde{\phi}_3}{d\phi_3} \right) d\phi_3.$$

First, we include a Breit-Wigner function corresponding to the decay with given width  $\Gamma_{\tilde{q}}$ . For the production of  $\tilde{q}\tilde{q}^*$  at leading order to be kinematically allowed there must be sufficient energy  $\sqrt{s}$  to constitute their masses. The second  $\Theta$  function restrains our subtraction to the cases where a subsequent decay is allowed.

We must introduce a new 3-particle phase space  $\phi_3 \rightarrow \tilde{\phi}_3$  similar to the Catani-Seymour formalism to remove only contributions from  $|\mathcal{M}_r|^2$  where  $\tilde{p}_{\text{res}}^2 = (p_2 + p_3)^2 = m_{\tilde{q}}^2$  is on-shell. Please note that the Breit-Wigner function is still evaluated in  $\phi_3$  as it evaluates to 1 otherwise. More details, especially on the explicit form of the Jacobian  $\frac{d\tilde{\phi}_3}{d\phi_3}$ , are given in [62] on the specific case of squark pair production.

We split the integration over the 3-particle phase space  $d\phi_3$  in a double resonant part with the diagram subtraction and the rest (non-resonant and single resonant). This allows the Monte-Carlo integration to converge faster by focusing on the dominating region of each part.

### 5.1.3. Quark antiquark initiated corrections

For a quark and antiquark entering our  $2 \rightarrow 3$  process we get following diagrams

In the diagrams above red indicates the need for a dipole subtraction and green for an on-shell resonance subtraction. New in this process is the appearance of gluinos. They can go on-shell now and might require a subtraction. Also, squarks in between a gaugino and gluino are not determined for fixed initial and final state any more (3, 4, 7, 8). Therefore, we iterate over the possible squarks, but one needs to be careful here since a diagram with the same topology, but different internal squarks will get a factor of 2 like an interference term. This factor of 2 appears naturally if we iterate over both internal squarks (one in  $\mathcal{M}$  and one in  $\mathcal{M}^*$ ). Furthermore, we must include all types of quarks in the final state. Given that the chargino changes particles from up-type to down-type and vice-versa and the neutralino does not, the easiest way of including all possible cases is to keep the couplings completely arbitrary in our computation and let them decide which processes are allowed. The downside of this is the large number diagrams entering the computation, but since the couplings will not change in one Monte-Carlo integration,

it is sufficient to compute the couplings, use only the non-zero ones and reuse them for the next integration point.

In table 6 we list the information for the dipoles again. The kernel here again depends on the polarized Born matrix element since the dipole is linked to the gluon entering our Born process.

Table 5: List of dipoles for quark-antiquark initial state.

Diagrams	dipole type	emitter	spectator	emitted	colour $c$	$\mathbf{T}_{\text{interm.}}^2$
5, 6	initial-final	(anti-)quark	squark	(anti-)quark	$-T_R C_A$	$C_A$
5, 6	initial-initial	(anti-)quark	quark	(anti-)quark	$-T_R C_A$	$C_A$

#### 5.1.4. Quark quark initiated correction

This final real correction is related to the quark antiquark case again by a crossing of the final state antiquark with the initial state quark

(5.25)

This case is very useful to check our previous case as it is very symmetric. First, we can effectively remove the diagrams with a gluino by giving it a high mass. On the other hand integrating over the first four diagrams must give the same result as if we integrate only over the last four. We directly notice that the dipoles are nearly the same as in the previous quark-antiquark case. The only difference is that the dipoles appear two times, either with initial quark  $q_a$  or  $q_b$ . The dipoles are just like the diagrams related by the crossing relation  $p_a \leftrightarrow p_b$ .

Table 6: List of dipoles for quark-quark initial state. Each dipole appear twice, but with different kinematics.

Diagrams	dipole type	emitter	spectator	emitted	colour $c$	$\mathbf{T}_{\text{interm.}}^2$
1, 2, 5, 6	initial-final	quark	squark	quark	$-T_R C_A$	$C_A$
1, 2, 5, 6	initial-initial	quark	quark	quark	$-T_R C_A$	$C_A$

Now that we finished the computation of the real corrections we can move on to the virtual corrections.

## 5.2. Virtual corrections

The second ingredient to our NLO computation are the virtual corrections. A step-by-step computation is given in appendix C. Though a symbolic computer driven approach is faster and more reliable. We include such an exemplary code in appendix C.4. As already outlined in the preparation to this part of the thesis we will apply on-shell renormalization, such that no loops on the legs of our Feynman diagrams must be calculated. We are left with computing self energies in section 5.2.1 and vertex corrections in section 5.2.2. After listing the box diagrams in section 5.2.3, we mention the extra finite counterterms and add the integrated Catani-Seymour dipoles.

### 5.2.1. Self energies

We need to compute quarks, squarks and the gluon self energies.

#### Quark self energy

For the quark self energy we get one extra contribution compared to the SM. This additional loop is displayed in eq. (5.26).

$$\text{Diagram} = \text{Diagram}_1 + \text{Diagram}_2 + \text{Diagram}_3 \quad (5.26)$$

The counterterms can be determined from eq. (4.48) and eq. (4.49) derived in section 4.3.1 and the self energies of a quark  $q_I$  (cf. appendix C.1.1). In the general massive case we find following self energies

$$\Sigma_S^L = \frac{g_s^2}{(4\pi)^2} C_F \delta_{\beta\alpha} m_q \left( (4B_0(p^2, m_q^2, 0) - 2) - \frac{1}{m_q} \sum_{\tilde{q}_i} (\mathcal{L}_{Ii} \mathcal{L}'_{Ii} m_{\tilde{g}} B_0(p^2, m_{\tilde{g}}^2, m_{\tilde{q}_i}^2)) \right) \quad (5.27)$$

$$\Sigma_V^L = \frac{g_s^2}{(4\pi)^2} C_F \delta_{\beta\alpha} \left( (2B_1(p^2, m_q^2, 0) + 1) + \sum_{\tilde{q}_i} (\mathcal{L}_{Ii} \mathcal{R}'_{Ii} B_1(p^2, m_{\tilde{g}}^2, m_{\tilde{q}_i}^2)) \right) \quad (5.28)$$

and the right-handed term similar with  $\mathcal{L} \leftrightarrow \mathcal{R}$ . From the parameters of the Passarino-Veltman integrals we can identify which term comes from which diagram. Since the  $m_{\tilde{g}}$  term is proportional to  $\mathcal{L}\mathcal{L}' = 0$ , it can be dropped for minimal squark mixing and we get for massless quarks

$$\delta Z_m = 0 \quad (5.29)$$

$$\delta Z_q^{L,R} = \frac{g_s^2}{(4\pi)^2} C_F (2B_1(0, m_{\tilde{g}}^2, m_{\tilde{q}_{L,R}}^2) + 2B_1(0, 0, 0)), \quad (5.30)$$



$$+ 2(m_{\tilde{g}}^2 - m_{\tilde{q}}^2)B_0(m_{\tilde{q}}^2, m_{\tilde{g}}^2, 0) + 2A_0(m_{\tilde{g}}^2) - A_0(m_{\tilde{q}}^2)), \quad (5.36)$$

$$\begin{aligned} \delta Z_{ii} = \dot{\Sigma}_{ii}(m_{\tilde{q}}^2) &= \frac{g_s^2}{(4\pi)^2} C_F (2B_0(m_{\tilde{q}}^2, 0, m_{\tilde{q}}^2) + 4m_{\tilde{q}}^2 \dot{B}_0(m_{\tilde{q}}^2, 0, m_{\tilde{q}}^2) \\ &+ 2(m_{\tilde{g}}^2 - m_{\tilde{q}}^2) \dot{B}_0(m_{\tilde{q}}^2, m_{\tilde{g}}^2, 0) - 2B_0(m_{\tilde{q}}^2, m_{\tilde{g}}^2, 0)). \end{aligned} \quad (5.37)$$

With  $B_0 \xrightarrow{\text{UV}} \Delta$  the UV limit comes out as

$$\delta Z_{ii} \xrightarrow{\text{UV}} \frac{g_s^2}{(4\pi)^2} C_F (2 - 2) \Delta = 0. \quad (5.38)$$

In the massive case however we separate  $i = j$  and  $i \neq j$  where only the former gets a mass renormalization.

$$\begin{aligned} \delta Z_{ii} = \dot{\Sigma}_{ii}(m_{\tilde{q}}^2) &= \frac{g_s^2}{(4\pi)^2} C_F (2B_0(m_{\tilde{q}}^2, 0, m_{\tilde{q}}^2) + 4m_{\tilde{q}}^2 \dot{B}_0(m_{\tilde{q}}^2, 0, m_{\tilde{q}}^2) \\ &+ 2(m_{\tilde{g}}^2 - m_{\tilde{q}}^2 + m_q^2 - 2m_{\tilde{g}}m_q \text{Re}[S_{i(I+3)}^* S_{iI}]) \dot{B}_0(m_{\tilde{q}}^2, m_{\tilde{g}}^2, m_q^2) \\ &- 2B_0(m_{\tilde{q}}^2, m_{\tilde{g}}^2, m_q^2)), \end{aligned} \quad (5.39)$$

$$\begin{aligned} \delta Z_{ij} \cdot (m_j^2 - m_i^2) = \Sigma_{ij}(m_j^2) - \Sigma_{ji}(m_i^2) &= \frac{g_s^2}{(4\pi)^2} C_F (4m_{\tilde{g}}m_q (S_{i(I+3)}^* S_{jI} + S_{j(I+3)} S_{iI}^*)) \\ &(B_0(m_{\tilde{q}_j}^2, m_{\tilde{g}}^2, 0) - B_0(m_{\tilde{q}_i}^2, m_{\tilde{g}}^2, 0)), \end{aligned} \quad (5.40)$$

$$\begin{aligned} \delta Z_{m_i}^2 m_i^2 = -\Sigma_{ii}(m_i^2) &= -\frac{g_s^2}{(4\pi)^2} C_F (4B_0(m_{\tilde{q}}^2, 0, m_{\tilde{q}}^2) - A_0(m_{\tilde{q}}^2) \\ &+ 2(m_{\tilde{g}}^2 - m_{\tilde{q}}^2 + m_q^2 + 2m_{\tilde{g}}m_{\tilde{q}} \text{Re}[S_{i(I+3)}^* S_{iI}]) B_0(m_{\tilde{q}}^2, m_{\tilde{g}}^2, 0) \\ &+ 2A_0(m_{\tilde{g}}^2) + 2A_0(m_q^2) - \sum_{k=1,2} |S_{ik}|^2 A_0(m_{\tilde{q}_k}^2)). \end{aligned} \quad (5.41)$$

Our results again agree with [24]. The renormalized squark self energy enters only in the u-diagram.

$$|\mathcal{M}_{\tilde{q}}^{\text{su}}|^2 = 2 \text{Re} \left\{ \left( \text{Diagram 1} \right) \int \left( \text{Diagram 2} + \text{Diagram 3} \right) \right\}. \quad (5.42)$$

### Gluon self energy

We also need to compute the gluon self energy since it gives finite contributions to the vertex counterterms. We encounter following Feynman diagrams

$$\text{Diagram 4} = \text{Diagram 5} + \text{Diagram 6} + \text{Diagram 7} + \text{Diagram 8} \quad (5.43)$$

$$+ \text{Diagram 9} + \text{Diagram 10} + \text{Diagram 11} + \text{Diagram 12}. \quad (5.44)$$

Their individual results are given in appendix C.1.3. The wave-function renormalization term is obtained from the transversal self energy  $\Sigma_t$  (see eq. (4.61))

$$\delta Z_g = -\text{Re} \left[ \frac{d\Sigma_t(p^2)}{dp^2} \right]_{p^2=0} \quad (5.45)$$

$$\begin{aligned} &= - \sum_{\text{heavy } q} \frac{g_s^2}{(4\pi)^2} \frac{2}{3} \left( 2m_q^2 \dot{B}_0(0, m_q^2, m_q^2) + B_0(0, m_q^2, m_q^2) - \frac{1}{3} \right) \\ &\quad - \sum_{\text{light } q} \frac{g_s^2}{(4\pi)^2} \frac{2}{3} (B_0(0, 0, 0)) \\ &\quad + \frac{g_s^2}{(4\pi)^2} (19 + 1) \frac{1}{4} (B_0(0, 0, 0)) \\ &\quad - \frac{g_s^2}{(4\pi)^2} \frac{2}{3} N_c \left( 2m_{\tilde{g}}^2 \dot{B}_0(0, m_{\tilde{g}}^2, m_{\tilde{g}}^2) + B_0(0, m_{\tilde{g}}^2, m_{\tilde{g}}^2) - \frac{1}{3} \right) \\ &\quad - \sum_{\tilde{q}} \frac{ig_s^2}{(4\pi)^2} T_R \frac{1}{3} \left( -(4m_{\tilde{q}}^2) \dot{B}_0(0, m_{\tilde{q}}^2, m_{\tilde{q}}^2) + B_0(0, m_{\tilde{q}}^2, m_{\tilde{q}}^2) + \frac{2}{3} \right). \end{aligned} \quad (5.46)$$

The first two terms come from the massive and massless quark loops. The term proportional to 19 comes from the gluon loop, and it is grouped together with the 1 from the ghost loop. Then come the gluino and the last line are the contributions from the squark loop. Taking the UV limit replaces  $B_0$  by  $\Delta$

$$\delta Z_g \xrightarrow{\text{UV}} \frac{g_s^2}{(4\pi)^2} \left( \underbrace{-\frac{2}{3}n_{lf} + 5}_{-2C_A + \frac{11C_A - 2n_{lf}}{3}} - \frac{2}{3} - \frac{2}{3}N_c - \sum_{\tilde{q}} \frac{1}{6} \right) \Delta \quad (5.47)$$

where made use of

$$\dot{B}_0(0, m^2, m^2) = \frac{1}{6m^2} \quad (5.48)$$

$$\epsilon B_0(0, m^2, m^2) = 1 \quad (5.49)$$

and neglected terms of  $\mathcal{O}(\epsilon)$ . The special case in eq. (5.48) is the reason why there is no finite part for the light quarks in contrast to the heavy quarks. It is practical to define  $\beta_0$  for light and heavy particles

$$\beta_0^L = \frac{11C_A - 2n_{lf}}{3} \quad (5.50)$$

$$\beta_0^H = -\frac{2}{3} - \frac{2}{3}N_c - \sum_{\tilde{q}} \frac{1}{6}, \quad (5.51)$$

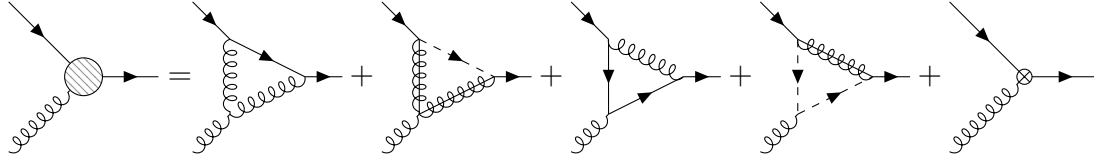
where  $n_{lf} = 5$  is the number of light quarks. This result is in agreement with the gluon wave-function renormalization given in [24] if we set  $\epsilon_{\text{UV}} = \epsilon_{\text{IR}}$  and consequently  $B_0(0, 0, 0) = 0$ .

### 5.2.2. Vertex corrections

In this segment we will look at the vertex corrections. Since they get a bit unhandy we focus on the UV divergent pieces whilst the full calculations are in appendix C.2.

### Quark-quark-gluon vertex

For the quark gluon vertex we get the SUSY contributions by replacing all loop particles with their superpartners.



$$(5.52)$$

The counterterm is expected to cancel the UV divergence and is constructed from the renormalization constants of involved particles and couplings

$$-\overline{\mathbf{UV}}[\Lambda] = \overline{\mathbf{UV}}[\Lambda_\times] = -ig_s T_{\beta\alpha}^a \gamma^\mu \delta_{IJ} \overline{\mathbf{UV}}[\delta Z_\alpha + \frac{1}{2}\delta Z_g + \delta Z_q]. \quad (5.53)$$

We explicitly give the divergence from our loop calculations

$$\overline{\mathbf{UV}}[\delta Z_\alpha + \frac{1}{2}\delta Z_g + \delta Z_q] \stackrel{!}{=} -\frac{g_s^2}{(4\pi)^2} T_R \left( 3C_A + C_A - \frac{1}{C_A} - \frac{1}{C_A} \right) \Delta \quad (5.54)$$

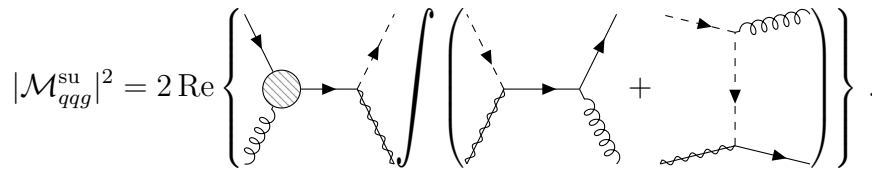
$$= -\frac{g_s^2}{(4\pi)^2} (C_A + 2C_F) \Delta \quad (5.55)$$

and using eq. (5.47) and eq. (5.31) gives us the divergence of the strong coupling renormalization constant

$$\overline{\mathbf{UV}}[\delta Z_\alpha] = \frac{g_s^2}{(4\pi)^2} (-C_A - 2C_F - \frac{1}{2}(-2C_A + \beta_0^L + \beta_0^H) + 2C_F) \Delta \quad (5.56)$$

$$= -\frac{g_s^2}{(4\pi)^2} \frac{\beta_0^L + \beta_0^H}{2} \Delta. \quad (5.57)$$

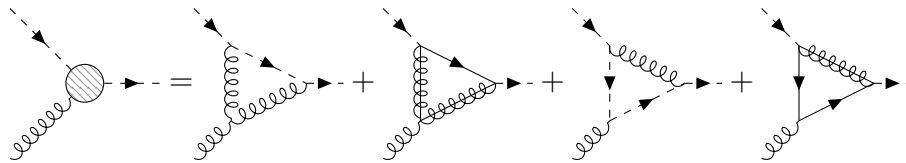
The UV divergence of the renormalization constant agrees with the ones presented in [9] and [24]. Again, the loop corrections to the  $qqg$ -vertex displayed must be combined with the two leading order diagrams



$$|\mathcal{M}_{qqg}^{\text{su}}|^2 = 2 \text{Re} \left\{ \left( \text{tree-level diagram} + \text{one-loop diagrams} \right) \right\}. \quad (5.58)$$

### Squark-squark-gluon vertex

The coupling of the gluon to a squark gets following NLO contributions



$$(5.59)$$

Looking at the UV divergence of these diagrams (cf. appendix C.2.2)

$$-\overline{\mathbf{UV}}[\Lambda] = \overline{\mathbf{UV}}[\Lambda_\times] = ig_s T_{\beta\alpha}^a (2p_1 + p_2)^\mu \delta_{ij} \overline{\mathbf{UV}}[\delta Z_\alpha + \frac{1}{2}\delta Z_g + \delta Z_{\tilde{q}}] \quad (5.60)$$

$$\overline{\mathbf{UV}}[\delta Z_\alpha + \frac{1}{2}\delta Z_g + \delta Z_{\tilde{q}}] \stackrel{!}{=} -\frac{g_s^2}{(4\pi)^2} T_R \left( \frac{3}{2}C_A + 2C_A - \frac{1}{C_A} - 2\frac{1}{C_A} - 2\frac{7}{4} \right) \Delta \quad (5.61)$$

$$= -\frac{g_s^2}{(4\pi)^2} C_A \Delta. \quad (5.62)$$

In the same fashion as for the  $qqg$  vertex, using the wave-function renormalization in eq. (5.47) and eq. (5.38) gives us the divergence of

$$\overline{\mathbf{UV}}[\delta Z_\alpha] = \frac{g_s^2}{(4\pi)^2} (-C_A - \frac{1}{2}(-2C_A + \beta_0^L + \beta_0^H)) \Delta \quad (5.63)$$

$$= -\frac{g_s^2}{(4\pi)^2} \frac{\beta_0^L + \beta_0^H}{2} \Delta \quad (5.64)$$

This is the same result as in previous chapter as it is expected. To include the loop corrections to the  $\tilde{q}\tilde{q}g$ -vertex the u-diagram with the loop gets connected to both Born diagrams

$$|\mathcal{M}_{\tilde{q}\tilde{q}g}^{\text{su}}|^2 = 2 \text{Re} \left\{ \int \left( \text{diagram 1} + \text{diagram 2} \right) \right\}. \quad (5.65)$$

### Quark-squark-gaugino vertex

The gaugino vertex gets only two loops

$$(5.66)$$

We compute the loop corrections to the  $q\tilde{q}\tilde{\chi}$ -vertex in appendix C.2.3. Since we do not renormalize the gaugino, the UV divergence must equal the difference of the quark  $\delta Z_q$  and squark  $\delta Z_{\tilde{q}}$  renormalization constants

$$-\overline{\mathbf{UV}}[\Lambda] = \overline{\mathbf{UV}}[\Lambda_\times] = ig_s (L'P_L + R'P_R) \overline{\mathbf{UV}}[\frac{1}{2}\delta Z_{\tilde{q}} + \frac{1}{2}\delta Z_q] \quad (5.67)$$



$$\overline{\mathbf{UV}}[\delta Z_{\tilde{q}} + \delta Z_q] = \overline{\mathbf{UV}}[\delta Z_q] = -\frac{g_s^2}{(4\pi)^2} 2C_F \Delta \quad (5.68)$$

And that is what we observe by looking at 5.31 and eq. (5.38). The vertex appears in both the s-channel and u-channel

$$|\mathcal{M}_{q\tilde{q}\chi}^{\text{su}}|^2 = 2 \text{Re} \left\{ \left( \text{diagram 1} + \text{diagram 2} \right) \int \left( \text{diagram 3} + \text{diagram 4} \right) \right\}. \quad (5.69)$$

### Gluino-gaugino-gluon vertex

The vertex of a gluino, gaugino and gluon does not appear at leading order or in the MSSM Lagrangian, but at higher orders it is realized as

$$\text{diagram} = \text{diagram 1} + \text{diagram 2} + \text{diagram 3} + \text{diagram 4}. \quad (5.70)$$

It therefore comes as no surprise that there are no UV divergences for all 4 diagrams combined, to be absorbed in counterterms.

$$|\mathcal{M}_{g\tilde{g}\chi}^{\text{su}}|^2 = 2 \text{Re} \left\{ \left( \text{diagram 1} \right) \int \left( \text{diagram 2} + \text{diagram 3} \right) \right\} \quad (5.71)$$

### 5.2.3. Boxes

The remaining potential diagrams for  $qg \rightarrow \tilde{\chi}\tilde{q}$  at the order of  $\mathcal{O}(\alpha_s^{3/2})$  are

$$\text{diagram} = \text{diagram 1} + \text{diagram 2} + \text{diagram 3} + \text{diagram 4} + \text{diagram 5} + \text{diagram 6} + \text{diagram 7} + \text{diagram 8}. \quad (5.72)$$

These box diagrams are combined, like all our virtuals, with both the s- and u-channel and no UV divergences remain.

$$|\mathcal{M}_{q\tilde{q}\chi g}^{\text{su}}|^2 = 2 \text{Re} \left\{ \left( \text{diagram 1} \right) \int \left( \text{diagram 2} + \text{diagram 3} \right) \right\} \quad (5.73)$$

### 5.2.4. Vertex counterterms

The counterterms for vertices follow directly from the wave-function renormalization constants calculated in the previous chapter. They will by definition cancel the UV poles since we chose the divergence of the running coupling that way. The running coupling however also gets a finite shift to decouple heavy particles such that only the gluon and five light quarks contribute to the running of  $\alpha_s$

$$\delta Z_{\alpha_s} = \frac{\alpha_s}{8\pi} \left[ -\frac{2}{3} \ln \frac{m_t^2}{\mu_R^2} - 2 \ln \frac{m_g^2}{\mu_R^2} - \frac{1}{6} \sum_{\bar{q}_i} \ln \frac{m_{\bar{q}_i}^2}{\mu_R^2} \right]. \quad (5.74)$$

This can be seen from the Slavnov-Taylor identities relating finite parts of the gluon  $\delta Z_g = -2\delta Z_{\alpha_s}$  to the coupling [9]. In our gluon renormalization eq. (5.46) we extracted the finite piece with the relation  $B_0(0, m^2, m^2) = \Delta - \ln \frac{m^2}{\mu^2}$  [54]. This procedure is called zero-momentum subtraction scheme in the literature [9] [24] and consistent with five-flavour  $\overline{\text{MS}}$  scheme used in parton distribution functions. We also have to include the finite SUSY restoring counterterms to our gaugino-squark-quark counterterm. They were already given in eq. (4.19).

### 5.2.5. Integrated dipoles

The integrated dipoles are defined through an insertion operator  $I$ .

$$\begin{aligned} \int d\sigma^A = & {}_m \langle 1, \dots, m | \mathbf{I}_{m+a+b}(\epsilon, \mu^2, \{p_i, m_i\}) | 1, \dots, m \rangle_m \\ & + \sum_{a'} \int_0^1 dx_{m,a'b} \langle 1, \dots, m; xp_a, p_b | K^{a,a'}(x) + P^{a,a'}(x, \mu_F^2) | 1, \dots, m; xp_a, p_b \rangle_{m,a'b} \\ & + \sum_{b'} \int_0^1 dx_{m,ab'} \langle 1, \dots, m; p_a, xp_b | K^{b,b'}(x) + P^{b,b'}(x, \mu_F^2) | 1, \dots, m; p_a, xp_b \rangle_{m,ab'} \end{aligned} \quad (5.75)$$

Where the operators  $\mathbf{K}$  and  $\mathbf{P}$  are finite collinear counterterms depending on the longitudinal momentum fraction  $x$ . The singular terms are included in  $\mathbf{I}$ :

$$\mathbf{I}_m(\epsilon, \mu_R^2; \{p_i, m_i\}) = -\frac{\alpha_s}{2\pi} \frac{(4\pi)^\epsilon}{\Gamma(1-\epsilon)} \sum_j \frac{1}{\mathbf{T}_j^2} \sum_{k \neq j} \mathbf{T}_j \mathbf{T}_k \quad (5.76)$$

$$\begin{aligned} & \left[ \mathbf{T}_j^2 \left( \frac{\mu^2}{s_{jk}} \right)^\epsilon \left( \nu_j(s_{jk}, m_j, m_k, m_F; \epsilon, \kappa) - \frac{\pi^2}{3} \right) \right. \\ & \left. + \Gamma_j(\mu, m_j, m_F; \epsilon) + \gamma_j(1 + \ln \frac{\mu^2}{s_{jk}}) + K_j + \mathcal{O}(\epsilon) \right] \end{aligned} \quad (5.77)$$

The finite constants  $\gamma_j$  and  $K_j$  as well as the dipole kernel functions  $\nu_j = \nu_j^S + \nu_j^{NS}$  can be found in the paper [38]. The parameters change with the use of different regularization

schemes [45]. However, there is no difference between CDR and HV schemes. This is also intuitively clear since we expect the procedure to kill all remaining  $\epsilon$  poles after renormalization and thereby the additional  $\mathcal{O}(\epsilon)$  terms from CDR do not contribute to the finite result. One also notices this in the different combinations of the leading order in the dipoles. The CDR LO can have terms of  $\mathcal{O}(\epsilon)$  whereas in HV this  $\epsilon$  is set to zero.

The evaluation of the integrated dipoles can again be summarized in a short table 7. It comes as no surprise that we already now these colour factors well from the unintegrated dipoles in our real correction.

Table 7: List of integrated dipoles for the virtual corrections.

Particle $j$	particle $k$	$s_{jk}$	colour $c = \langle \mathbf{T}_j \mathbf{T}_k \rangle$	Casimir $\mathbf{T}_j^2$
squark	quark	$2p_a p_1$	$\frac{T_R}{C_A}$	$C_F$
quark	squark	$2p_a p_1$	$\frac{T_R}{C_A}$	$C_F$
quark	gluon	$2p_a p_b$	$-T_R C_A$	$C_F$
gluon	quark	$2p_a p_b$	$-T_R C_A$	$C_A$
gluon	squark	$2p_b p_1$	$-T_R C_A$	$C_A$
squark	gluon	$2p_b p_1$	$-T_R C_A$	$C_F$

The collinear remainder  $\mathbf{P} + \mathbf{K}$  can be directly implemented from the aforementioned dipole formalism papers and was already included for our process in **Resummino**.

## 6. Numerical tests

Since such lengthy calculations carry a high probability of making of (most likely insignificant) mistakes, we will go through several (primarily numeric) tests and comparisons to ensure that the final results are correct. The specific SUSY scenario and mass spectrum should not matter in performing these checks. An obvious exception is the regularization and subtraction of on-shell resonances since they only appear for specific mass ordering.

### 6.1. Leading Order

We checked our new implementation of the leading order process against **SunderCalc**, **Prospino2**[63] and **MadGraph**[41]. The relative errors  $\Delta\sigma/\sigma$  in table 8 shows good agreement which is crucial for continuing with further tests.

Table 8: Relative errors between several programs calculating squark-electroweakino production.

Process $p + p \rightarrow$	SunderCalc	Resummino	MadGraph	Prospino2
$u + g \rightarrow \tilde{u}_L + \tilde{\chi}_1^0$	0%	0.02%	0.04%	0.03%
$d + g \rightarrow \tilde{d}_L + \tilde{\chi}_1^0$	0%	0.03%	0.01%	0.04%
$\bar{u} + g \rightarrow \tilde{\bar{u}}_L + \tilde{\chi}_1^0$	0%	0.04%	0.3%	0.03%
$\bar{d} + g \rightarrow \tilde{\bar{d}}_L + \tilde{\chi}_1^0$	0%	0.05%	0.05%	0.03%
$u + g \rightarrow \tilde{d}_L + \tilde{\chi}_1^+$	0%	0.02%	0.3%	0.01%
$d + g \rightarrow \tilde{u}_L + \tilde{\chi}_1^-$	0%	0.03%	0.05%	0.01%
$\bar{u} + g \rightarrow \tilde{\bar{d}}_L + \tilde{\chi}_1^-$	0%	0.04%	0.3%	0.01%
$\bar{d} + g \rightarrow \tilde{\bar{u}}_L + \tilde{\chi}_1^+$	0%	0.05%	0.04%	0.01%

#### 6.1.1. Polarized matrix element

We also expect the polarized matrix element to be consistent with our averaged calculation. To explicitly check this we only need to contract the tensor with  $-g^{\mu\nu}$  (the gluon polarization sum) and scale it with the values of table 3. For example in the SS case ( $\mathcal{M}_s \mathcal{M}_s^\dagger$ ) we get

$$-q^2(-4p_2p_b + m_2^2 - m_1^2 + 2p_a p_1) \quad (6.1)$$

after applying slightly modified momentum conservation  $-2p_2p_b + m_2^2 = m_1^2 - 2p_a p_1$  and including the omitted factors we get

$$q^2(2p_2p_b) \frac{2C_A C_F g_s^2 (R^2 + L^2)}{96s^2} = \langle \mathcal{M}_s \rangle^2 \quad (6.2)$$

ensuring us that the computation is consistent with eq. (3.16).

### 6.1.2. MadGraph

In the prompt after starting MG5\_aMC we enter

```
MG5_aMC> import model EWKino_NLO_UFO
MG5_aMC> generate p p > ul n1 QCD=1
MG5_aMC> output L0
MG5_aMC> launch
```

to get the production of a left-up-squark and a neutralino from the specified UFO model[24]. Now L0/Cards/param\_card.dat<sup>2</sup> needs to be set as well as the PDFs and the factorization scale in L0/Cards/run\_card.dat.

## 6.2. Real corrections

### 6.2.1. Dipole subtraction

We can check that the dipoles cancel the divergence of the real corrections point wise. In fig. 4 adding together the two most contributing dipoles (5+6) results in the same divergence as our real correction matrix element as  $p_t$  approaches 0. The fig. 5 shows a cancellation over 7-8 orders of magnitude. But with  $p_t$  getting too low we loose some cancellation due to numeric rounding errors, resulting in the peak at  $p_t \approx 0$ . This low contributing region where the cancellation does not work any more is excluded from our integration.

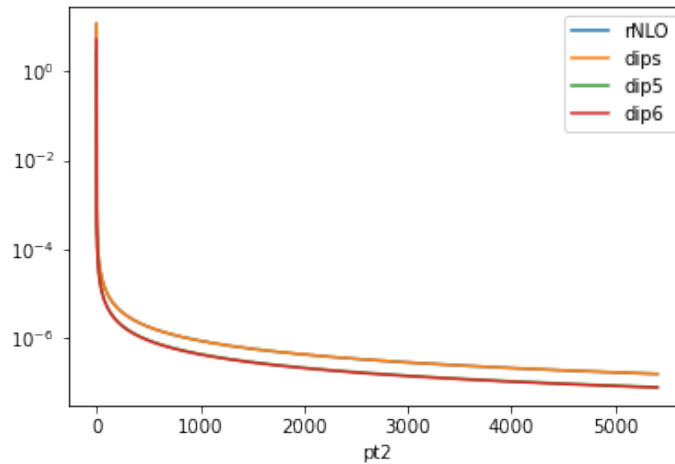


Figure 4: Divergence structure of an arbitrary phase space point as  $p_t$  goes to 0.

<sup>2</sup>MadGraph always need the decay data. It can be copied from the param\_card\_default.dat

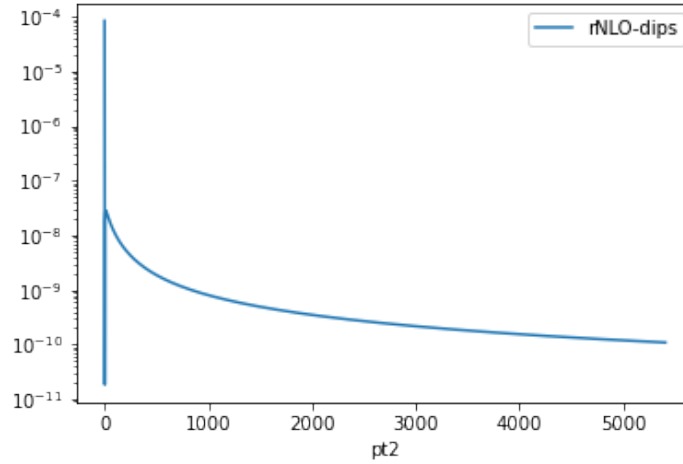


Figure 5: Point wise cancellation of IR divergence by subtracting the dipoles (dips) from the real matrix element (rNLO).

Let us look at the impact of the dipole subtraction on our integrated result. On the left side of fig. 6 we see that, without the dipole subtraction, going to a lower  $p_t$ -cut results in an increased cross-section. This is to be expected as we include more of the divergence displayed in fig. 4. If we now perform the dipole subtraction the divergence is eliminated and our result does not depend on the  $p_t$ -cut any more (right side).

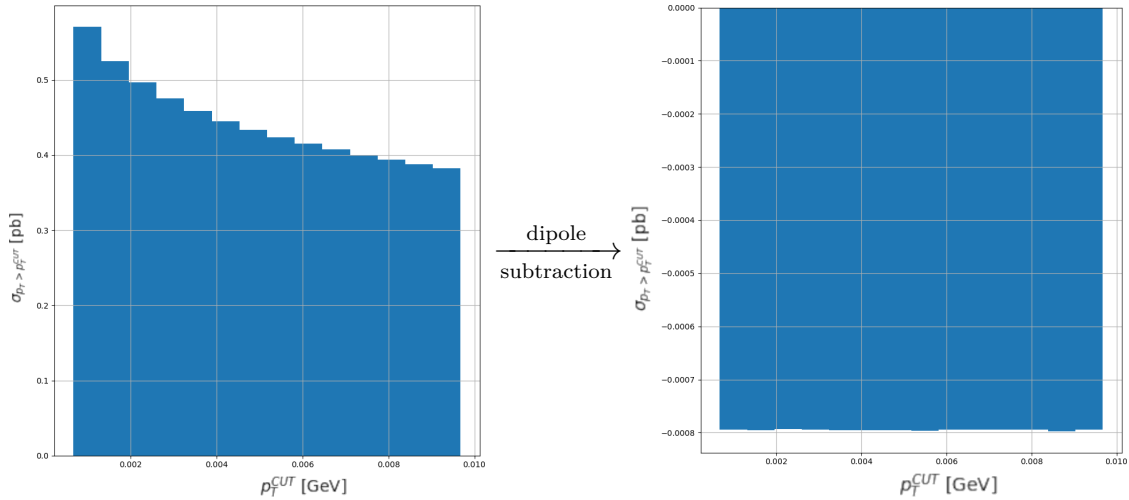


Figure 6: Integrated cross-section with varied  $p_t$ -cut. The left plot is just the real emission cross section without dipole subtraction. In the plot on the right the subtraction is enabled.

During checking our dipoles against other implementations we notice significant differences in the  $7 \times 4$  matrix used to combine the polarized dipoles (appendix D.1). But most of the elements do not contribute such that the final subtraction term and cross-section turn out to be the same.

### 6.2.2. On-shell subtraction

In fig. 7 and fig. 8 we see that our result does not depend (much) on the width  $\Gamma$ , even though the non-subtracted results differ significantly (orange, blue). The widths are  $\Gamma_{\tilde{q}} = m_{\tilde{q}} \cdot 10^{-2}$  and  $\Gamma_{\tilde{q}} = m_{\tilde{q}} \cdot 10^{-3}$ . They give roughly the same cross-section after the subtraction (red, green).

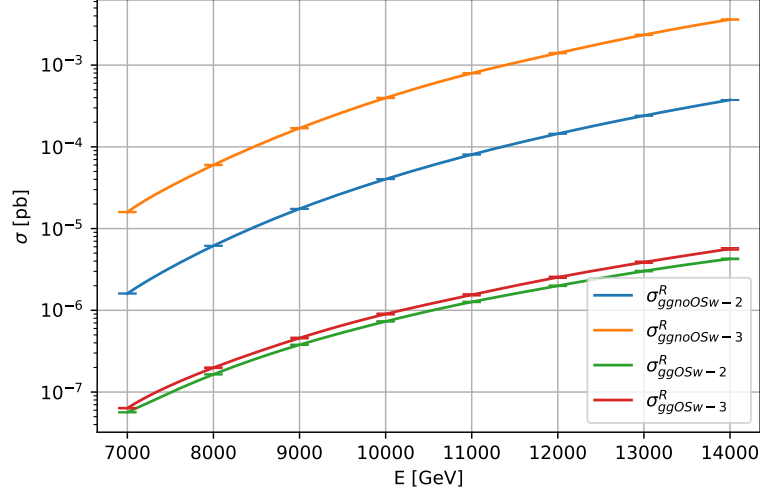


Figure 7: On shell subtraction with different widths in  $g + g \rightarrow \tilde{u}_L + \tilde{\chi}_2^0$

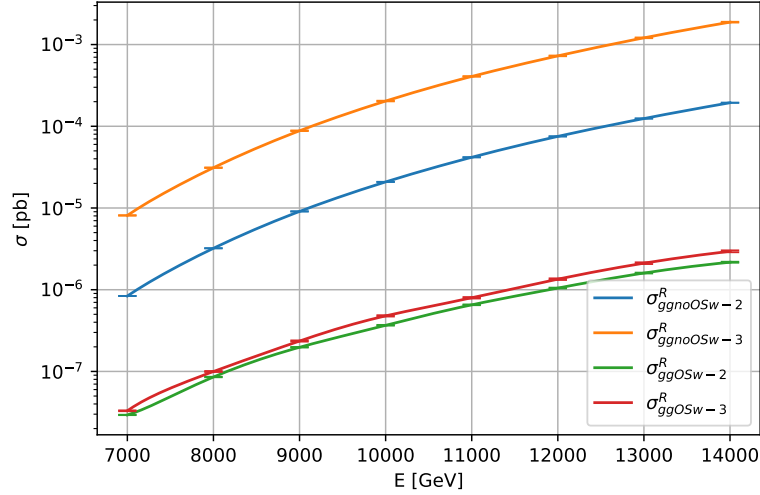


Figure 8: On shell subtraction with different widths in  $g + g \rightarrow \tilde{d}_L + \tilde{\chi}_1^+$

### 6.2.3. Total Reals

One interesting observation is a flipping of the sign in the total real correction when either the squark mass or hadronic center-of-mass energy is varied (fig. 9). We observed such a sign flip for all real corrections individually but at different masses. It is strongly related to the dipole and on-shell subtraction since we would expect the squared matrix

element to be positive. This was already observed in [9] with which we compare our computation. We use **SPheno**[64] to reproduce the spectrum SPS1a<sub>1000</sub> where the mass of the gluino is increased to 1 TeV from the original SPS1a of [65]. The parameters and masses are shown in table 9. Unfortunately LHAPDF[66] does no longer support the cteq6 set, nonetheless using CT14lo/CT14nlo gives good agreement as shown in fig. 9.

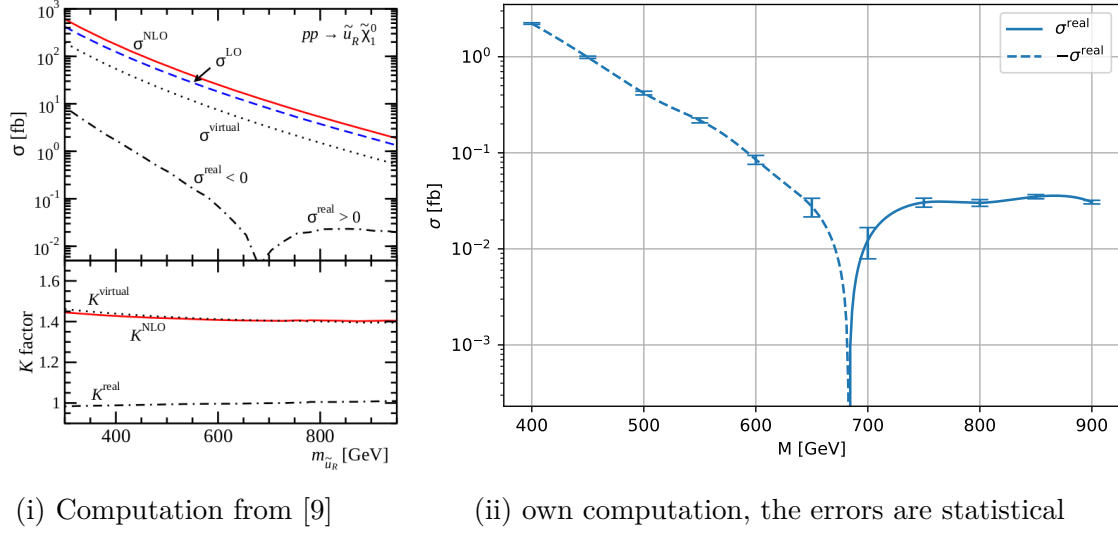


Figure 9: Sign flip of the real correction in  $pp \rightarrow \tilde{u}_R \chi_1^0$

Table 9: SPS1a<sub>1000</sub> parameter definitions [65] and resulting masses from **SPheno**. The gluino mass was manually increased to 1 TeV.

Parameter	$m_0$	$m_{1/2}$	$A_0$	$\tan \beta$	$\text{sign } \mu$
Value [GeV]	100	250	-100	$10\text{GeV}^{-1}$	+
Particle	$m_{\tilde{u}_R}$	$m_{\tilde{\chi}_1^0}$	$m_{\tilde{g}}$		
Mass [GeV]	550	97	1000		

## 6.3. Virtuals

### 6.3.1. Madgraph

To get only the virtual contributions from **MadGraph** `QCD=1` gets replaced by `[virt=QCD]`. For the s channel we force the intermediate particle to be an up-quark.

```
MG5_aMC> generate p p > u > ul n1 [virt=QCD]
```

Instead for the u channel we forbid up-quarks as the intermediate particle.

```
MG5_aMC> generate p p > ul n1 $$ u [virt=QCD]
```



In the resulting directory `SubProcesses/P0 Ug_*/loop_matrix.ps` we find a complete pictorial list of loop diagrams. To inspect a subset or single diagrams the parameter `-loop_filter='id==1 or id==2'` accepting a pythonic expression can be used and the ids come from the unfiltered list. `MadGraph` uses the axial gauge for the polarization sums of the gluon, and just a metric tensor  $g^{\mu\nu}$  for internal gluons

$$\sum_i \epsilon^{\mu*}(p) \epsilon^\nu(p) = -g^{\mu\nu} + \frac{p^\mu q^\nu + q^\mu p^\nu}{p \cdot q} - \frac{q^2 p^\nu p^\mu}{(p \cdot q)^2}. \quad (6.3)$$

If we want to know more details of the calculation we perform following changes in the generated process directory `SubProcesses/P0 Ug_*/`

#### **MadLoop5\_resources/MadLoopParams.dat:**

1. `MLReductionLib 1`, to use `CutTools`.
2. `CTModeRun 1`
3. `HelicityFilterLevel 0`
4. `DoubleCheckHelicityFilter .FALSE.`

#### **check\_sa.f:**

1. `READPS = .TRUE.`, if we want to use our own `PS.input` file.
2. `ML5_0_SLOOPMATRIX_THRES(P,MATELEM,...) →`  
`ML5_0_SLOOPMATRIXHEL_THRES(P,1,MATELEM,...)`, where 1 is the helicity id as specified in `ML5_0_HelConfigs.dat`.

#### **CT\_interface.f**

1. `WRITE(*,*) 'CutTools: Loop ID',ID,' =',RES(1),RES(2),RES(3)`, gets uncommented.

And in order to be sure that no UV counterterms are included, remove all UV and UVLOOP HELAS[42] calls from `helas_calls_ampb_1.f`. Then,

```
$ make && ./check
```

gives the poles (UV+IR combined) and finite loop results.

One remaining complication comes from the rational  $R_2$  term, defined as

$$R_2 = \lim_{\epsilon \rightarrow 0} \frac{1}{(2\pi)^4} \int d^d \bar{q} \frac{\tilde{N}}{\bar{D}_0 \bar{D}_1 \dots \bar{D}_{m-1}}, \quad (6.4)$$

where the loop denominators are given in  $d = 4 - 2\epsilon$  and the numerator in  $d - 4$  dimensions to transform the FDH scheme result to the HV scheme[44]. These finite contributions are already included in the model as `R2` counterterms and can not be reassigned to single loops. For our process they were calculated in [67]. Therefore, only a subset of loops corresponding to the  $R_2$  can be checked (they have the same `R2GC...` counterterm), unless we are sure the nominator of a single loop does not depend on  $\epsilon$ . If the nominator includes no  $\epsilon$ ,  $R_2$  can be ignored.

If we want to check the parametrization of the Passarino-Veltman tensors, we need to change the `vendor/CutTools/src/avh/avh_olo.f90` file in our `MadGraph` installation. By setting `punit=6` and recompiling `CutTools` we get more information on our loop integrals.

One remaining discrepancy between our computation and `MadGraph`'s individual diagram calculations is a factor of 2 in the finite and both divergent  $\epsilon$  pole contributions whenever a triple-gluon-vertex appears (and in the model counterterms). This is most likely related to the fixing of the gauge. The factor is not compatible with our integrated dipoles and counterterms.

We are however convinced in our computation being correct since the double divergent  $\epsilon^{-2}$  are regularization scheme independent and given as

$$\mathbf{I}_m(\epsilon, \mu^2; \{p_i, m_i\}) = \sum_j \frac{1}{\epsilon^2} \sum_{k \neq j} \mathbf{T}_j \mathbf{T}_k + \mathcal{O}(1/\epsilon) = -\frac{1}{\epsilon^2} \sum_j \mathbf{T}_j^2 + \mathcal{O}(1/\epsilon), \quad (6.5)$$

where  $j$  only runs over massless particles and we used colour conservation  $\sum_{k \neq j} \mathbf{T}_k = -\mathbf{T}_j$  and this is in agreement with our results.  $\mathbf{T}_j^2$  is just the quadratic Casimir operator in given particle's representation and consequently there is no colour correlation with the Born process [39].

### 6.3.2. Pole cancellation

First, we observe that our previously analytical calculated counterterms exactly cancel the UV contribution from our automatically constructed virtuals. The total IR poles (or after renormalization, the remaining  $\epsilon$  poles if we do not distinguish between UV and IR) must cancel against the poles from the integrated dipoles. As explained above the double poles are easier to check since they do not have a regularization scheme dependence and no conversion from different common prefactors (e.g.  $r_\Gamma$  or  $\Gamma(1 \pm \epsilon)$ ) needs to be considered. We confirm that all  $\epsilon$  poles get cancelled in our computation.

## 7. Results

Finally, we can obtain precise cross sections for squark electroweakino production with reasonable confidence in our computation. We average the final state masses for both the central renormalization and factorization scales  $\mu_0 = \mu_R = \mu_F = \frac{1}{2}(m_{\tilde{q}} + m_{\tilde{\chi}})$ . In fig. 10 we present our correction to the leading order process again for the parameters of [9] at 7 TeV LHC energy.

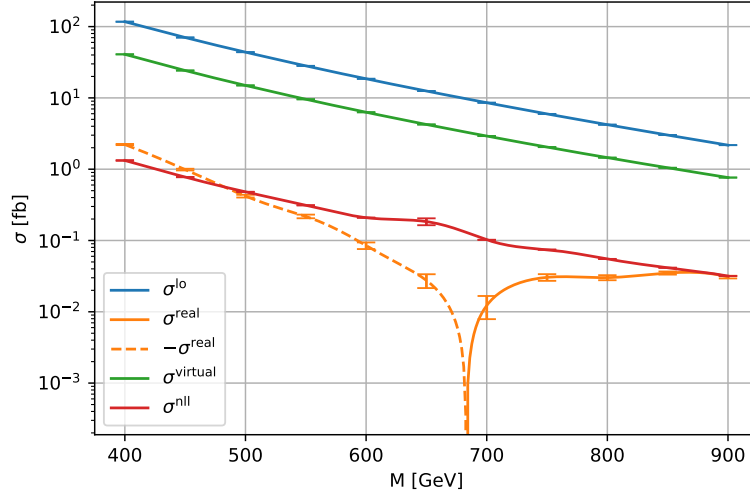


Figure 10: Cross section for  $pp \rightarrow \tilde{u}_R \chi_1^0$  at  $\sqrt{s} = 7$  TeV using CT14LO as the PDF. The SUSY spectrum is given in table 9. We vary the mass of the squark keeping the difference between left- and right-handed squark constant. The uncertainties stem from the convergence of our Monte-Carlo integration.

First looking at the virtuals we observe that our results are lower than our comparison result (fig. 9i) for a small squark mass of 400 GeV, but also in good agreement for 800 GeV. This is most likely due to using different PDFs. However, it could also be a difference coming from the collinear remainder  $\mathbf{P} + \mathbf{K}$ , which dominates the virtual corrections. The contribution from the resummation is of roughly the same order as our real corrections and should be included if one aims for a precision at the level of the reals. The MSSM parameterization SPS1a has however been excluded by the LHC 13 TeV data.

We present the result to a more recent exemplary best fit parameterization of the pMSSM from [6]. This parameterization includes constraints from LHC data at 13 TeV as well as PICO, XENON1T, PandaX-II and  $(g - 2)_\mu$  and is displayed with the resulting masses in table 10. The neutralino mass is small compared to the squark and gluino. By excluding the  $(g - 2)_\mu$  data the neutralino mass would get larger  $\sim 1$  TeV while the squark and gluino get reduced to  $\sim 1$  TeV and  $\sim 2$  TeV, respectively.

It must be emphasized that these results are preliminary. In fig. 11 we again vary the mass of our up-type squarks and as expected the cross section drops linearly on a logarithmic scale with increasing squark mass.

Table 10: Best fit MSSM parameters from [6] and resulting masses.

	$M_1$	$M_2$	$M_3$	$\tan \beta$	$\mu$	$m_{A_0}$	$A_{t,b,\tau}$	$M_{(U,D,Q)_{1,2}}$
[GeV]	252	254	-3861	36 GeV <sup>-1</sup>	1333	4015	2770	4044
	$M_{(U,D,Q)_3}$	$M_{(L,E)_{1,2}}$	$M_{(L,E)_3}$	$\Rightarrow$	$m_{\tilde{u}_R}$	$m_{\tilde{\chi}_1^0}$	$m_{\tilde{g}}$	
[GeV]	1667	351	465		4065	249	3901	

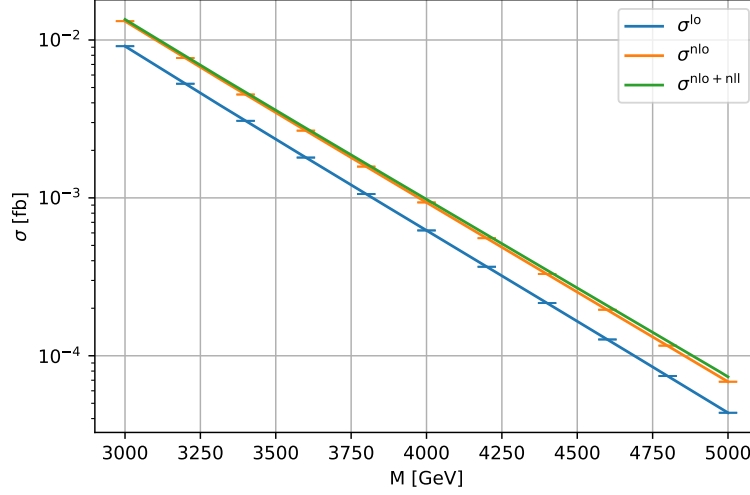


Figure 11: Cross section for  $pp \rightarrow \tilde{u}_R \chi_1^0$  at  $\sqrt{s} = 13$  TeV using CT14LO as the PDF. The SUSY spectrum is given in table 10. We vary the mass of the squark keeping the difference between left- and right-handed squark constant. The uncertainties come from the convergence of our Monte-Carlo integration.

If we rescale our cross sections by the leading order result

$$K = \frac{\sigma_{\text{NLO,NLO+NLL}}}{\sigma_{\text{LO}}} \quad (7.1)$$

we get the plot in fig. 12. Both relative NLO and NLO+NLL contributions rise with the squark mass. This is to be expected from threshold resummation since the phase space gets more restricted and the logarithmic remainders get even larger.

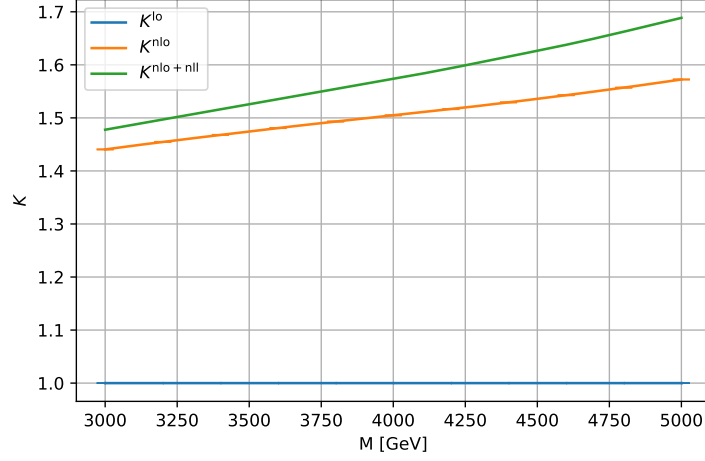


Figure 12:  $K$  for  $pp \rightarrow \tilde{u}_R \chi_1^0$  at  $\sqrt{s} = 13$  TeV using CT14LO as the PDF. The SUSY spectrum is given in table 10. We vary the mass of the squark keeping the difference between left- and right-handed squark constant. The uncertainties come from the convergence of our Monte-Carlo integration.

A better quantity than statistical Monte-Carlo uncertainties for the precision of a prediction comes from the dependence of the result on the unphysical renormalization and factorization scales. This is shown in fig. 13 where the scales are varied around the central scale  $\mu_0$ . In the first panel both scales are equal, whereas in the remaining plots one scale is fixed and the other is varied. We observe a clear improvement from LO to NLO. Apart from the point at  $\mu_F = 10\mu_0$  and  $\mu_R = 0.1\mu_0$  the inclusion of the NLL corrections reduces the variance of the cross sections even further. The general trend of our scale dependence is similar to that of [9].

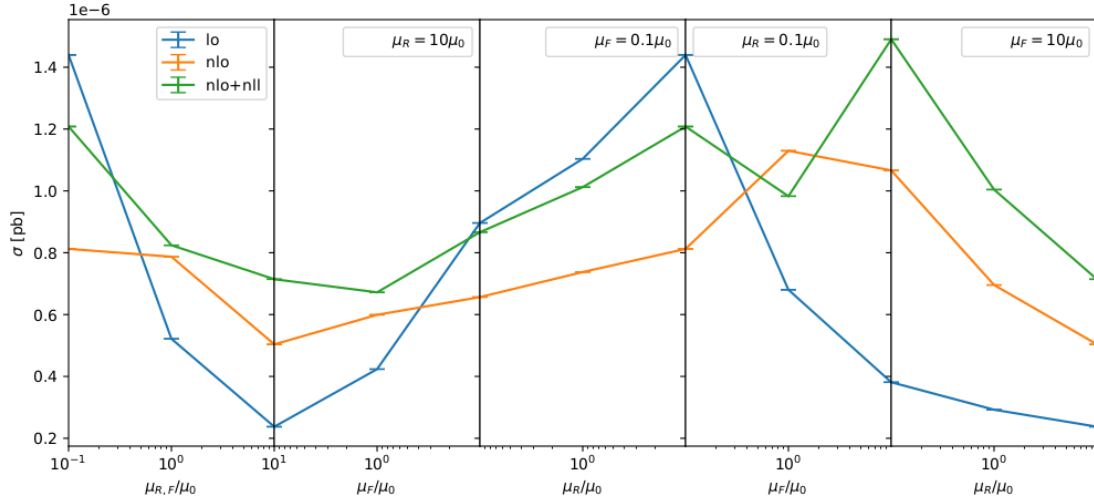


Figure 13: Profile of renormalization and factorization scale dependence of  $pp \rightarrow \tilde{u}_R \chi_1^0$  at  $\sqrt{s} = 13$  TeV using CT14LO as the PDF. The SUSY spectrum is given in table 10. The uncertainties come from the convergence of our Monte-Carlo integration.

## 8. Conclusion

We presented our next-to-leading order computation of squark electroweakino production and explained several methods to test our calculation. To the presented extent our computations agree with the results of alternatives, namely **Prospino2** and **MadGraph**. The necessity of the inclusion of threshold resummation for a highly restricted phase space was observed when we investigated a best fit pMSSM parametrization of a global fit of several experiments. Apart from the high complexity of combining all the methods outlined, we encountered no obstacle to moving to a fully automated calculation.

## 9. Outlook

In this work we focused on (re-)producing consistent results, but our actual code still is relatively slow and can be optimized. Most checks were performed for the dominating up-squark neutralino production case. Explicitly checking the chargino and mixed top-squark cases will ensure consistency in handling the couplings also beyond leading order.

Further performance improvements might be possible by splitting the virtual loops with a massive gluino which contribute less into a separate integration. To ensure that our results are correct I want to verify the calculation of the collinear remainder  $\mathbf{P} + \mathbf{K}$  as well as resummation ingredients, the soft anomalous dimension and hard matching coefficient.

After final optimization the main purpose of the investigation of precision predictions of squark electroweakino production, the exploration of phenomenological and experimental interesting regions, will become feasible for a large parameter space. The uncertainties presented in this thesis were all statistical uncertainties originating from the convergence of our Monte Carlo integration. A better and more physical uncertainty can be obtained through a variation of the scales. The impact of using different parton distribution functions on the NLO and NLL predictions should be explored in the future. The realization of listed refinements will be done at the start of my PhD.

## 10. References

- [1] B. Abi et al. “Measurement of the Positive Muon Anomalous Magnetic Moment to 0.46 ppm”. In: *Phys. Rev. Lett.* 126 (14 Apr. 2021), p. 141801. DOI: 10.1103/PhysRevLett.126.141801. URL: <https://link.aps.org/doi/10.1103/PhysRevLett.126.141801>.
- [2] S. Bilenky. “Neutrino oscillations: from an historical perspective to the present status”. In: (2016). DOI: 10.1016/j.nuclphysb.2016.01.025. eprint: [arXiv:1602.00170](https://arxiv.org/abs/1602.00170).
- [3] Martin Bauer and Tilman Plehn. *Yet Another Introduction to Dark Matter*. 2017. eprint: [arXiv:1705.01987](https://arxiv.org/abs/1705.01987).
- [4] CMS Collaboration. “Search for electroweak production of charginos and neutralinos in multilepton final states in proton-proton collisions at  $\sqrt{s} = 13$  TeV”. In: (2017). DOI: 10.1007/JHEP03(2018)166. eprint: [arXiv:1709.05406](https://arxiv.org/abs/1709.05406).
- [5] E. Aprile et al. “First Dark Matter Search Results from the XENON1T Experiment”. In: (2017). DOI: 10.1103/PhysRevLett.119.181301. eprint: [arXiv:1705.06655](https://arxiv.org/abs/1705.06655).
- [6] E. Bagnaschi et al. “Likelihood Analysis of the pMSSM11 in Light of LHC 13-TeV Data”. In: (2017). DOI: 10.1140/epjc/s10052-018-5697-0. eprint: [arXiv:1710.11091](https://arxiv.org/abs/1710.11091).
- [7] CERN Yellow Reports: Monographs. *CERN Yellow Reports: Monographs, Vol. 10 (2020): High-Luminosity Large Hadron Collider (HL-LHC): Technical design report*. en. 2020. DOI: 10.23731/CYRM-2020-0010. URL: <https://e-publishing.cern.ch/index.php/CYRM/issue/view/127>.
- [8] Christoph Englert et al. “Autofocusing searches in jets plus missing energy”. In: *Phys. Rev. D* 83 (9 May 2011), p. 095009. DOI: 10.1103/PhysRevD.83.095009. URL: <https://link.aps.org/doi/10.1103/PhysRevD.83.095009>.
- [9] T. Binoth et al. “Automized Squark-Neutralino Production to Next-to-Leading Order”. In: (2011). DOI: 10.1103/PhysRevD.84.075005. eprint: [arXiv:1108.1250](https://arxiv.org/abs/1108.1250).
- [10] J. Fiaschi and M. Klasen. “Neutralino/chargino pair production at NLO+NLL with resummation-improved PDFs for LHC Run II”. In: (2018). DOI: 10.1103/PhysRevD.98.055014. eprint: [arXiv:1805.11322](https://arxiv.org/abs/1805.11322).
- [11] Juri Fiaschi, Michael Klasen, and Marthijn Sunder. “Slepton pair production with aNNLO+NNLL precision”. In: *Journal of High Energy Physics* 2020.4 (Apr. 2020). DOI: 10.1007/jhep04(2020)049. URL: [https://doi.org/10.1007/jhep04\(2020\)049](https://doi.org/10.1007/jhep04(2020)049).
- [12] B. Fuks, M. Klasen, and M. Rothering. “Soft gluon resummation for associated gluino-gaugino production at the LHC”. In: (2016). DOI: 10.1007/JHEP07(2016)053. eprint: [arXiv:1604.01023](https://arxiv.org/abs/1604.01023).
- [13] Amit Chakraborty et al. “Monojet Signatures from Heavy Colored Particles: Future Collider Sensitivities and Theoretical Uncertainties”. In: (2018). DOI: 10.1140/epjc/s10052-018-6149-6. eprint: [arXiv:1805.05346](https://arxiv.org/abs/1805.05346).
- [14] *Search for electroweak production of charginos and neutralinos in proton-proton collisions at  $\sqrt{s}=13$  TeV*. Tech. rep. Geneva: CERN, 2021. URL: <http://cds.cern.ch/record/2752640>.
- [15] CMS Collaboration. “Search for direct top squark pair production in events with one lepton, jets, and missing transverse momentum at 13 TeV with the CMS experiment”. In: (2019). DOI: 10.1007/JHEP05(2020)032. eprint: [arXiv:1912.08887](https://arxiv.org/abs/1912.08887).

- 
- [16] Tilman Plehn. “Measuring the MSSM Lagrangean”. In: (2004). eprint: [arXiv:hep-ph/0410063](#).
  - [17] Sebastian A. R. Ellis and Bob Zheng. “Reaching for Squarks and Gauginos at a 100 TeV p-p Collider”. In: (2015). DOI: [10.1103/PhysRevD.92.075034](#). eprint: [arXiv:1506.02644](#).
  - [18] Lasse Kiesow. “Higher-order corrections for squark-gaugino production at the LHC”. MA thesis. Westfälische Wilhelms-Universität Münster, 2017. URL: [https://www.uni-muenster.de/imperia/md/content/physik\\_tp/theses/klasen/kiesow\\_msc.pdf](https://www.uni-muenster.de/imperia/md/content/physik_tp/theses/klasen/kiesow_msc.pdf).
  - [19] Benjamin Fuks et al. “Precision predictions for electroweak superpartner production at hadron colliders with Resummino”. In: (2013). DOI: [10.1140/epjc/s10052-013-2480-0](#). eprint: [arXiv:1304.0790](#).
  - [20] Stephen P. Martin. “A Supersymmetry Primer”. In: (1997). DOI: [10.1142/9789812839657\\_0001](#). eprint: [arXiv:hep-ph/9709356](#).
  - [21] Moritz Meinecke. “SUSY-QCD Corrections to the (Co)Annihilation of Neutralino Dark Matter within the MSSM”. dissertation. Westfälischen Wilhelms-Universität Münster, 2015. URL: [https://www.uni-muenster.de/imperia/md/content/physik\\_tp/theses/klasen/meinecke\\_phd.pdf](https://www.uni-muenster.de/imperia/md/content/physik_tp/theses/klasen/meinecke_phd.pdf).
  - [22] Marcel Rothering. “Precise predictions for supersymmetric particle production at the LHC”. dissertation. Westfälischen Wilhelms-Universität Münster, 2016. URL: [https://www.uni-muenster.de/imperia/md/content/physik\\_tp/theses/klasen/rothering\\_phd.pdf](https://www.uni-muenster.de/imperia/md/content/physik_tp/theses/klasen/rothering_phd.pdf).
  - [23] David Regalado Lamprea. “Precision computations for gaugino and scalar dark matter”. dissertation. Westfälischen Wilhelms-Universität Münster, 2018. URL: [https://www.uni-muenster.de/imperia/md/content/physik\\_tp/theses/klasen/rothering\\_phd.pdf](https://www.uni-muenster.de/imperia/md/content/physik_tp/theses/klasen/rothering_phd.pdf).
  - [24] Stefano Frixione et al. “Automated simulations beyond the Standard Model: supersymmetry”. In: (2019). DOI: [10.1007/JHEP12\(2019\)008](#). eprint: [arXiv:1907.04898](#).
  - [25] Sidney Coleman and Jeffrey Mandula. “All Possible Symmetries of the  $S$  Matrix”. In: *Phys. Rev.* 159 (5 July 1967), pp. 1251–1256. DOI: [10.1103/PhysRev.159.1251](#). URL: <https://link.aps.org/doi/10.1103/PhysRev.159.1251>.
  - [26] Rudolf Haag, Jan T. opuszaski, and Martin Sohnius. “All possible generators of supersymmetries of the S-matrix”. In: *Nuclear Physics B* 88.2 (Mar. 1975), pp. 257–274. DOI: [10.1016/0550-3213\(75\)90279-5](#). URL: [https://doi.org/10.1016/0550-3213\(75\)90279-5](https://doi.org/10.1016/0550-3213(75)90279-5).
  - [27] Benjamin Fuks. *Supersymmetry - When Theory Inspires Experimental Searches*. 2014. eprint: [arXiv:1401.6277](#).
  - [28] B. C. Allanach et al. “SUSY Les Houches Accord 2”. In: (2007). DOI: [10.1016/j.cpc.2008.08.004](#). eprint: [arXiv:0801.0045](#).
  - [29] Janusz Rosiek. “Complete set of Feynman rules for the MSSM – ERRATUM”. In: (1995). DOI: [10.1103/PhysRevD.41.3464](#). eprint: [arXiv:hep-ph/9511250](#).
  - [30] A. Denner et al. “Compact Feynman rules for Majorana fermions”. In: *Physics Letters B* 291.3 (Sept. 1992), pp. 278–280. DOI: [10.1016/0370-2693\(92\)91045-b](#). URL: [https://doi.org/10.1016/0370-2693\(92\)91045-b](https://doi.org/10.1016/0370-2693(92)91045-b).



- 
- [31] R. Kleiss, I. Malamos, and G. v. d. Oord. “Majoranized Feynman rules”. In: (2009). DOI: 10.1140/epjc/s10052-009-1158-0. eprint: [arXiv:0906.3388](#).
  - [32] J. Kuipers, T. Ueda, and J. A. M. Vermaseren. *Code Optimization in FORM*. 2013. eprint: [arXiv:1310.7007](#).
  - [33] Matthias Jamin and Markus E. Lautenbacher. “TRACER version 1.1”. In: 74.2 (Feb. 1993), pp. 265–288. DOI: 10.1016/0010-4655(93)90097-v. URL: [https://doi.org/10.1016/0010-4655\(93\)90097-v](https://doi.org/10.1016/0010-4655(93)90097-v).
  - [34] Vladyslav Shtabovenko, Rolf Mertig, and Frederik Orellana. “FeynCalc 9.3: New features and improvements”. In: (2020). DOI: 10.1016/j.cpc.2020.107478. eprint: [arXiv:2001.04407](#).
  - [35] Toichiro Kinoshita. “Mass Singularities of Feynman Amplitudes”. In: *Journal of Mathematical Physics* 3.4 (1962), pp. 650–677. DOI: 10.1063/1.1724268. eprint: <https://doi.org/10.1063/1.1724268>. URL: <https://doi.org/10.1063/1.1724268>.
  - [36] T. D. Lee and M. Nauenberg. “Degenerate Systems and Mass Singularities”. In: *Phys. Rev.* 133 (6B Mar. 1964), B1549–B1562. DOI: 10.1103/PhysRev.133.B1549. URL: <https://link.aps.org/doi/10.1103/PhysRev.133.B1549>.
  - [37] Stefano Catani and Michael H. Seymour. “A General Algorithm for Calculating Jet Cross Sections in NLO QCD”. In: (1996). DOI: 10.1016/S0550-3213(96)00589-5. eprint: [arXiv:hep-ph/9605323](#).
  - [38] Stefano Catani et al. “The Dipole Formalism for Next-to-Leading Order QCD Calculations with Massive Partons”. In: (2002). DOI: 10.1016/S0550-3213(02)00098-6. eprint: [arXiv:hep-ph/0201036](#).
  - [39] Stefano Catani, Stefan Dittmaier, and Zoltan Trocsanyi. “One-loop Singular Behaviour of QCD and SUSY QCD Amplitudes with Massive Partons”. In: (2000). DOI: 10.1016/S0370-2693(01)00065-X. eprint: [arXiv:hep-ph/0011222](#).
  - [40] G. Altarelli and G. Parisi. “Asymptotic freedom in parton language”. In: 126.2 (Aug. 1977), pp. 298–318. DOI: 10.1016/0550-3213(77)90384-4. URL: [https://doi.org/10.1016/0550-3213\(77\)90384-4](https://doi.org/10.1016/0550-3213(77)90384-4).
  - [41] J. Alwall et al. “The automated computation of tree-level and next-to-leading order differential cross sections, and their matching to parton shower simulations”. In: (2014). DOI: 10.1007/JHEP07(2014)079. eprint: [arXiv:1405.0301](#).
  - [42] H. Murayama, I. Watanabe, and Kaoru Hagiwara. “HELAS: HELicity amplitude subroutines for Feynman diagram evaluations”. In: (Jan. 1992).
  - [43] Adrian Signer and Dominik Stockinger. “Using Dimensional Reduction for Hadronic Collisions”. In: (2008). DOI: 10.1016/j.nuclphysb.2008.09.016. eprint: [arXiv:0807.4424](#).
  - [44] Celine Degrande. “Automatic evaluation of UV and R2 terms for beyond the Standard Model Lagrangians: a proof-of-principle”. In: (2014). DOI: 10.1016/j.cpc.2015.08.015. eprint: [arXiv:1406.3030](#).
  - [45] Stefano Catani, Michael H. Seymour, and Zoltán Trócsányi. “Regularization Scheme Independence and Unitarity in QCD Cross Sections”. In: (1996). DOI: 10.1103/PhysRevD.55.6819. eprint: [arXiv:hep-ph/9610553](#).
  - [46] William B. Kilgore. “Regularization Schemes and Higher Order Corrections”. In: (2011). DOI: 10.1103/PhysRevD.83.114005. eprint: [arXiv:1102.5353](#).

- 
- [47] C. Gnendiger et al. “To  $d$ , or not to  $d$ : recent developments and comparisons of regularization schemes”. In: *The European Physical Journal C* 77.7 (July 2017). DOI: 10.1140/epjc/s10052-017-5023-2. URL: <https://doi.org/10.1140/epjc/s10052-017-5023-2>.
  - [48] Zoltan Kunszt, Adrian Signer, and Zoltán Trócsányi. “One-loop helicity amplitudes for all  $2 \rightarrow 2$  processes in QCD and N=1 supersymmetric Yang-Mills theory”. In: (1993). DOI: 10.1016/0550-3213(94)90456-1. eprint: [arXiv:hep-ph/9305239](https://arxiv.org/abs/hep-ph/9305239).
  - [49] William B. Kilgore. “The Four Dimensional Helicity Scheme Beyond One Loop”. In: (2012). DOI: 10.1103/PhysRevD.86.014019. eprint: [arXiv:1205.4015](https://arxiv.org/abs/1205.4015).
  - [50] F. Jegerlehner. “Facts of life with gamma(5)”. In: (2000). DOI: 10.1007/s100520100573. eprint: [arXiv:hep-th/0005255](https://arxiv.org/abs/hep-th/0005255).
  - [51] T. Hahn and M. Perez-Victoria. “Automatized One-Loop Calculations in 4 and D dimensions”. In: (1998). DOI: 10.1016/S0010-4655(98)00173-8. eprint: [arXiv:hep-ph/9807565](https://arxiv.org/abs/hep-ph/9807565).
  - [52] G. 't Hooft and M. Veltman. “Scalar one-loop integrals”. In: *Nuclear Physics B* 153 (Jan. 1979), pp. 365–401. DOI: 10.1016/0550-3213(79)90605-9. URL: [https://doi.org/10.1016/0550-3213\(79\)90605-9](https://doi.org/10.1016/0550-3213(79)90605-9).
  - [53] G. Passarino and M. Veltman. “One-loop corrections for  $e+e^-$  annihilation into  $\mu+\mu^-$  in the Weinberg model”. In: *Nuclear Physics B* 160.1 (Nov. 1979), pp. 151–207. DOI: 10.1016/0550-3213(79)90234-7. URL: [https://doi.org/10.1016/0550-3213\(79\)90234-7](https://doi.org/10.1016/0550-3213(79)90234-7).
  - [54] K. Kovarik. “Hitchhikers guide to renormalization”. unpublished manuscript.
  - [55] Ansgar Denner. “Techniques for the calculation of electroweak radiative corrections at the one-loop level and results for W-physics at LEP200”. In: (2007). eprint: [arXiv:0709.1075](https://arxiv.org/abs/0709.1075).
  - [56] Matthew D. Schwartz. *Quantum Field Theory and the Standard Model*. Cambridge University Press, Mar. 2014. ISBN: 978-1-107-03473-0, 978-1-107-03473-0.
  - [57] S. Heinemeyer, H. Rzehak, and C. Schappacher. “Proposals for Bottom Quark/Squark Renormalization in the Complex MSSM”. In: (2010). DOI: 10.1103/PhysRevD.82.075010. eprint: [arXiv:1007.0689](https://arxiv.org/abs/1007.0689).
  - [58] Tilman Plehn. “Lectures on LHC Physics”. In: (2009). DOI: 10.1007/978-3-642-24040-9. eprint: [arXiv:0910.4182](https://arxiv.org/abs/0910.4182).
  - [59] S. Catani and L. Trentadue. “Resummation of the QCD perturbative series for hard processes”. In: *Nuclear Physics B* 327.2 (Nov. 1989), pp. 323–352. DOI: 10.1016/0550-3213(89)90273-3. URL: [https://doi.org/10.1016/0550-3213\(89\)90273-3](https://doi.org/10.1016/0550-3213(89)90273-3).
  - [60] P. Nogueira. “Automatic Feynman Graph Generation”. In: *Journal of Computational Physics* 105.2 (Apr. 1993), pp. 279–289. DOI: 10.1006/jcph.1993.1074. URL: <https://doi.org/10.1006/jcph.1993.1074>.
  - [61] Wolfgang Hollik, Jonas M. Lindert, and Davide Pagani. “NLO corrections to squark-squark production and decay at the LHC”. In: (2012). DOI: 10.1007/JHEP03(2013)139. eprint: [arXiv:1207.1071](https://arxiv.org/abs/1207.1071).
  - [62] Ryan Gavin et al. “Matching Squark Pair Production at NLO with Parton Showers”. In: (2013). DOI: 10.1007/JHEP10(2013)187. eprint: [arXiv:1305.4061](https://arxiv.org/abs/1305.4061).

- 
- [63] Tilman Plehn. *Prospino2*. URL: <https://www.thphys.uni-heidelberg.de/~plehn/index.php?show=prospino>.
  - [64] Werner Porod. “SPHeno, a program for calculating supersymmetric spectra, SUSY particle decays and SUSY particle production at  $e^+ e^-$  colliders”. In: (2003). DOI: 10.1016/S0010-4655(03)00222-4. eprint: [arXiv:hep-ph/0301101](https://arxiv.org/abs/hep-ph/0301101).
  - [65] B. C. Allanach et al. “The Snowmass Points and Slopes: Benchmarks for SUSY Searches”. In: (2002). DOI: 10.1007/s10052-002-0949-3. eprint: [arXiv:hep-ph/0202233](https://arxiv.org/abs/hep-ph/0202233).
  - [66] Andy Buckley et al. “LHAPDF6: parton density access in the LHC precision era”. In: (2014). DOI: 10.1140/epjc/s10052-015-3318-8. eprint: [arXiv:1412.7420](https://arxiv.org/abs/1412.7420).
  - [67] Hua-Sheng Shao and Yu-Jie Zhang. “Feynman Rules for the Rational Part of One-loop QCD Corrections in the MSSM”. In: (2012). DOI: 10.1007/s13130-012-4240-2. eprint: [arXiv:1205.1273](https://arxiv.org/abs/1205.1273).
  - [68] Malin Sjö Dahl. “ColorMath - A package for color summed calculations in  $SU(N_c)$ ”. In: (2012). DOI: 10.1140/epjc/s10052-013-2310-4. eprint: [arXiv:1211.2099](https://arxiv.org/abs/1211.2099).
  - [69] Roman Poya, Antonio J. Gil, and Rogelio Ortigosa. “A high performance data parallel tensor contraction framework: Application to coupled electro-mechanics”. In: *Computer Physics Communications* (2017). DOI: [http://dx.doi.org/10.1016/j.cpc.2017.02.016](https://doi.org/10.1016/j.cpc.2017.02.016). URL: <http://www.sciencedirect.com/science/article/pii/S0010465517300681>.
  - [70] Aaron Meurer et al. “SymPy: symbolic computing in Python”. In: *PeerJ Computer Science* 3 (Jan. 2017), e103. ISSN: 2376-5992. DOI: 10.7717/peerj-cs.103. URL: <https://doi.org/10.7717/peerj-cs.103>.
  - [71] *Catch2*. <https://github.com/catchorg/Catch2>. 2021.

## Appendix

### A. Feynman rules

All momenta go into the vertex. We adopt the generalized couplings and conventions from [22]:

- First Greek letters ( $\alpha, \beta, \dots$ ) denote fundamental colour indices.
- Middle Greek letters ( $\mu, \nu, \dots$ ) denote Lorentz indices.
- Lowercase beginning Latin letters ( $a, b, \dots$ ) refer adjoint colour indices.
- Uppercase middle Latin letters ( $I, J, \dots$ ) are generation indices.
- Lowercase middle Latin letters ( $i, j, \dots$ ) label sfermions.
- Lowercase middle Latin letters ( $k, \dots$ ) indicate different neutralinos or charginos.

#### A.1. Standard model

##### A.1.1. Propagators

$$\begin{aligned}
 \alpha \longrightarrow \beta &= \frac{i(\not{p} + m)}{p^2 - m^2} \delta_{\beta\alpha} \\
 \mu a \text{ wavy } \nu b &= \begin{cases} \frac{-i}{p^2} \delta_{ab} g_{\mu\nu} & \text{Feynman gauge} \\ \frac{-i}{p^2} \delta_{ab} (g_{\mu\nu} - \frac{n^\mu p^\nu + n^\nu p^\mu}{p \cdot n} + \frac{n^2 p^\nu p^\nu}{(p \cdot n)^2}) & \text{axial gauge, } n \cdot p \neq 0 \end{cases} \\
 a \text{ dashed } b &= \frac{i}{p^2} \delta_{ba}
 \end{aligned}$$

##### A.1.2. Vertices

$$\begin{aligned}
 \begin{array}{c} \text{Diagram: A vertex with three incoming wavy lines. The left line is labeled } g_a^\mu \text{ and } p_1. \text{ The top-right line is labeled } g_b^\nu \text{ and } p_2. \text{ The bottom-right line is labeled } g_c^\lambda \text{ and } p_3. \end{array} &= -g_s f_{abc} \Gamma^{\mu\nu\lambda} \\
 &= -g_s f_{abc} (g^{\mu\nu} (p_1 - p_2)^\lambda + g^{\nu\lambda} (p_2 - p_3)^\mu + g^{\mu\lambda} (p_3 - p_1)^\nu)
 \end{aligned}$$

$$\begin{aligned}
 \begin{array}{c} \text{Diagram: A vertex with two incoming wavy lines. The left line is labeled } q_{I\beta} \text{ and } g_a^\mu. \text{ The top-right line is labeled } \bar{q}_{J\alpha}. \end{array} &= -ig_s \gamma^\mu T_{\alpha\beta}^a \delta_{IJ} \\
 \begin{array}{c} \text{Diagram: A vertex with one incoming wavy line labeled } g_a^\mu \text{ and one incoming dashed line labeled } \bar{c}^c \text{ and } p. \text{ The outgoing dashed line is labeled } c^b. \end{array} &= g_s p^\mu f^{abc}
 \end{aligned}$$

## A.2. Minimal supersymmetric standard model

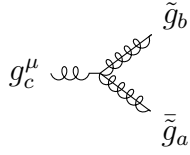
The displayed rules are a subset taken from the complete set [29].

### A.2.1. Propagators

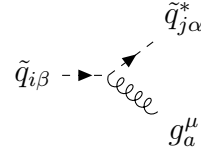
$$\alpha \text{ --- } \beta = \frac{i}{p^2 - m^2} \delta_{\alpha\beta}$$

$$a \text{ --- } b = \frac{i(\not{p} + m)}{p^2 - m^2} \delta_{ab}$$

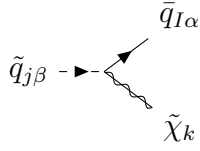
### A.2.2. Vertices



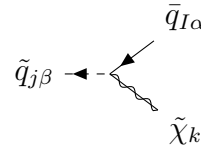
$$= -ig_s f_{abc} \gamma^\mu$$



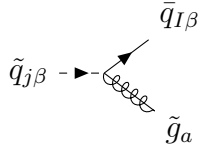
$$= ig_s (p_{\tilde{q}_\alpha}^\mu - p_{\tilde{q}_\beta}^\mu) T_{\alpha\beta}^a \delta_{ij}$$



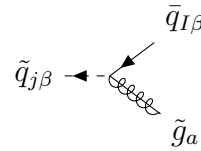
$$= i(L_{Ijk} P_L + R_{Ijk} P_R) \delta_{\alpha\beta}$$



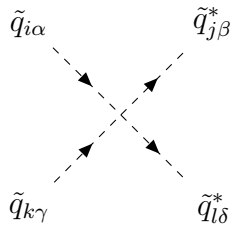
$$= i(L'_{Ijk} P_L + R'_{Ijk} P_R) \delta_{\alpha\beta}$$



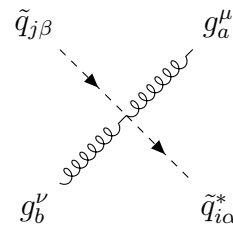
$$= ig_s (\mathcal{L}_{Ij} P_L + \mathcal{R}_{Ij} P_R) T_{\alpha\beta}^a$$



$$= ig_s (\mathcal{L}'_{Ij} P_L + \mathcal{R}'_{Ij} P_R) T_{\alpha\beta}^a$$



$$= -i(X_{ijkl} \delta_{\alpha\beta} \delta_{\gamma\delta} + Y_{ijkl} \delta_{\alpha\delta} \delta_{\gamma\beta} + Z_{ijkl} \delta_{\alpha\gamma} \delta_{\beta\delta})$$



$$= ig_s^2 (T^a T^b + T^b T^a)_{\alpha\beta} g^{\mu\nu} \delta^{ij}$$

## B. Polarized Born matrix element

Here we will compute the prefactors to the Polarized matrix element. At the end we also present the expressions in a format closely related to the actual implementation.<sup>3</sup> The matrix elements for squark gaugino production are

$$M_s = \bar{u}(p_2) i (LP_L + RP_R) i \left( \frac{\not{q}}{q^2} \right) (-i) g_s \gamma^\mu u(p_a) \epsilon^\mu (q - p_a) T_{a_3, a_1}^{b_1} \quad (\text{B.1})$$

$$M_s^\dagger = -\bar{u}(p_a) \gamma^\nu \left( \frac{\not{q}}{q^2} \right) i (L^* P_R + R^* P_L) i (-i) g_s u(p_2) \epsilon^{\nu*} (q - p_a) T_{a_3, a_1}^{b_1*} \quad (\text{B.2})$$

$$M_u = \bar{u}(p_2) i (LP_L + RP_R) u(p_a) (-i) g_s \frac{((p_a^\mu - p_2^\mu) - (-q^\mu + p_2^\mu)) i}{(p_a - p_2)^2 - M_U^2} \epsilon^\mu (q - p_1) T_{a_2, a_3}^{b_1} \quad (\text{B.3})$$

$$M_u^\dagger = -\bar{u}(p_a) i (L^* P_R + R^* P_L) u(p_2) (-i) g_s \frac{((p_a^\nu - p_2^\nu) - (-q^\nu + p_2^\nu)) i}{(p_a - p_2)^2 - M_U^2} \epsilon^{\nu*} (q - p_1) T_{a_2, a_3}^{b_1*}. \quad (\text{B.4})$$

In the following computations we are going to drop the  $\epsilon$  polarization since we want to calculate the polarized matrix element.

### B.1. SS case

Summing over spins gives the usual spinor trace

$$\sum_{\text{spin}} M_s M_s^\dagger = \text{Tr} \left[ (\not{p}_2 + m_2) (LP_L + RP_R) \left( \frac{\not{q}}{q^2} \right) \gamma^\mu \not{p}_a \gamma^\nu \left( \frac{\not{q}}{q^2} \right) (L^* P_R + R^* P_L) \right]. \quad (\text{B.5})$$

$$g_s^2 \epsilon^{\nu*} T_{a_3, a_1}^{b_1*} \epsilon^\mu T_{a_3, a_1}^{b_1} \quad (\text{B.6})$$

$$= \text{Tr} \left[ (\not{p}_2) (LP_L + RP_R) \left( \frac{\not{q}}{q^2} \right) \gamma^\mu \not{p}_a \gamma^\nu \left( \frac{\not{q}}{q^2} \right) (L^* P_R + R^* P_L) \right]. \quad (\text{B.7})$$

$$g_s^2 \epsilon^{\nu*} T_{a_3, a_1}^{b_1*} \epsilon^\mu T_{a_3, a_1}^{b_1}. \quad (\text{B.8})$$

We let Mathematica evaluate the expression to

$$\begin{aligned} \text{Tr} \left[ (\not{p}_2) (LP_L + RP_R) \left( \frac{\not{q}}{q^2} \right) \gamma^\mu \not{p}_a \gamma^\nu \left( \frac{\not{q}}{q^2} \right) (L^* P_R + R^* P_L) \right] = 2 \big( \\ L^2 \bar{q}^2 \bar{g}^{\text{munu}} (\cdot \overline{p_2 p_a}) - 2L^2 \bar{g}^{\text{munu}} (\cdot \overline{p_2 \bar{q}}) (\cdot \overline{p_a \bar{q}}) + R^2 \bar{q}^2 \bar{g}^{\text{munu}} (\cdot \overline{p_2 p_a}) - 2R^2 \bar{g}^{\text{munu}} (\cdot \overline{p_2 \bar{q}}) (\cdot \overline{p_a \bar{q}}) \\ + 2i (L^2 - R^2) \bar{q}^{\text{nu}} \bar{\epsilon}^{\text{munup} \overline{p_a \bar{q}}} - 2i (L^2 - R^2) \bar{q}^{\text{mu}} \bar{\epsilon}^{\text{nup} \overline{p_a \bar{q}}} - iL^2 \bar{q}^2 \bar{\epsilon}^{\text{munup} \overline{p_2 p_a}} \\ + 2iL^2 (\cdot \overline{p_a \bar{q}}) \bar{\epsilon}^{\text{munup} \overline{p_2 \bar{q}}} - L^2 \bar{q}^2 \bar{p}^{\text{mu}} \bar{p}^{\text{a nu}} - L^2 \bar{q}^2 \bar{p}^{\text{a mu}} \bar{p}^{\text{2 nu}} + 2L^2 \bar{q}^{\text{mu}} \bar{p}^{\text{a nu}} (\cdot \overline{p_2 \bar{q}}) \\ + 2L^2 \bar{p}^{\text{a mu}} \bar{q}^{\text{nu}} (\cdot \overline{p_2 \bar{q}}) + iR^2 \bar{q}^2 \bar{\epsilon}^{\text{munup} \overline{p_2 p_a}} - 2iR^2 (\cdot \overline{p_a \bar{q}}) \bar{\epsilon}^{\text{munup} \overline{p_2 \bar{q}}} - R^2 \bar{q}^2 \bar{p}^{\text{mu}} \bar{p}^{\text{a nu}} \\ - R^2 \bar{q}^2 \bar{p}^{\text{a mu}} \bar{p}^{\text{2 nu}} + 2R^2 \bar{q}^{\text{mu}} \bar{p}^{\text{a nu}} (\cdot \overline{p_2 \bar{q}}) + 2R^2 \bar{p}^{\text{a mu}} \bar{q}^{\text{nu}} (\cdot \overline{p_2 \bar{q}}) \big). \end{aligned} \quad (\text{B.9})$$

<sup>3</sup>The analytic calculations are given in  $p_a p_b \rightarrow p_1 p_2 p_3$  kinematic nomenclature. The implementation expressions however use  $p_1 p_2 \rightarrow k_1 k_2 k_3$ .

We only have to keep terms symmetric in  $\mu\nu$

$$\begin{aligned} \text{Tr} \left[ (\not{p}_2)(LP_L + RP_R)(\frac{\not{q}}{q^2})\gamma^\mu \not{p}_a \gamma^\nu (\frac{\not{q}}{q^2})(L^*P_R + R^*P_L) \right] = 2 \left( \right. \\ L^2 \bar{q}^2 \bar{g}^{\text{munu}} (\cdot \bar{p}_2 \bar{p}_a) - 2L^2 \bar{g}^{\text{munu}} (\cdot \bar{p}_2 \bar{q}) (\cdot \bar{p}_a \bar{q}) + R^2 \bar{q}^2 \bar{g}^{\text{munu}} (\cdot \bar{p}_2 \bar{p}_a) - 2R^2 \bar{g}^{\text{munu}} (\cdot \bar{p}_2 \bar{q}) (\cdot \bar{p}_a \bar{q}) \\ - L^2 \bar{q}^2 \bar{p}_2^{\text{mu}} \bar{p}_a^{\text{nu}} - L^2 \bar{q}^2 \bar{p}_a^{\text{mu}} \bar{p}_2^{\text{nu}} + 2L^2 \bar{q}^{\text{mu}} \bar{p}_a^{\text{nu}} (\cdot \bar{p}_2 \bar{q}) + 2L^2 \bar{p}_a^{\text{mu}} \bar{q}^{\text{nu}} (\cdot \bar{p}_2 \bar{q}) \\ \left. - R^2 \bar{q}^2 \bar{p}_2^{\text{mu}} \bar{p}_a^{\text{nu}} - R^2 \bar{q}^2 \bar{p}_a^{\text{mu}} \bar{p}_2^{\text{nu}} + 2R^2 \bar{q}^{\text{mu}} \bar{p}_a^{\text{nu}} (\cdot \bar{p}_2 \bar{q}) + 2R^2 \bar{p}_a^{\text{mu}} \bar{q}^{\text{nu}} (\cdot \bar{p}_2 \bar{q}) \right) \quad (\text{B.10}) \end{aligned}$$

and can determine the prefactors to our vector of Lorentz tensors (here without the common prefactors  $2g_s^2(L^2 + R^2)C_A C_F$  and the propagator denominator).

$$\begin{aligned} g^{\mu\nu} &\rightarrow p_2 \cdot p_a q^2 - 2p_2 \cdot q p_a \cdot q = q^2 (p_2 p_a - p_2 q) \\ &= q^2 \left( p_2 p_a - \left( m_2^2 + p_2 p_1 + \frac{1}{2} m_1^2 - \frac{1}{2} m_1^2 \right) \right) \\ &= q^2 \left( p_2 p_a - \frac{1}{2} (q^2 + \Delta M^2) \right) = \frac{1}{2} - \text{Q2} * (\text{Dn\_k2mp1\_MQ+Q2}) \quad (\text{B.11}) \end{aligned}$$

$$p_a^\mu p_a^\nu \rightarrow 0 \quad (\text{B.12})$$

$$q^\mu q^\nu \rightarrow 0 \quad (\text{B.13})$$

$$p_1^\mu p_1^\nu \rightarrow 0 \quad (\text{B.14})$$

$$p_a^\mu q^\nu + p_a^\nu q^\mu \rightarrow 2p_2 q - q^2 = q^2 + \Delta M^2 - q^2 = \frac{1}{2} 2 * \text{dM2o} \quad (\text{B.15})$$

$$p_a^\mu p_1^\nu + p_a^\nu p_1^\mu \rightarrow +q^2 = \frac{1}{2} 2 * \text{Q2} \quad (\text{B.16})$$

$$q^\mu p_1^\nu + q^\nu p_1^\mu \rightarrow 0 \quad (\text{B.17})$$

## B.2. UU case

The u channel squared case is fully analog to previous SS case.

$$\begin{aligned} \sum_{\text{spin}} M_u M_u^\dagger &= \text{Tr} \left[ (\not{p}_2 + m_2)(LP_L + RP_R)(\not{p}_a)(L^*P_R + R^*P_L) \right] \epsilon^{\nu*}(q - p_1) \epsilon^\mu(q - p_1) \\ &\quad \frac{((p_a^\mu - p_2^\mu) - (-q^\mu + p_2^\mu))((p_a^\nu - p_2^\nu) - (-q^\nu + p_2^\nu))}{(p_a - p_2)^2 - M_U^2} \frac{T_{a_2, a_3}^{b_1} {}^* T_{a_2, a_3}^{b_1}}{(p_a - p_2)^2 - M_U^2} g_s^2 \quad (\text{B.18}) \end{aligned}$$

Where the trace gives

$$\text{Tr} \left[ (\not{p}_2 + m_2)(LP_L + RP_R)(\not{p}_a)(L^*P_R + R^*P_L) \right] = 2(L^2 + R^2)(\cdot \bar{p}_2 \bar{p}_a) \quad (\text{B.19})$$

and the momenta from the squark-squark-gluon vertices simplify to

$$((p_a^\mu - p_2^\mu) - (-q^\mu + p_2^\mu))((p_a^\nu - p_2^\nu) - (-q^\nu + p_2^\nu)) = (p_a + 2p_1 - q)^\mu (p_a + 2p_1 - q)^\nu. \quad (\text{B.20})$$

In the end we have following prefactors to the Lorentz-tensors.

$$g^{\mu\nu} \rightarrow 0 \quad (\text{B.21})$$

$$p_a^\mu p_a^\nu \rightarrow p_2 p_a = \text{P1K2} \quad (\text{B.22})$$

$$q^\mu q^\nu \rightarrow p_2 p_a = \text{P1K2} \quad (\text{B.23})$$

$$p_1^\mu p_1^\nu \rightarrow 4 p_2 p_a = 4 * \text{P1K2} \quad (\text{B.24})$$

$$p_a^\mu q^\nu + p_a^\nu q^\mu \rightarrow -p_2 p_a = -\text{P1K2} \quad (\text{B.25})$$

$$p_a^\mu p_1^\nu + p_a^\nu p_1^\mu \rightarrow 2 p_2 p_a = 2 * \text{P1K2} \quad (\text{B.26})$$

$$q^\mu p_1^\nu + q^\nu p_1^\mu \rightarrow -2 p_2 p_a = -2 * \text{P1K2} \quad (\text{B.27})$$

### B.3. SU case

The evaluation for the interference term is again the same procedure.

$$\sum_{\text{spin}} M_s M_u^\dagger = \text{Tr} \left[ (\not{p}_2 + m_2) (L P_L + R P_R) \left( \frac{\not{q}}{q^2} \right) \gamma^\mu \not{p}_a (L^* P_R + R^* P_L) \right] \\ \frac{((p_a^\nu - p_2^\nu) - (-q^\nu + p_2^\nu))}{(p_a - p_2)^2 - M_U^2} \epsilon^{\nu*} (q - p_1) T_{a_2, a_3}^{b_1} \epsilon^\mu (q - p_a) T_{a_3, a_1}^{b_1} g_s^2 \quad (\text{B.28})$$

With the trace

$$\text{Tr} \left[ (\not{p}_2 + m_2) (L P_L + R P_R) \left( \frac{\not{q}}{q^2} \right) \gamma^\mu \not{p}_a (L^* P_R + R^* P_L) \right] = \\ 2 \left( L^2 + R^2 \right) (\overline{p}^{\text{mu}} (-\cdot \overline{p} a \overline{q})) + \overline{q}^{\text{mu}} (\cdot \overline{p} 2 \overline{p} a) + \overline{p} a^{\text{mu}} (\cdot \overline{p} 2 \overline{q}) + 2i \left( L^2 - R^2 \right) \epsilon^{\text{mup} 2 \overline{p} a \overline{q}} \quad (\text{B.29})$$

and the imaginary antisymmetric  $\epsilon$  term can be dropped due to symmetry and being imaginary. Simplification of the momenta gives

$$((p_a^\nu - p_2^\nu) - (-q^\nu + p_2^\nu)) = (p_a + 2p_1 - q)^\nu. \quad (\text{B.30})$$

We must symmetrize the resulting expression in  $\mu\nu$ . Since the dipole is symmetric, any antisymmetric contributions from pol. Born vanishes. We also multiply by 2 since it is an interference term. We do this computation first for generic prefactors  $X$  and  $Y$  and add a purely antisymmetric  $R$  such that our expression is symmetric.

$$X p_a^\mu q^\nu + Y p_a^\nu q^\mu = (X + R) p_a^\mu q^\nu + (Y - R) p_a^\nu q^\mu \quad (\text{B.31})$$

$$X + R \stackrel{!}{=} (Y - R) \implies X - Y = -2R \implies X + R = Y - R = \frac{X + Y}{2} \quad (\text{B.32})$$

With this result the prefactors can be determined:

$$g^{\mu\nu} \rightarrow 0 \quad (\text{B.33})$$

$$p_a^\mu p_a^\nu \rightarrow 2 p_2 q = \Delta M^2 + q^2 = \frac{1}{2} 2 * (\text{Q2} + \text{dM2o}) \quad (\text{B.34})$$

$$q^\mu q^\nu \rightarrow -2 (-p_a q + p_2 p_a) = q^2 - 2 p_a p_2 = \frac{1}{2} 2 * (\text{Q2} - 2 * \text{P1K2}) \quad (\text{B.35})$$

$$p_1^\mu p_1^\nu \rightarrow 2 \cdot 2 p_a q = 2 q^2 = \frac{1}{2} 4 * \text{Q2} \quad (\text{B.36})$$



$$\begin{aligned}
p_a^\mu q^\nu + p_a^\nu q^\mu &\rightarrow 2\frac{1}{2}((-p_2q) + (-p_aq + p_2p_a)) = -\frac{1}{2}(\Delta M^2 + q^2) + \left(-\frac{1}{2}q + p_2p_a\right) \\
&= -q^2 - \frac{1}{2}\Delta M^2 + p_2p_a = \frac{1}{2}(-2*Q2-Dn\_k2mp1\_MQ)
\end{aligned} \tag{B.37}$$

$$p_a^\mu p_1^\nu + p_a^\nu p_1^\mu \rightarrow 2\frac{1}{2}(2p_2q + p_aq) = \Delta M^2 + q^2 + \frac{1}{2}q^2 = \frac{1}{2}(3*Q2+2*dM2o) \tag{B.38}$$

$$q^\mu p_1^\nu + q^\nu p_1^\mu \rightarrow 2\frac{1}{2}(2(-p_aq + p_2p_a) - p_aq) = \frac{1}{2}(-3q^2 + 4p_2p_a) = \frac{1}{2}(-3*Q2+4*P1K2) \tag{B.39}$$

## C. Virtual corrections

Many of these corrections are closely related to the computations in [18], however we include several fixes and missing diagrams. We also use the definition

$$\mu^{4-D} \int \frac{d^D l}{(2\pi)^D} = \frac{i}{16\pi^2} \int_l. \tag{C.1}$$

In the last segment (appendix C.4) we will present our `FeynCalc` to compute all the virtuals automatically.

### C.1. Self energies

#### C.1.1. Quark self energies

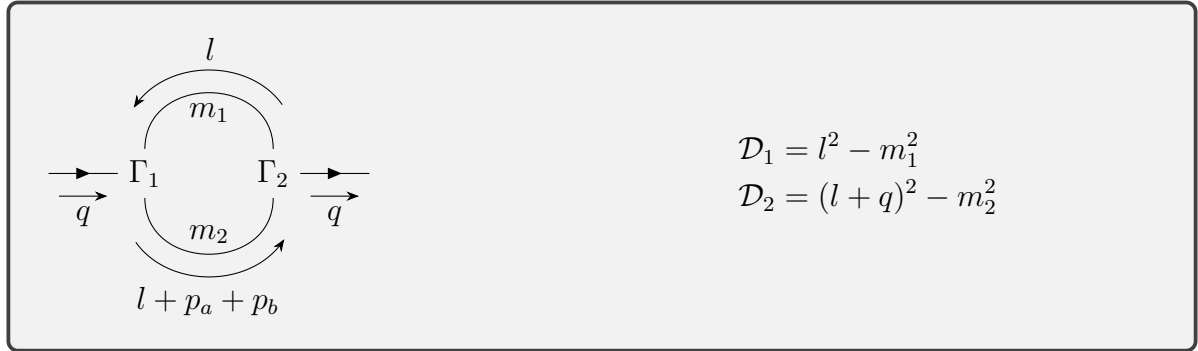
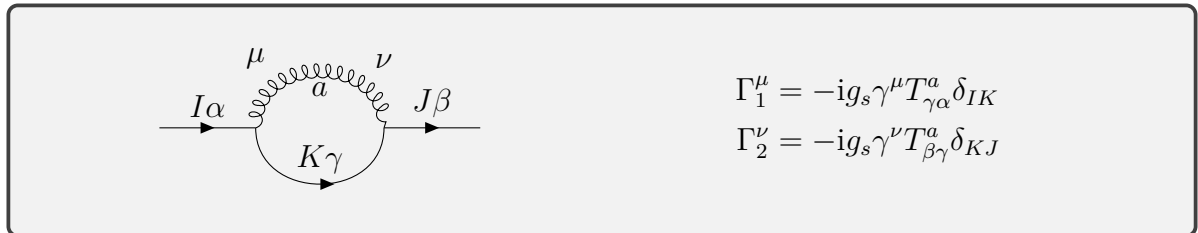


Figure 14: Parametrization of the  $q$  self energy

#### Gluon-quark loop



$$-i\Sigma_{\beta\alpha}(q^2, m_q^2, 0) \quad (C.2)$$

$$= \mu^{4-D} \int \frac{d^D l}{(2\pi)^D} \Gamma_2^\nu \frac{i(\not{l} + \not{q} + m_q)}{\mathcal{D}_2} \Gamma_1^\mu \frac{-ig_{\mu\nu}}{\mathcal{D}_1} \quad (C.3)$$

$$= -\frac{ig_s^2}{(4\pi)^2} T_{\beta\gamma}^a T_{\gamma\alpha}^a \int_l \frac{\gamma^\mu (\not{l} + \not{q}) \gamma^\mu + Dm_q}{\mathcal{D}_1 \mathcal{D}_2} \quad (C.4)$$

$$= -\frac{ig_s^2}{(4\pi)^2} C_F \delta_{\beta\alpha} \int_l \frac{(2-D)(\not{l} + \not{q}) + Dm_q}{\mathcal{D}_1 \mathcal{D}_2} \quad (C.5)$$

$$= -\frac{ig_s^2}{(4\pi)^2} C_F \delta_{\beta\alpha} ((2-D)(\gamma^\mu B^\mu) + Dm_q B_0) \quad (C.6)$$

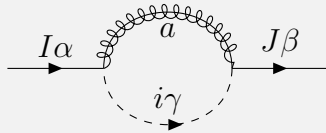
$$= -\frac{ig_s^2}{(4\pi)^2} C_F \delta_{\beta\alpha} ((2-D)\not{q}(-B_1) + Dm_q B_0) \quad (C.7)$$

$$= -\frac{ig_s^2}{(4\pi)^2} C_F \delta_{\beta\alpha} ((4-D-2)\not{q}(-B_1) + (D-4+4)m_q B_0) \quad (C.8)$$

$$= -\frac{ig_s^2}{(4\pi)^2} C_F \delta_{\beta\alpha} (\not{q}(2B_1 + 1) + m_q(4B_0 - 2)) \quad (C.9)$$

Where we inserted eq. (E.6) for the colour algebra, used  $\gamma$ -matrices in  $D$  dimensions eq. (E.12) and applied the tensor reduction of  $B_1$  eq. (E.17). In the last step the multiplication with  $2\epsilon = (D-4)$  is taken from table 11.

### Gluino-squark loop



$$\Gamma_1 = ig_s(\mathcal{L}'P_L + \mathcal{R}'P_R)_{Ii}T_{\gamma\alpha}^a$$

$$\Gamma_2 = ig_s(\mathcal{L}P_L + \mathcal{R}P_R)_{Ji}T_{\beta\gamma}^a$$

$$-i\Sigma_{\beta\alpha}(q^2, m_{\tilde{g}}^2, m_{\tilde{q}}^2) \quad (C.10)$$

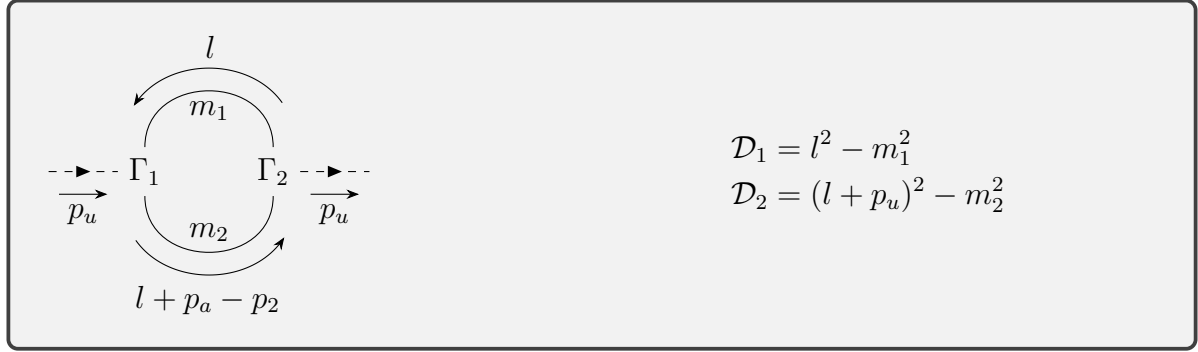
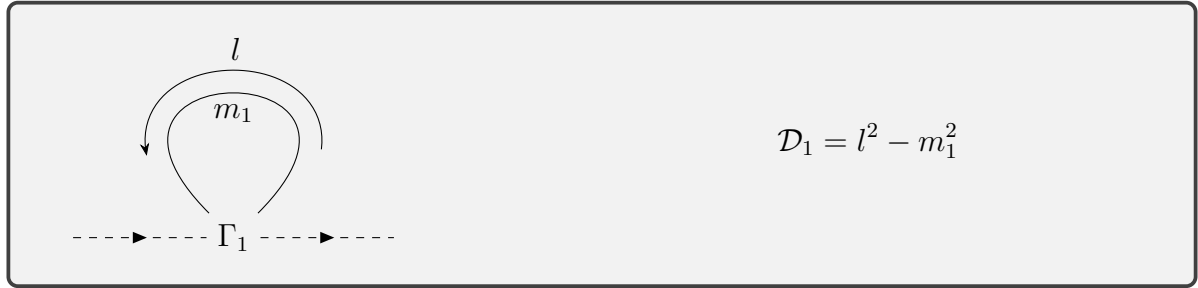
$$= \mu^{4-D} \int \frac{d^D l}{(2\pi)^D} \Gamma_2 \frac{i(-\not{l} + m_{\tilde{g}})}{\mathcal{D}_1} \Gamma_1 \frac{i}{\mathcal{D}_2} \quad (C.11)$$

$$= \frac{ig_s^2}{(4\pi)^2} C_F \delta_{\beta\alpha} \left( -(\mathcal{L}\mathcal{R}'P_L + \mathcal{R}\mathcal{L}'P_R)\not{q}B_1 + (\mathcal{L}\mathcal{L}'P_L + \mathcal{R}\mathcal{R}'P_R)m_{\tilde{g}}B_0 \right) \quad (C.12)$$

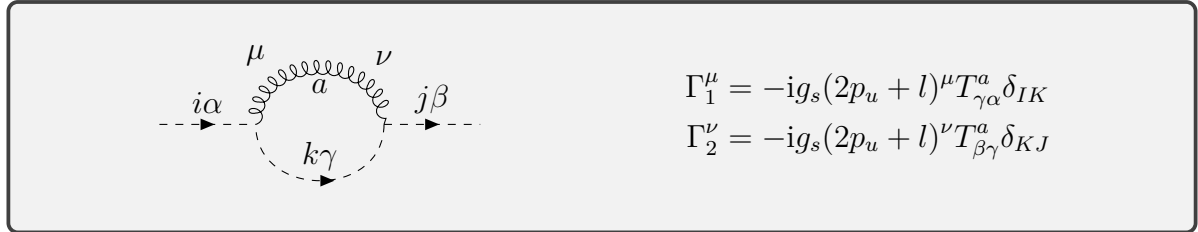
$$= -\frac{ig_s^2}{(4\pi)^2} C_F \delta_{\beta\alpha} (\mathcal{L}_{Ii}\mathcal{R}'_{Ii}P_L + \mathcal{R}_{Ii}\mathcal{L}'_{Ii}P_R)\not{q}B_1 \quad (C.13)$$

The terms proportional to the single  $m_{\tilde{g}}$  can be dropped for minimal squark mixing (See eq. (2.14)). Furthermore for massless quarks the restriction  $I = J$  applies since then there are no off-diagonal elements in the squark mixing matrix.

## C.1.2. Squark self energies

Figure 15: Parametrization of the  $\tilde{q}$  self energyFigure 16: Parametrization of the  $\tilde{q}$  self energy with 4 point vertices

## Gluon-squark loop



$$-i\Sigma_{\beta\alpha}(p_u^2, 0, m_{\tilde{q}_i}) \quad (C.14)$$

$$= \mu^{4-D} \int \frac{d^D l}{(2\pi)^D} \Gamma_2^\nu \frac{i}{\mathcal{D}_2} \Gamma_1^\mu \frac{-ig_{\mu\nu}}{\mathcal{D}_1} \quad (C.15)$$

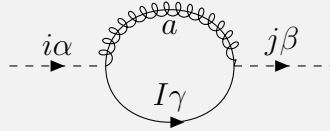
$$= -\frac{ig_s^2}{(4\pi)^2} C_F \delta_{ij} \delta_{\beta\alpha} \int_l \frac{(2p_u + l)^2}{\mathcal{D}_1 \mathcal{D}_2} \quad (C.16)$$

$$= -\frac{ig_s^2}{(4\pi)^2} C_F \delta_{ij} \delta_{\beta\alpha} (4(B_0 + B_1)p_u^2 + B^{\mu\mu}) \quad (C.17)$$

$$= -\frac{ig_s^2}{(4\pi)^2} C_F \delta_{ij} \delta_{\beta\alpha} (4(B_0 + B_1)p_u^2 + A_0(m_{\tilde{q}_i}^2)) \quad (\text{C.18})$$

$$= -\frac{ig_s^2}{(4\pi)^2} C_F \delta_{ij} \delta_{\beta\alpha} (2B_0 p_u^2 + 2m_{\tilde{q}}^2 B_0 - A_0(m_{\tilde{q}_i}^2)) \quad (\text{C.19})$$

### Gluino-quark loop



$$\begin{aligned} \Gamma_1 &= ig_s (\mathcal{L}P_L + \mathcal{R}P_R)_{Ii} T_{\gamma\alpha}^a \\ \Gamma_2 &= ig_s (\mathcal{L}'P_L + \mathcal{R}'P_R)_{Ij} T_{\beta\gamma}^a \end{aligned}$$

$$-i\Sigma_{\beta\alpha}(p_u^2, m_{\tilde{g}}^2, m_{q_I}^2) \quad (\text{C.20})$$

$$= \mu^{4-D} \int \frac{d^D l}{(2\pi)^D} (-1) \text{Tr} \left[ \Gamma_2 \frac{i(l + m_{\tilde{g}})}{\mathcal{D}_1} \Gamma_1 \frac{i(l + \not{p}_u + m_{q_I})}{\mathcal{D}_2} \right] \quad (\text{C.21})$$

$$= -\frac{ig_s^2}{(4\pi)^2} C_F \delta_{\beta\alpha} \int_l \text{Tr} \left[ \frac{((\mathcal{L}'\mathcal{R}P_L + \mathcal{R}'\mathcal{L}P_R)(l^2 + l \cdot \not{p}_u) + (\mathcal{L}'\mathcal{L}P_L + \mathcal{R}'\mathcal{R}P_R)m_{\tilde{g}}m_{q_I})}{\mathcal{D}_1 \mathcal{D}_2} \right] \quad (\text{C.22})$$

$$= -\frac{ig_s^2}{(4\pi)^2} C_F \delta_{\beta\alpha} \int_l \frac{2((\mathcal{L}'\mathcal{R} + \mathcal{R}'\mathcal{L})(l^2 + l \cdot p_u) + (\mathcal{L}'\mathcal{L} + \mathcal{R}'\mathcal{R})m_{\tilde{g}}m_{q_I})}{\mathcal{D}_1 \mathcal{D}_2} \quad (\text{C.23})$$

$$= -\frac{ig_s^2}{(4\pi)^2} C_F \delta_{\beta\alpha} 2 \left( (\mathcal{L}'\mathcal{R} + \mathcal{R}'\mathcal{L})(B^{\mu\mu} + p_u^2 B_1) + (\mathcal{L}'\mathcal{L} + \mathcal{R}'\mathcal{R})m_{\tilde{g}}m_{q_I} B_0 \right) \quad (\text{C.24})$$

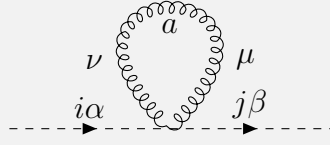
$$= -\frac{ig_s^2}{(4\pi)^2} C_F \delta_{\beta\alpha} 2 \left( (\mathcal{L}'\mathcal{R} + \mathcal{R}'\mathcal{L})(A_0(m_{\tilde{q}}^2) + m_{\tilde{g}}^2 B_0 + p_u^2 B_1) + (\mathcal{L}'\mathcal{L} + \mathcal{R}'\mathcal{R})m_{\tilde{g}}m_{q_I} B_0 \right) \quad (\text{C.25})$$

$$= -\frac{ig_s^2}{(4\pi)^2} C_F \delta_{\beta\alpha} 2 \left( (\mathcal{L}'\mathcal{R} + \mathcal{R}'\mathcal{L}) \left( \frac{1}{2} A_0(m_{\tilde{q}}^2) + \frac{1}{2} m_{\tilde{g}}^2 B_0 + \frac{1}{2} (A_0(m_{\tilde{g}}^2) - (p_u^2 - m_{\tilde{q}}^2) B_0) \right) \right. \\ \left. + (\mathcal{L}'\mathcal{L} + \mathcal{R}'\mathcal{R})m_{\tilde{g}}m_{q_I} B_0 \right) \quad (\text{C.26})$$

$$(\text{C.27})$$

The terms proportional to the single  $m_{\tilde{g}}$  can be dropped for minimal squark mixing (See eq. (2.14)). Furthermore, for massless quarks the restriction  $I = J$  applies since then there are no off-diagonal elements in the squark mixing matrix.

### Gluon loop



$$\Gamma_1^{\mu\nu} = ig_s^2 (T^a T^a + T^a T^a)_{\beta\alpha} g^{\mu\nu} \delta_{ij}$$

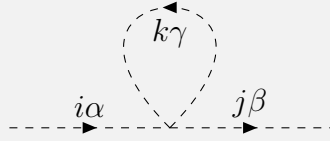
$$-i\Sigma_{\beta\alpha}(0) \quad (C.28)$$

$$= \mu^{4-D} \int \frac{d^D l}{(2\pi)^D} \Gamma_1^{\mu\nu} \frac{-ig^{\mu\nu}}{\mathcal{D}_1} \quad (C.29)$$

$$= \frac{ig_s^2}{(4\pi)^2} 2C_F \delta_{ij} \delta_{\beta\alpha} D A_0(0) \quad (C.30)$$

$$= 0 \quad (C.31)$$

### Squark loop



$$\Gamma_1 = -i(X_{ijkk}\delta_{\beta\alpha}\delta_{\gamma\gamma} + Y_{ijkk}\delta_{\beta\gamma}\delta_{\gamma\alpha})$$

Only the  $X$  and  $Y$  couplings are proportional to  $g_s$  so  $Z$  can be dropped for our purposes.

$$-i\Sigma_{\beta\alpha}(m_{\tilde{q}_k}^2) \quad (C.32)$$

$$= \mu^{4-D} \int \frac{d^D l}{(2\pi)^D} \Gamma_1 \frac{i}{\mathcal{D}_1} \quad (C.33)$$

$$= \frac{i}{(4\pi)^2} \delta_{\beta\alpha} (N_c X_{ijkk} + Y_{ijkk}) A_0(m_{\tilde{q}_k}^2) \quad (C.34)$$

### Same squark types

For a  $\tilde{U}\tilde{U}\tilde{U}\tilde{U}$  or  $\tilde{D}\tilde{D}\tilde{D}\tilde{D}$  vertex

$$Y_{ilkj} = X_{ijkl} = g_s^2 \frac{1}{6} (3X_{\tilde{q}}^{il} X_{\tilde{q}}^{kj} - X_{\tilde{q}}^{ij} X_{\tilde{q}}^{kl}) \quad (C.35)$$

and

$$X_{\tilde{q}}^{il} = \delta^{ij} - 2R_{\tilde{q}}^{ij} = \begin{cases} \delta^{ij} - 2S_{\tilde{U}}^{Ii*} S_{\tilde{U}}^{Ij} \\ \delta^{ij} - 2S_{\tilde{D}}^{Ii} S_{\tilde{D}}^{Ij*} \end{cases} \quad (C.36)$$

holds. For vanishing mixing this results in

$$-i\Sigma_{\beta\alpha}(m_{\tilde{q}_i}^2) = \frac{i}{(4\pi)^2} \delta_{\beta\alpha} \delta_{ij} \left( N_c \frac{3}{6} - \frac{1}{6} \right) A_0(m_{\tilde{q}_k}^2) \quad (\text{C.37})$$

$$= \frac{i}{(4\pi)^2} \delta_{\beta\alpha} \delta_{ij} C_F A_0(m_{\tilde{q}_i}^2) \quad (\text{C.38})$$

### Different squark types

For a  $\tilde{U}\tilde{U}\tilde{D}\tilde{D}$  vertex

$$X_{ijkl} = -X_{\tilde{U}}^{ij} X_{\tilde{D}}^{lk} \quad (\text{C.39})$$

$$Y_{ijkl} = 3X_{\tilde{U}}^{ij} X_{\tilde{D}}^{lk} \quad (\text{C.40})$$

$$(\text{C.41})$$

results in

$$\Sigma_{\beta\alpha} = 0 \quad (\text{C.42})$$

### Combined

$$-i\Sigma_{\beta\alpha}(m_{\tilde{q}_k}^2) = - \sum_{k=1,2} \frac{ig_s^2 C_F}{(4\pi)^2} \delta_{\beta\alpha} |S_{ik}|^2 A_0(m_{\tilde{q}_k}^2) \quad (\text{C.43})$$

#### C.1.3. Gluon self energies

The gluon self energy can be split in a longitudinal and a transversal part.

$$\Sigma^{ba}(p^2) = \delta^{ba} \left( (g_{\mu\nu} - \frac{p^\mu p^\nu}{p^2}) \Sigma_t(p^2) + (\frac{p^\mu p^\nu}{p^2}) \Sigma_l(p^2) \right) \quad (\text{C.44})$$

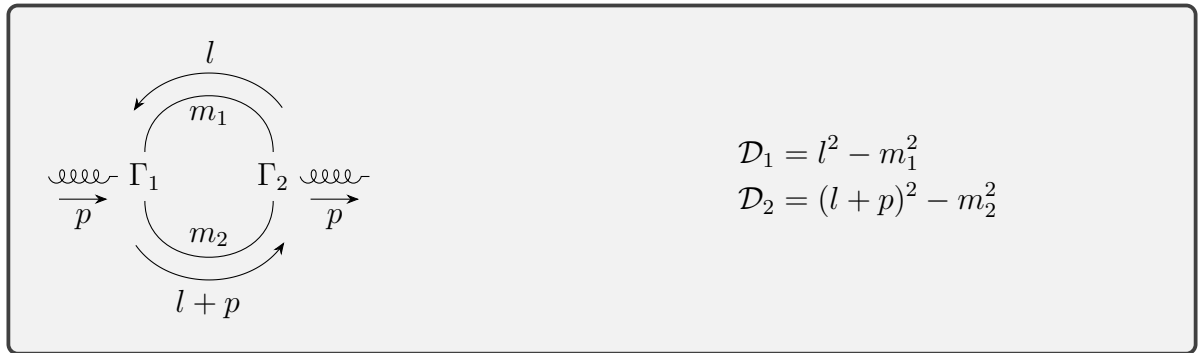


Figure 17: Parametrization of the  $g$  self energy

Figure 18: Parametrization of the  $g$  self energy with 4 point vertices**Quark-quark loop**

$$-i\Sigma^{ba}(p^2, m_{q_I}^2, m_{q_J}^2) \quad (C.45)$$

$$=(-1)\mu^{4-D} \int \frac{d^D l}{(2\pi)^D} \text{Tr} \left[ \Gamma_2^\nu \frac{i(l + m_{q_I})}{\mathcal{D}_1} \Gamma_1^\mu \frac{i(l + \not{p} + m_{q_J})}{\mathcal{D}_2} \right] \quad (C.46)$$

$$= -\frac{ig_s^2}{(4\pi)^2} (T_R \delta_{ba}) \int_l \frac{\text{Tr} [\gamma^\nu \not{l} \gamma^\mu (\not{l} + \not{p})] + 4g^{\mu\nu} m_q^2}{\mathcal{D}_1 \mathcal{D}_2} \quad (C.47)$$

$$= -\frac{ig_s^2}{(4\pi)^2} (T_R \delta_{ba}) \int_l 4 \frac{l^\mu (l + p)^\nu - g^{\mu\nu} l \cdot (l + p) + l^\nu (l + p)^\mu + g^{\mu\nu} m_q^2}{\mathcal{D}_1 \mathcal{D}_2} \quad (C.48)$$

$$= -\frac{ig_s^2}{(4\pi)^2} (T_R \delta_{ba}) 2 \frac{p^2 g^{\mu\nu} - p^\mu p^\nu}{p^2} \frac{((D-2)p^2 + 4m_q^2)B_0 - 2(D-2)A_0(m_q^2)}{(D-1)} \quad (C.49)$$

$$\begin{aligned} -i\Sigma_t(p^2) &= -\frac{ig_s^2}{(4\pi)^2} \frac{2}{3} \left( (p^2 + 2m_q^2)B_0(p^2, m_q^2, m_q^2) \right. \\ &\quad \left. - \frac{1}{3}(p^2 - 4m_q^2)\epsilon B_0(p^2, m_q^2, m_q^2) - 2A_0(m_q^2) \right) \end{aligned} \quad (C.50)$$

$$-i\Sigma_l(p^2) = 0 \quad (C.51)$$

where we used

$$\frac{D-2}{D-1} = \frac{2}{3} - \frac{2}{9}\epsilon + \mathcal{O}(\epsilon^2) \quad (C.52)$$

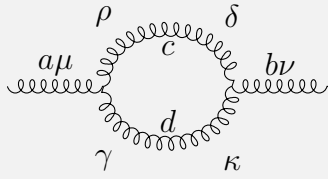
$$\frac{1}{D-1} = \frac{1}{3} + \frac{2}{9}\epsilon + \mathcal{O}(\epsilon^2) \quad (C.53)$$

in the last step. For massless quarks however

$$-i\Sigma_t(p^2) = -\frac{ig_s^2}{(4\pi)^2} \frac{2}{9} (3 - \epsilon) (p^2 B_0(p^2, 0, 0)) \quad (C.54)$$

$$-i\Sigma_l(p^2) = 0. \quad (C.55)$$

### Gluon-gluon loop



$$\Gamma_1^{\gamma\rho\mu} = -g_s \Gamma^{\rho\gamma\mu} f^{cda}$$

$$\Gamma_2^{\delta\kappa\nu} = -g_s \Gamma^{\delta\kappa\nu} f^{cdb}$$

$$-i\Sigma^{ba}(p^2, 0, 0) \quad (C.56)$$

$$= \frac{1}{2} \mu^{4-D} \int \frac{d^D l}{(2\pi)^D} \Gamma_2^{\delta\kappa\nu} \frac{-ig^{\delta\rho}}{\mathcal{D}_1} \Gamma_1^{\gamma\rho\mu} \frac{-ig^{\gamma\kappa}}{\mathcal{D}_2} \quad (C.57)$$

$$= -\frac{ig_s^2}{(4\pi)^2} (2N_c T_R \delta^{ba}) \frac{1}{2} \int_l \frac{(g^{\delta\kappa}(-2l-p)^\nu + g^{\kappa\nu}(l+2p)^\delta + g^{\nu\delta}(-p+l)^\kappa)}{\mathcal{D}_1 \mathcal{D}_2} \quad (C.58)$$

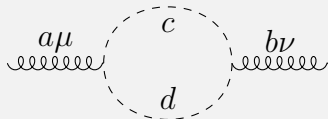
$$\times (-1)(g^{\rho\gamma}(-2l-p)^\mu + g^{\gamma\mu}(l+2p)^\rho + g^{\mu\rho}(-p+l)^\gamma) g^{\delta\rho} g^{\gamma\kappa} \quad (C.59)$$

$$= -\frac{ig_s^2}{(4\pi)^2} (2N_c T_R \delta^{ba}) \frac{1}{4} B_0 \frac{(5-6D)p^2 g^{\mu\nu} + (7D-6)p^\mu p^\nu}{(D-1)} \quad (C.60)$$

$$-i\Sigma_t(p^2) = \frac{ig_s^2}{(4\pi)^2} N_c \frac{6D-5}{4(D-1)} p^2 B_0(p^2, 0, 0) \quad (C.61)$$

$$-i\Sigma_l(p^2) = -\frac{ig_s^2}{(4\pi)^2} N_c \frac{1}{4} p^2 B_0(p^2, 0, 0) \quad (C.62)$$

### Ghost-ghost loop



$$\Gamma_1^\mu = -g_s l^\mu f^{dca}$$

$$\Gamma_2^\nu = -g_s (l+p)^\nu f^{cdb}$$



$$-i\Sigma^{ba}(p^2, 0, 0) \quad (C.63)$$

$$= (-1)\mu^{4-D} \int \frac{d^D l}{(2\pi)^D} \Gamma_2^\nu \frac{i}{\mathcal{D}_1} \Gamma_1^\mu \frac{i}{\mathcal{D}_2} \quad (C.64)$$

$$= \frac{ig_s^2}{(4\pi)^2} (-2N_c T_R \delta_{ba}) \int_l \frac{l^\mu (l+p)^\nu}{\mathcal{D}_1 \mathcal{D}_2} \quad (C.65)$$

$$= \frac{ig_s^2}{(4\pi)^2} (-2N_c T_R \delta_{ba}) (B^{\mu\nu} + p^\nu B^\mu) \quad (C.66)$$

$$= \frac{ig_s^2}{(4\pi)^2} (-2N_c T_R \delta_{ba}) (g^{\mu\nu} B_{00} + p^\mu p^\nu B_{11} + p^\nu B^\mu) \quad (C.67)$$

$$= \frac{ig_s^2}{(4\pi)^2} (-2N_c T_R \delta_{ba}) (g^{\mu\nu} \frac{1}{2(D-1)} p^2 B_1 - p^\mu p^\nu \frac{D}{2(D-1)} B_1 + p^\nu p^\mu B_1) \quad (C.68)$$

$$= -\frac{ig_s^2}{(4\pi)^2} (-2N_c T_R \delta_{ba}) \frac{1}{2} (g^{\mu\nu} \frac{1}{2(D-1)} p^2 B_0 + p^\mu p^\nu \frac{D-2}{2(D-1)} B_0) \quad (C.69)$$

$$-i\Sigma_t(p^2) = \frac{ig_s^2}{(4\pi)^2} N_c \frac{1}{4(D-1)} p^2 B_0(p^2, 0, 0) \quad (C.70)$$

$$-i\Sigma_l(p^2) = \frac{ig_s^2}{(4\pi)^2} N_c \frac{1}{4} p^2 B_0(p^2, 0, 0) \quad (C.71)$$

We notice that the longitudinal contributions between the ghost and the gluon loop cancel.

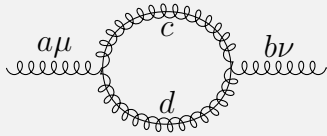
### Gluon loop



$$\Gamma_1^{\mu\nu\rho\kappa} \propto g_s^2$$

$$-i\Sigma^{ba}(0) \propto A_0(0) = 0 \quad (C.72)$$

### Gluino-gluino loop



$$\begin{aligned} \Gamma_1^\mu &= g_s \gamma^\mu f^{dca} \delta_{IJ} \\ \Gamma_2^\nu &= g_s \gamma^\nu f^{cdb} \delta_{IJ} \end{aligned}$$

$$-i\Sigma^{ba}(p^2, m_{\tilde{g}}^2, m_{\tilde{g}}^2) \quad (C.73)$$

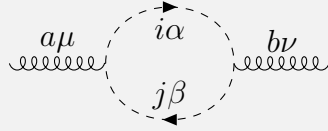
$$= (-\frac{1}{2})\mu^{4-D} \int \frac{d^D l}{(2\pi)^D} \text{Tr} \left[ \Gamma_2^\nu \frac{i(\not{l} + m_{\tilde{g}})}{\mathcal{D}_1} \Gamma_1^\mu \frac{i(\not{l} + \not{p} + m_{\tilde{g}})}{\mathcal{D}_2} \right] \quad (C.74)$$

Giving us the same contribution from the trace as in the massive quark loop case. The colour factor changes from  $T^2$  to  $f^2$  and thereby  $T_R \rightarrow 2N_c T_R$  resulting in total rescaling by  $N_c$ .

$$-i\Sigma_t(p^2) = -\frac{ig_s^2}{(4\pi)^2} N_c \frac{((D-2)p^2 + 4m_{\tilde{g}}^2)B_0(p^2, m_{\tilde{g}}^2, m_{\tilde{g}}^2) - 2(D-2)A_0(m_{\tilde{g}}^2)}{(D-1)} \quad (C.75)$$

$$-i\Sigma_l(p^2) = 0 \quad (C.76)$$

### Squark-squark loop



$$\begin{aligned} \Gamma_1^\mu &= ig_s(2l+p)^\mu T_{\beta\alpha}^a \delta_{ij} \\ \Gamma_2^\nu &= ig_s(2l+p)^\nu T_{\alpha\beta}^b \delta_{ij} \end{aligned}$$

$$-i\Sigma^{ba}(p^2, m_{\tilde{q}_i}^2, m_{\tilde{q}_j}^2) \quad (C.77)$$

$$= \mu^{4-D} \int \frac{d^D l}{(2\pi)^D} \Gamma_2^\nu \frac{i}{\mathcal{D}_1} \Gamma_1^\mu \frac{i}{\mathcal{D}_2} \quad (C.78)$$

$$= \frac{ig_s^2}{(4\pi)^2} (T_R \delta^{ba}) \int_l \frac{(2l+p)^\mu (2l+p)^\nu}{\mathcal{D}_1 \mathcal{D}_2} \quad (C.79)$$

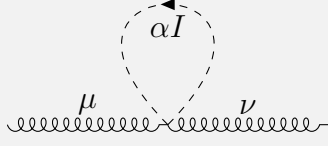
$$= \frac{ig_s^2}{(4\pi)^2} (T_R \delta^{ba}) (4B^{\mu\nu} + 4p^\mu p^\nu B_1 + B_0 p^\mu p^\nu) \quad (C.80)$$

$$= \frac{ig_s^2}{(4\pi)^2} \frac{(T_R \delta^{ba})}{(D-1)} \left( (4m_{\tilde{q}}^2 - p^2)(g^{\mu\nu} - \frac{p^\mu p^\nu}{p^2}) B_0 + 2A_0(m_{\tilde{q}}^2) \left( (D-2) \frac{p^\mu p^\nu}{p^2} + g^{\mu\nu} \right) \right) \quad (C.81)$$

$$-i\Sigma_t(p^2) = \frac{ig_s^2}{(4\pi)^2} (T_R) \frac{1}{(D-1)} \left( (4m_{\tilde{q}}^2 - p^2) B_0(p^2, m_{\tilde{q}}^2, m_{\tilde{q}}^2) + 2A_0(m_{\tilde{q}}^2) \right) \quad (C.82)$$

$$-i\Sigma_l(p^2) = \frac{ig_s^2}{(4\pi)^2} (T_R) 2A_0(m_{\tilde{q}}^2) \quad (C.83)$$

### Squark loop



$$\Gamma_1^{\mu\nu} = ig_s^2 (T^a T^b + T^b T^a)_{\alpha\alpha}$$

$$-i\Sigma^{ba}(m_{\tilde{q}_I}^2) \quad (C.84)$$

$$= \mu^{4-D} \int \frac{d^D l}{(2\pi)^D} \Gamma_1^{\nu\mu} \frac{i}{\mathcal{D}_1} \quad (C.85)$$

$$= -\frac{ig_s^2}{(4\pi)^2} \delta^{ba} A_0(m_{\tilde{q}_I}^2) g^{\mu\nu} \quad (C.86)$$

$$-i\Sigma_t(p^2) = -\frac{ig_s^2}{(4\pi)^2} A_0(m_{\tilde{q}_I}^2) \quad (C.87)$$

$$-i\Sigma_l(p^2) = -\frac{ig_s^2}{(4\pi)^2} A_0(m_{\tilde{q}_I}^2) \quad (C.88)$$

This longitudinal part cancels the squark-squark-loop contribution.

## C.2. Vertex corrections

### C.2.1. Quark-quark-gluon vertex

We compute the loop corrections to the  $qqg$ -vertex using the parametrization displayed in fig. 19.

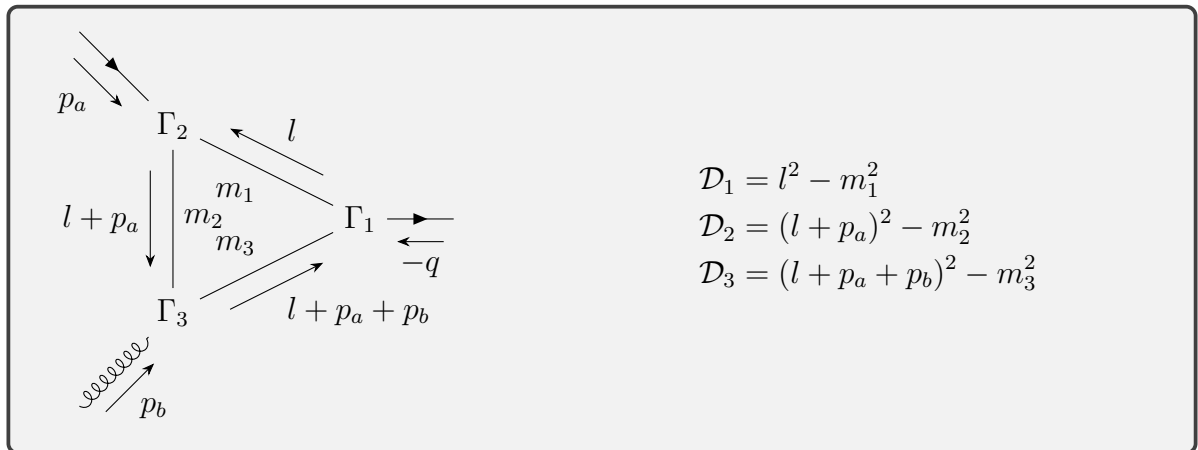
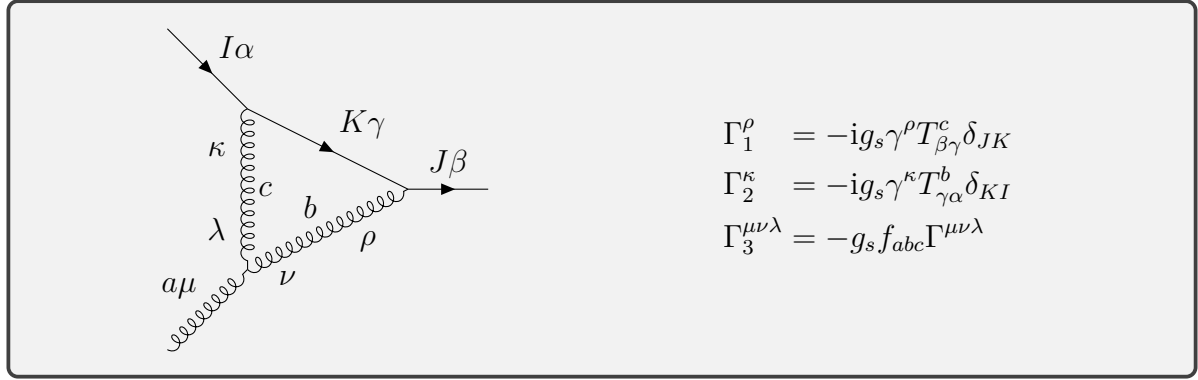


Figure 19: Parametrization of the  $qqg$ -vertex

### Quark-gluon-gluon loop



$$\Lambda_{\beta\alpha}^{\mu a}(0, 0, q^2, 0, 0, 0) \quad (C.89)$$

$$= \mu^{4-D} \int \frac{d^D l}{(2\pi)^D} \Gamma_1^\rho \frac{-i \not{l}}{\mathcal{D}_1} \Gamma_2^\kappa \frac{-ig_{\kappa\lambda}}{\mathcal{D}_2} \Gamma_3^{\mu\nu\lambda} \frac{-ig_{\nu\rho}}{\mathcal{D}_3} \quad (C.90)$$

$$= -\frac{g_s^3}{(4\pi)^2} \int_l \frac{\gamma^\nu \not{l} \gamma^\lambda (g^{\mu\nu}(l + p_a + 2p_b)^\lambda + g^{\nu\lambda}(-(2l + 2p_a + p_b))^\mu + g^{\mu\lambda}(l + p_a - p_b)^\nu)}{\mathcal{D}_1 \mathcal{D}_2 \mathcal{D}_3} \quad (C.91)$$

$$= \frac{ig_s^3}{(4\pi)^2} C_A T_R T_{\beta\alpha}^a \delta_{IJ} (\gamma^\mu ((\not{p}_b - \not{p}_a) \gamma_\sigma C^\sigma - C^{\sigma\sigma}) + (2-D) \gamma_\sigma (2C^{\sigma\mu} + C^\sigma (2p_a + p_b)^\mu) - \gamma^\mu (C^{\sigma\sigma} + \gamma_\sigma C^\sigma (\not{p}_a + 2\not{p}_b))) \quad (C.92)$$

To get the counterterm we consider only the UV divergent part  $\overline{\text{UV}}$  by looking at table 11:

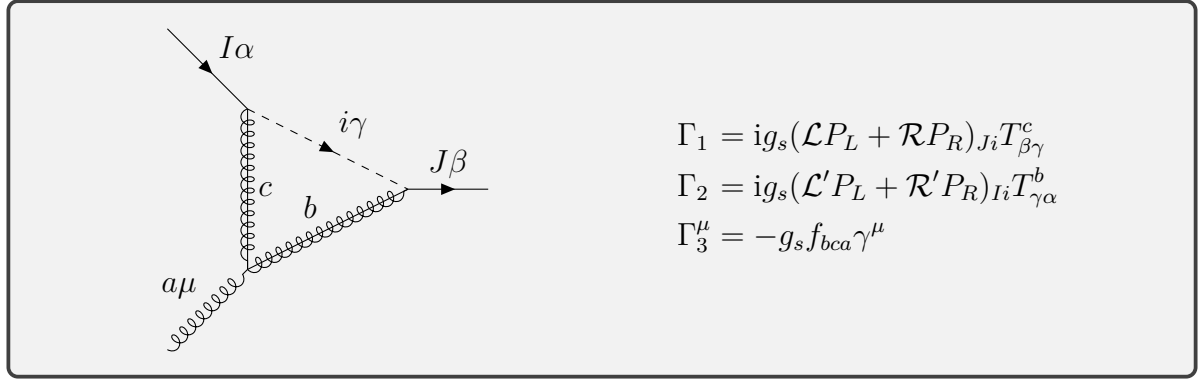
$$\overline{\text{UV}}[\Lambda] = \frac{ig_s^3}{(4\pi)^2} C_A T_R T_{\beta\alpha}^a \delta_{IJ} \gamma^\mu (-4 - 4 - 4) \left(\frac{1}{4} \Delta\right) \quad (C.93)$$

In contrast the vertex divergence in `FeynCalc`/`MadGraph` is

$$\overline{\text{UV}}[\Lambda] = \frac{ig_s^3}{(4\pi)^2} C_A T_R T_{\beta\alpha}^a \delta_{IJ} \gamma^\mu (-4) \left(\frac{1}{4} \Delta\right). \quad (C.94)$$

It appears as if  $C^{\sigma\sigma} = 0$  was used for the massless case.

## Squark-gluino-gluino loop



$$\Lambda_{\beta\alpha}^{\mu a}(0, 0, q^2, m_{\tilde{q}_i}^2, m_{\tilde{g}}^2, m_{\tilde{g}}^2) \quad (\text{C.95})$$

$$= \mu^{4-D} \int \frac{d^D l}{(2\pi)^D} \Gamma_1 \frac{i(\not{l} + \not{p}_a + \not{p}_b + m_{\tilde{g}})}{\mathcal{D}_3} \Gamma_3^\mu \frac{i(\not{l} + \not{p}_a + m_{\tilde{g}})}{\mathcal{D}_2} \Gamma_2 \frac{i}{\mathcal{D}_1} \quad (\text{C.96})$$

$$\begin{aligned} &= \frac{ig_s^3}{(4\pi)^2} C_A T_R T_{\beta\alpha}^a \left( (\mathcal{L}\mathcal{R}'P_L + \mathcal{R}\mathcal{L}'P_R) \int_l \frac{\gamma^\mu m_{\tilde{g}}^2 + (\not{l} + \not{p}_a + \not{p}_b)\gamma^\mu(\not{l} + \not{p}_a)}{\mathcal{D}_1 \mathcal{D}_2 \mathcal{D}_3} \right. \\ &\quad \left. + (\mathcal{L}\mathcal{L}'P_L + \mathcal{R}\mathcal{R}'P_R) \int_l \frac{m_{\tilde{g}}\gamma^\mu(\not{l} + \not{p}_a) + (\not{l} + \not{p}_a + \not{p}_b)\gamma^\mu m_{\tilde{g}}}{\mathcal{D}_1 \mathcal{D}_2 \mathcal{D}_3} \right) \quad (\text{C.97}) \end{aligned}$$

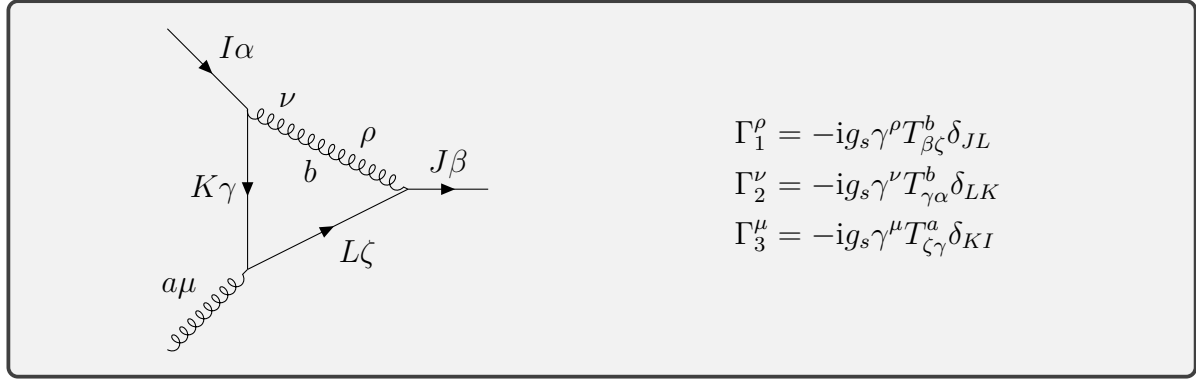
$$\begin{aligned} &= \frac{ig_s^3}{(4\pi)^2} C_A T_R T_{\beta\alpha}^a \left( (\mathcal{L}_{Ji}\mathcal{R}'_{Ii}P_L + \mathcal{R}_{Ji}\mathcal{L}'_{Ii}P_R) \left( C_0(\gamma^\mu m_{\tilde{g}}^2 + (\not{p}_a + \not{p}_b)\gamma^\mu \not{p}_a) - 2\gamma_\sigma C^{\mu\sigma} \right. \right. \\ &\quad \left. \left. + \gamma^\mu C^{\sigma\sigma} + C^\sigma(\gamma_\sigma \gamma^\mu \not{p}_a + (\not{p}_a + \not{p}_b)\gamma^\mu \gamma_\sigma) \right) + (\mathcal{L}_{Ji}\mathcal{L}'_{Ii}P_L + \mathcal{R}_{Ji}\mathcal{R}'_{Ii}P_R) \right. \\ &\quad \left. \left( C^\sigma(\gamma_\sigma \gamma^\mu m_{\tilde{g}} + m_{\tilde{g}}\gamma^\mu \gamma_\sigma) + C_0(m_{\tilde{g}}\gamma^\mu \not{p}_a + (\not{p}_a + \not{p}_b)\gamma^\mu m_{\tilde{g}}) \right) \right) \quad (\text{C.98}) \end{aligned}$$

The terms proportional to the single  $m_{\tilde{g}}$  can be dropped for minimal squark mixing (See eq. (2.14)).

To get the counterterm we consider only the UV divergent part  $\overline{\text{UV}}$  by looking at table 11:

$$\overline{\text{UV}}[\Lambda] = \frac{ig_s^3}{(4\pi)^2} C_A T_R T_{\beta\alpha}^a (-2)\gamma^\mu (-2+4) \left(\frac{1}{4}\Delta\right) \quad (\text{C.99})$$

### Quark-quark-gluon loop



$$\Lambda_{\beta\alpha}^{\mu a}(0, 0, q^2, 0, 0, 0) \quad (C.100)$$

$$= \mu^{4-D} \int \frac{d^D l}{(2\pi)^D} \Gamma_1^\rho \frac{i(l + \not{p}_a + \not{p}_b)}{\mathcal{D}_3} \Gamma_3^\mu \frac{i(l + \not{p}_a)}{\mathcal{D}_2} \Gamma_2^\nu \frac{-ig_{\nu\rho}}{\mathcal{D}_1} \quad (C.101)$$

$$= -\frac{ig_s^3}{(4\pi)^2} T_{\beta\zeta}^b T_{\zeta\gamma}^a T_{\gamma\alpha}^b \int_l \frac{\gamma_\nu (l + \not{p}_a + \not{p}_b) \gamma^\mu (l + \not{p}_a) \gamma^\nu}{\mathcal{D}_1 \mathcal{D}_2 \mathcal{D}_3} \quad (C.102)$$

$$= \frac{ig_s^3}{(4\pi)^2} \frac{T_R}{C_A} T_{\beta\alpha}^a \delta_{JI} \gamma_\nu \left( 2C^{\mu\sigma} \gamma_\sigma - \gamma^\mu C^{\sigma\sigma} + C^\sigma (\gamma_\sigma \gamma^\mu \not{p}_a + (\not{p}_a + \not{p}_b) \gamma^\mu \gamma_\sigma) \right) \quad (C.103)$$

$$+ C_0 (\not{p}_a + \not{p}_b) \gamma^\mu \not{p}_a \gamma^\nu \quad (C.104)$$

To get the counterterm we consider only the UV divergent part  $\overline{\mathbf{UV}}$  by looking at table 11:

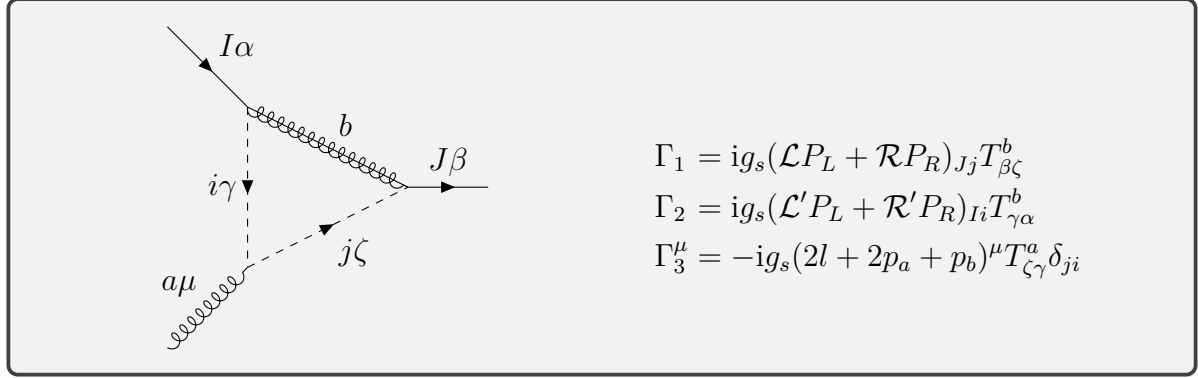
$$\overline{\mathbf{UV}}[\Lambda] = \frac{ig_s^3}{(4\pi)^2} \frac{T_R}{C_A} T_{\beta\alpha}^a \delta_{IJ} \gamma^\mu (-2)(2-4) \left( \frac{1}{4} \Delta \right) \quad (C.105)$$

The extra factor  $-2$  comes from the remaining  $\gamma$ -matrices. In contrast, the vertex divergence in `FeynCalc`/`MadGraph` is

$$\overline{\mathbf{UV}}[\Lambda] = \frac{ig_s^3}{(4\pi)^2} \frac{T_R}{C_A} T_{\beta\alpha}^a \delta_{IJ} \gamma^\mu (-2)(2) \left( \frac{1}{4} \Delta \right). \quad (C.106)$$

It appears as if  $C^{\sigma\sigma} = 0$  was used for the massless case.

### Squark-squark-gluino loop



$$\Lambda_{\beta\alpha}^{\mu a}(0, 0, q^2, m_{\tilde{g}}^2, m_{\tilde{q}_i}^2, m_{\tilde{q}_i}^2) \quad (\text{C.107})$$

$$= \mu^{4-D} \int \frac{d^D l}{(2\pi)^D} \Gamma_1 \frac{i(\not{l} + m_{\tilde{g}})}{\mathcal{D}_1} \Gamma_2 \frac{i}{\mathcal{D}_2} \Gamma_3^\mu \frac{i}{\mathcal{D}_3} \quad (\text{C.108})$$

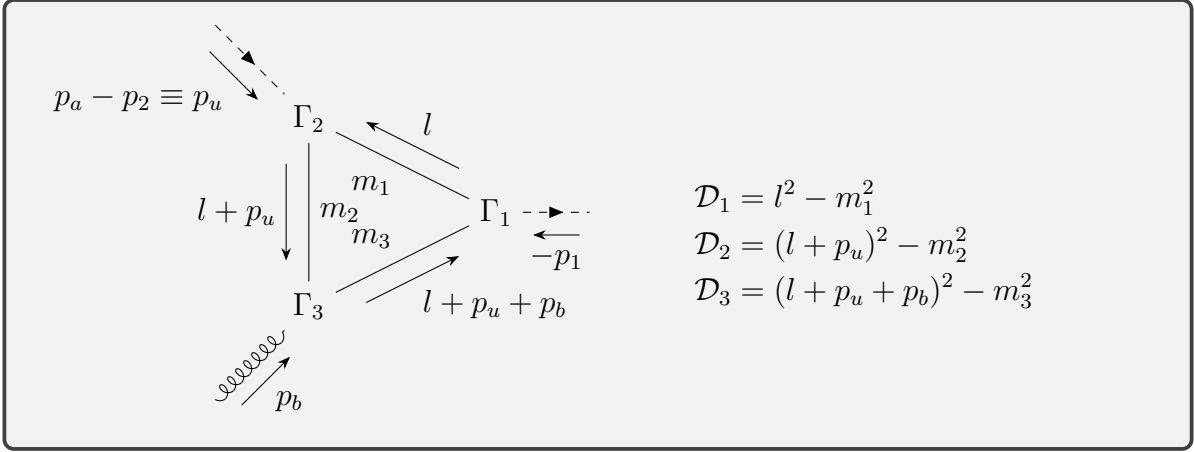
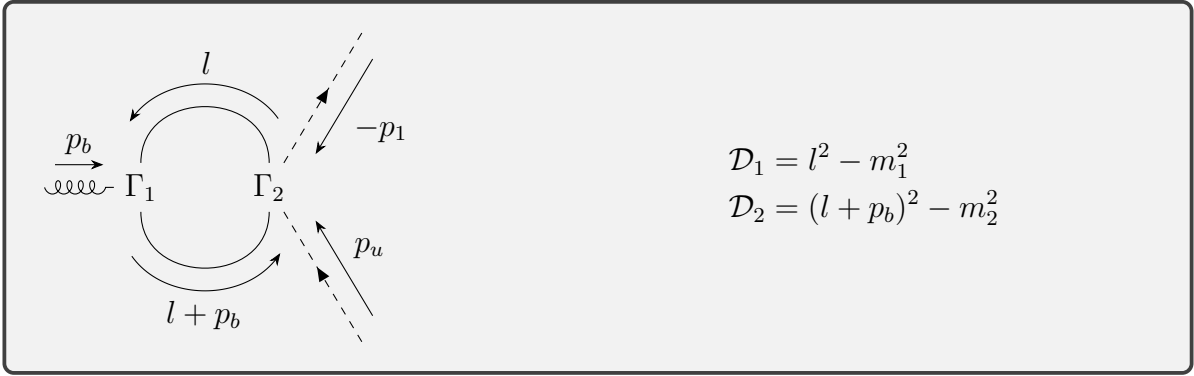
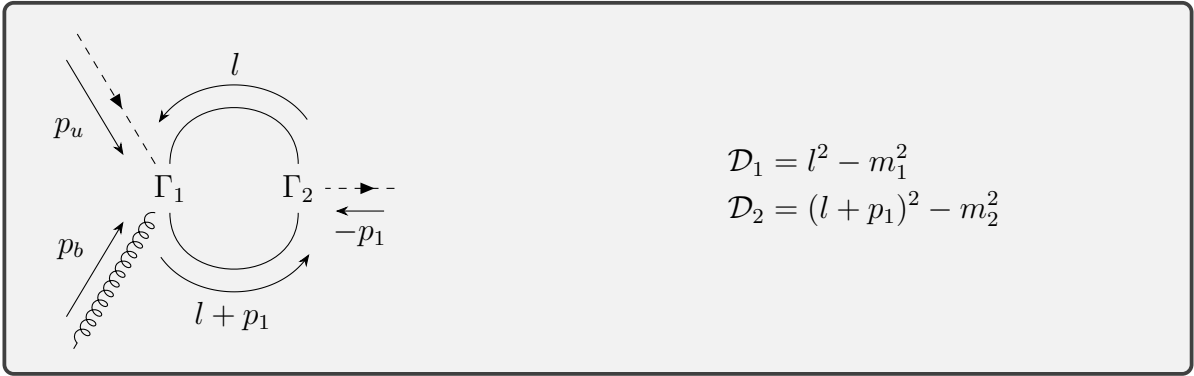
$$\begin{aligned} &= -\frac{ig_s^3}{(4\pi)^2} \frac{T_R}{C_A} T_{\beta\alpha}^a ((\mathcal{L}_{Ji}\mathcal{R}'_{Ii}P_L + \mathcal{R}_{Ji}\mathcal{L}'_{Ii}P_R)\gamma_\sigma (2C^{\sigma\mu} + C^\sigma(2p_a + p_b^\mu)) \\ &\quad (\mathcal{L}_{Ji}\mathcal{L}'_{Ii}P_L + \mathcal{R}_{Ji}\mathcal{R}'_{Ii}P_R)m_{\tilde{g}}(2C^\mu + C_0(2p_a + p_b^\mu)) \end{aligned} \quad (\text{C.109})$$

The term proportional to the single  $m_{\tilde{g}}$  can be dropped for minimal squark mixing (See eq. (2.14)). To get the counterterm we consider only the UV divergent part  $\overline{\mathbf{UV}}$  by looking at table 11:

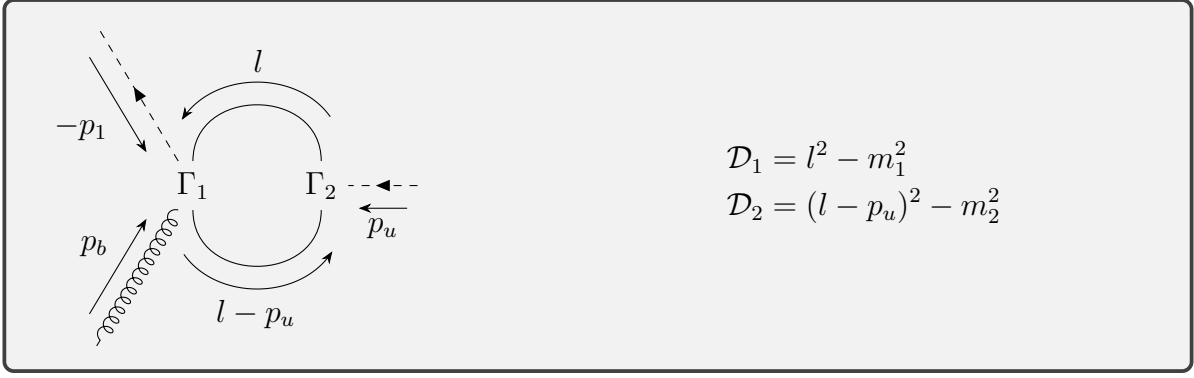
$$\overline{\mathbf{UV}}[\Lambda] = -\frac{ig_s^3}{(4\pi)^2} \frac{T_R}{C_A} T_{\beta\alpha}^a \gamma^\mu (-2)(2)(\frac{1}{4}\Delta) \quad (\text{C.110})$$

#### C.2.2. Squark-squark-gluon vertex

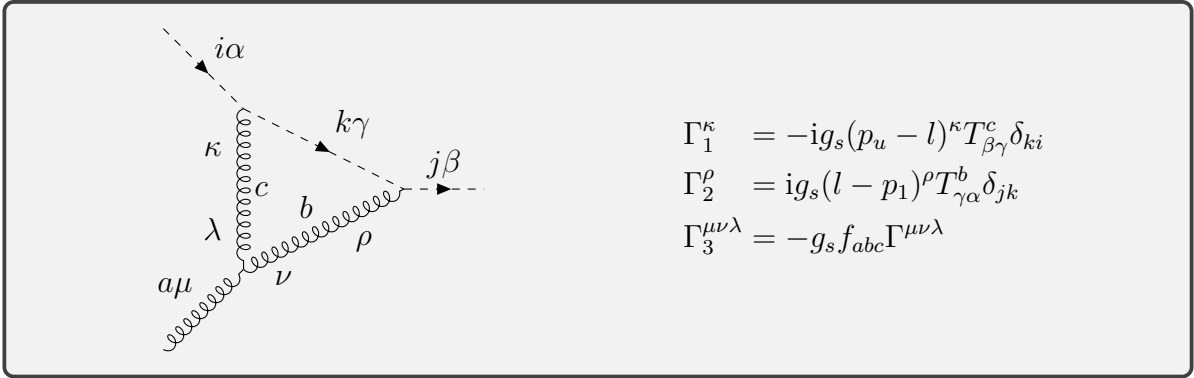
We compute the loop corrections to the  $\tilde{q}\tilde{q}g$ -vertex using the parametrization displayed in fig. 20.

Figure 20: Parametrization of the  $\tilde{q}\tilde{q}g$ -vertexFigure 21: Parametrization of the  $\tilde{q}\tilde{q}g$ -vertexFigure 22: Parametrization of the  $\tilde{q}\tilde{q}g$ -vertex



Figure 23: Parametrization of the  $\tilde{q}\tilde{q}g$ -vertex

### Squark-gluon-gluon loop



$$\Lambda_{\beta\alpha}^{\mu a}(p_u^2, 0, m_{\tilde{q}}^2, m_{\tilde{q}}^2, 0, 0) \quad (\text{C.111})$$

$$= \mu^{4-D} \int \frac{d^D l}{(2\pi)^D} \Gamma_3^{\mu\nu\lambda} \frac{-ig_{\lambda\kappa}}{\mathcal{D}_2} \Gamma_1^\kappa \frac{i}{\mathcal{D}_1} \Gamma_2^\rho \frac{-ig_{\rho\nu}}{\mathcal{D}_3} \quad (\text{C.112})$$

$$= -\frac{g_s^3}{(4\pi)^2} \int_l \frac{\Gamma^{\mu\nu\lambda}(p_u - l)^\nu (l - p_1)^\lambda}{\mathcal{D}_1 \mathcal{D}_2 \mathcal{D}_3} f_{abc} T_{\beta\gamma}^c T_{\gamma\alpha}^b \quad (\text{C.113})$$

given

$$\Gamma^{\mu\nu\lambda} = -g^{\mu\nu}(2p_b + l + p_u)^\lambda + g^{\nu\lambda}(2l + 2p_u + p_b)^\mu - g^{\mu\lambda}(l + p_u - p_b)^\nu \quad (\text{C.114})$$

results in

$$\Gamma^{\mu\nu\lambda}(p_u - l)^\nu (l - p_1)^\lambda = p_u^\mu(4p_u \cdot l + 2p_b \cdot l - 4l^2) \quad (\text{C.115})$$

$$+ p_b^\mu(p_u \cdot p_b + 2p_u \cdot l - p_b \cdot l - 2l^2) \quad (\text{C.116})$$

$$+ l^\mu(-4p_u^2 - 4p_u \cdot p_b + 4p_u \cdot l + 2p_b \cdot l) \quad (\text{C.117})$$

and thus giving following vertex correction with the same arguments for the  $C$ -tensors:

$$\Lambda_{\gamma\beta}^{\mu a}(p_u^2, p_b^2 = 0, p_1^2 = m_{\bar{q}}^2, m_{\bar{q}}^2, 0, 0) = \frac{ig_s^3}{32\pi^2} C_A T_{\gamma\beta}^a \left[ p_u^\mu (C^\nu (4p_u + 2b)^\nu - 4C^{\nu\nu}) \right. \\ \left. + p_b^\mu (C^\nu (2p_u - p_b)^\nu - 2C^{\nu\nu} + C_0 p_u \cdot p_b) \right. \\ \left. - C^\mu (4p_u^2 + 4p_u \cdot p_b) + C^{\mu\nu} (4p_u^\nu - 2p_b^\nu) \right] \quad (\text{C.118})$$

where the colour algebra has been simplified  $f_{abc} T_{\beta\alpha}^c T_{\gamma\beta}^b = -i C_A T_R T_{\gamma\alpha}^a$ . Now we can apply the tensor-coefficients from eq. (4.30) and arrive at

$$\Lambda_{\gamma\alpha}^{\mu a} = -\frac{ig_s^3}{32\pi^2} C_A T_{\gamma\alpha}^a \left[ +p_u^\mu (-C_1 m_{\bar{q}}^2 + C_1 U + C_2 m_{\bar{q}}^2 - C_2 U \right. \\ \left. + 4C_{00} + C_{11} m_{\bar{q}}^2 - C_{11} U - C_{22} m_{\bar{q}}^2 + C_{22} U - 4DC_{00}) \right. \\ \left. + p_b^\mu \left( \frac{1}{2} C_0 m_{\bar{q}}^2 - \frac{1}{2} C_0 U - \frac{1}{2} C_1 m_{\bar{q}}^2 + \frac{5}{2} C_1 U - \frac{3}{2} C_2 m_{\bar{q}}^2 - \frac{1}{2} C_2 U \right. \right. \\ \left. \left. + 2C_{00} - 2C_{11} U - C_{12} m_{\bar{q}}^2 + C_{12} U + C_{22} m_{\bar{q}}^2 + C_{22} U - 2DC_{00} \right) \right] \quad (\text{C.119})$$

with  $p_1^2 = m_{\bar{q}}^2$  and  $p_u^2 = U$  which arise due to  $p_u \cdot p_b = \frac{1}{2}(p_1^2 - p_b^2 - p_u^2)$ . This can be embedded in to

$$2M_v M_u^* = -2 \frac{1}{96(p_u^2 - m_{\bar{q}}^2)^2} \epsilon^{*\mu} \epsilon^\nu \text{Tr} [i(L' P_L + R' P_R) \not{p}_a (-i(LP_L + RP_R)) (\not{p}_2 + m_\chi) \\ \underbrace{(-ig_s)(p_u^\mu C_u + p_b^\mu C_b) T_{\gamma\beta}^a}_{\Lambda_{\gamma\alpha}^{\mu a}} ig_s (p_1^\nu + p_u^\nu) T_{\beta\gamma}^a] \quad (\text{C.120})$$

with averaging factors of quark spin  $\frac{1}{2}$ , colour  $\frac{1}{3}$ , gluon polarisation  $\frac{1}{2}$  and colour  $\frac{1}{8}$ .  $C_u$  and  $C_b$  are the terms proportional to the momenta in eq. (C.119). The fermion traces are evaluated with **FORM**. In our computation we get exactly half of what **MadGraph** gives as result for  $\epsilon_{\text{UV}}^{-1} + \epsilon_{\text{IR}}^{-1}, \epsilon_{\text{IR}}^{-2}$  and the finite contribution. This also is the case for the  $uug$ -vertex'  $ugg$ -loop.

Notes:

- in axial gauge ( $\sum_i \epsilon_\mu \epsilon_\nu^* = -g_{\mu\nu} + \frac{n^\mu p^\nu + n^\nu p^\mu}{p \cdot n} - \frac{n^2 p^\nu p^\nu}{(p \cdot n)^2}$ ,  $n = q$  or  $n = p_a$ )  $C_b$  won't contribute since the gluon momentum contracted with the polarization sum vanishes.
- Also only  $C_2$  and  $C_{22}$  contribute to the  $\epsilon_{\text{IR}}^{-2}$  term.
- The  $\epsilon_{\text{IR}}^{-2}$  of  $C_u$  is  $\frac{g_s^2 C_A}{32\pi^2}$ .
- Only these two vertex loops with a triple gluon differ from **MadGraph**'s vertex computations
- Only these two vertex loops give  $\epsilon_{\text{IR}}^{-2}$  contributions

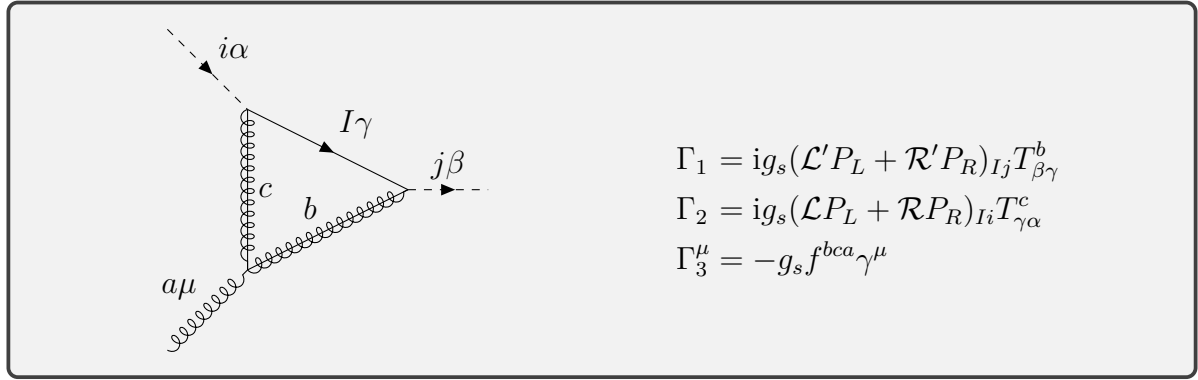
- The same factor 2 is missing in separate unpublished automatic calculation (SunderCalc).

To get the counterterm we consider only the UV divergent part  $\overline{\mathbf{UV}}$  by looking at table 11:

$$\overline{\mathbf{UV}}[\Lambda] = -\frac{ig_s^3}{(4\pi)^2} T_R C_A T_{\beta\alpha}^a \delta_{ij} (2p_u + p_b)^\mu (-4 \cdot 2 + 2) \left(\frac{1}{4} \Delta\right) \quad (\text{C.121})$$

$$= \frac{ig_s^3}{(4\pi)^2} \frac{3}{2} T_R C_A \Delta T_{\beta\alpha}^a \delta_{ij} (2p_u + p_b)^\mu \quad (\text{C.122})$$

### Quark-gluino-gluino loop



$$\Lambda_{\beta\alpha}^{\mu a}(p_u^2, 0, m_{\tilde{q}}^2, m_{q_I}^2, m_{\tilde{g}}^2, m_{\tilde{g}}^2) \quad (\text{C.123})$$

$$= \mu^{4-D} \int \frac{d^D l}{(2\pi)^D} (-1) \text{Tr} \left[ \Gamma_1 \frac{i(l + m_{q_I})}{\mathcal{D}_1} \Gamma_2 \frac{i(l + \not{p}_u + m_{\tilde{g}})}{\mathcal{D}_2} \Gamma_3^\mu \frac{i(l + \not{p}_u + \not{p}_b + m_{\tilde{g}})}{\mathcal{D}_3} \right] \quad (\text{C.124})$$

$$= -\frac{g_s^3}{(4\pi)^2} \underbrace{f^{bca} T_{\beta\gamma}^b T_{\gamma\alpha}^c}_{iC_A T_R T_{\beta\alpha}^a} \quad (\text{C.125})$$

$$\int_l \text{Tr} \left[ \frac{(\mathcal{L}' P_L + \mathcal{R}' P_R)(l + m_{q_I})(\mathcal{L} P_L + \mathcal{R} P_R)(l + \not{p}_u + m_{\tilde{g}}) \gamma^\mu (l + \not{p}_u + \not{p}_b + m_{\tilde{g}})}{\mathcal{D}_1 \mathcal{D}_2 \mathcal{D}_3} \right] \quad (\text{C.126})$$

$$= -\frac{ig_s^3}{(4\pi)^2} C_A T_R T_{\beta\alpha}^a \quad (\text{C.127})$$

$$\int_l \text{Tr} \left[ \frac{(\mathcal{L}' \mathcal{R} P_L + \mathcal{R}' \mathcal{L} P_R)(l)(l + \not{p}_u + m_{\tilde{g}}) \gamma^\mu (l + \not{p}_u + \not{p}_b + m_{\tilde{g}})}{\mathcal{D}_1 \mathcal{D}_2 \mathcal{D}_3} \right] \quad (\text{C.128})$$

$$\int_l \text{Tr} \left[ \frac{(\mathcal{L}' \mathcal{L} P_L + \mathcal{R}' \mathcal{R} P_R)(m_{q_I})(l + \not{p}_u + m_{\tilde{g}}) \gamma^\mu (l + \not{p}_u + \not{p}_b + m_{\tilde{g}})}{\mathcal{D}_1 \mathcal{D}_2 \mathcal{D}_3} \right] \quad (\text{C.129})$$

$$= -\frac{ig_s^3}{(4\pi)^2} C_A T_R T_{\beta\alpha}^a \quad (C.130)$$

$$\int_l \frac{2(\mathcal{L}'\mathcal{R} + \mathcal{R}'\mathcal{L}) \left( l^\mu(l^2 + m_{\tilde{g}}^2 - p_u \cdot p_b) + (l \cdot p_b) p_u^\mu + (l \cdot p_u + l^2)(2p_u + p_b)^\mu \right)}{\mathcal{D}_1 \mathcal{D}_2 \mathcal{D}_3} \quad (C.131)$$

$$\int_l \frac{2(\mathcal{L}'\mathcal{L} + \mathcal{R}'\mathcal{R}) m_{q_I} m_{\tilde{g}} (2l + 2p_u + p_b)^\mu}{\mathcal{D}_1 \mathcal{D}_2 \mathcal{D}_3} \quad (C.132)$$

$$= -\frac{ig_s^3}{(4\pi)^2} C_A T_R T_{\beta\alpha}^a 2 \left( (\mathcal{L}'\mathcal{L} + \mathcal{R}'\mathcal{R}) m_{q_I} m_{\tilde{g}} (2C^\mu + (2p_u + p_b)^\mu C_0) + (\mathcal{L}'\mathcal{R} + \mathcal{R}'\mathcal{L}) \right. \quad (C.133)$$

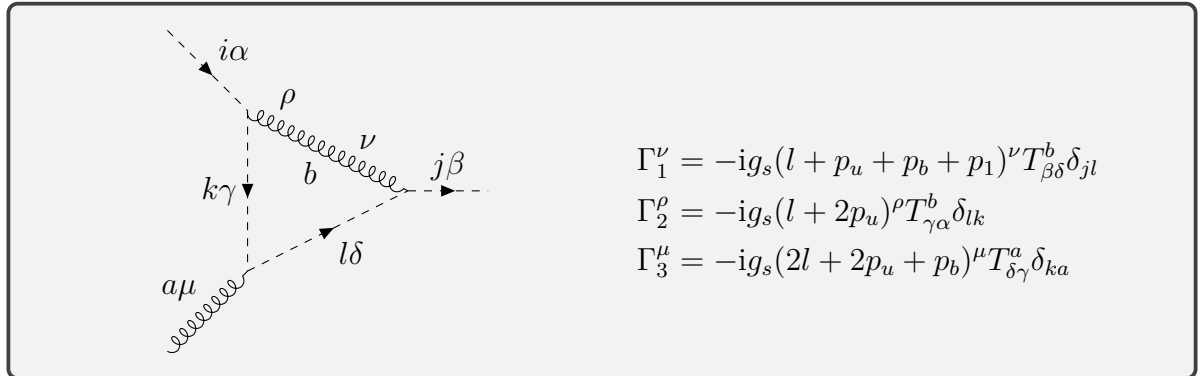
$$\left. \left( C^{\sigma\sigma\mu} + C^{\sigma\sigma} (2p_u + p_b)^\mu + C^\sigma (p_b^\sigma p_u^\mu + p_u^\sigma (2p_u + p_b)^\mu) + C^\mu (m_{\tilde{g}}^2 - p_u \cdot p_b) \right) \right) \quad (C.134)$$

To get the counterterm we consider only the UV divergent part  $\overline{\mathbf{UV}}$  by looking at table 11:

$$\overline{\mathbf{UV}}[\Lambda] = -\frac{ig_s^3}{(4\pi)^2} T_R C_A 2 \frac{1}{2} (-2) T_{\beta\alpha}^a (2p_u + p_b)^\mu (4) \left( \frac{1}{4} \Delta \right) \quad (C.135)$$

$$= \frac{ig_s^2}{(4\pi)^2} T_R C_A 2 \Delta T_{\beta\alpha}^a \delta_{ij} (2p_u + p_b)^\mu \quad (C.136)$$

### Gluon squark squark loop



$$\Lambda_{\beta\alpha}^{\mu a}(p_u^2, 0, m_{\tilde{q}}^2, 0, m_{\tilde{q}}^2, m_{\tilde{q}}^2) \quad (C.137)$$

$$= \mu^{4-D} \int \frac{d^D l}{(2\pi)^D} \Gamma_1^\nu \frac{-ig^{\rho\nu}}{\mathcal{D}_1} \Gamma_2^\rho \frac{i}{\mathcal{D}_2} \Gamma_3^\mu \frac{i}{\mathcal{D}_3} \quad (C.138)$$

$$= -\frac{ig_s^3}{(4\pi)^2} \underbrace{T_{\beta\delta}^b T_{\gamma\alpha}^b T_{\delta\gamma}^a}_{-\frac{T_R}{C_A} T_{\beta\alpha}^a} \delta_{ij} \int_l \frac{(l + p_u + p_b + p_1) \cdot (l + 2p_u)(2l + 2p_u + p_b)^\mu}{\mathcal{D}_1 \mathcal{D}_2 \mathcal{D}_3} \quad (C.139)$$

$$= \frac{ig_s^3}{(4\pi)^2} \frac{T_R}{C_A} T_{\beta\alpha}^a \delta_{ij} \left( (C_0(2p_u + p_b)^\mu + 2C^\mu)(p_u^2 + p_b \cdot p_u + p_1 \cdot p_u) \right) \quad (C.140)$$

$$+C^{\sigma\sigma}(2p_u + p_b)^\mu + 2C^{\sigma\sigma\mu} + (2C^{\sigma\mu} + C^\sigma(2p_u + p_b)^\mu)(4p_u + 2p_b)^\sigma) \quad (\text{C.141})$$

$$(\text{C.142})$$

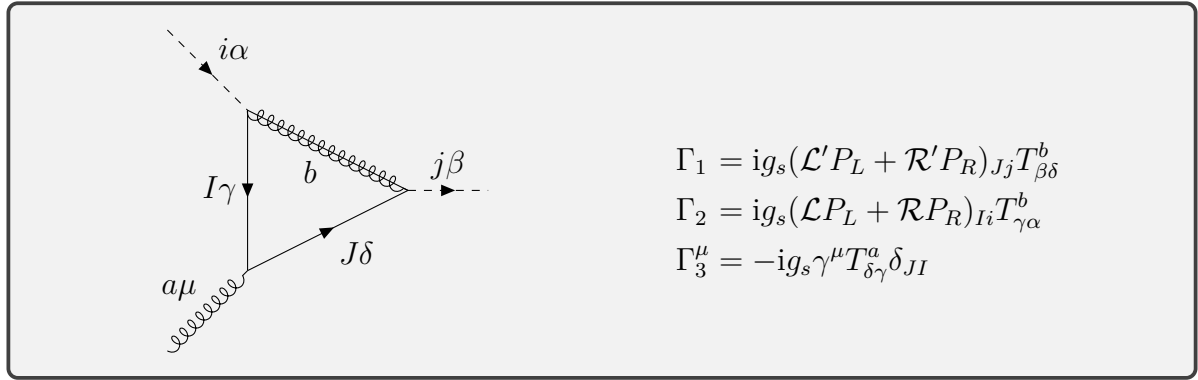
In the last step  $p_1 = p_u + p_b$  has been replaced.

To get the counterterm we consider only the UV divergent part  $\overline{\text{UV}}$  by looking at table 11:

$$\overline{\text{UV}}[\Lambda] = \frac{ig_s^3}{(4\pi)^2} \frac{T_R}{C_A} T_{\beta\alpha}^a \delta_{ij} (2p_u + p_b)^\mu \left( (4+4)\left(\frac{1}{4}\Delta\right) + (2 \cdot 6 \cdot 2)\left(-\frac{1}{12}\Delta\right) \right) \quad (\text{C.143})$$

$$= -\frac{ig_s^3}{(4\pi)^2} \frac{T_R}{C_A} \Delta T_{\beta\alpha}^a \delta_{ij} (2p_u + p_b)^\mu \quad (\text{C.144})$$

### Gluino quark quark loop



$$\Lambda_{\beta\alpha}^{\mu a}(p_u^2, 0, m_{\tilde{q}}^2, m_{\tilde{g}}^2, m_{q_I}^2, m_{q_I}^2) \quad (\text{C.145})$$

$$= \mu^{4-D} \int \frac{d^D l}{(2\pi)^D} (-1) \text{Tr} \left[ \Gamma_1 \frac{i(l + \not{p}_u + \not{p}_b + m_{q_I})}{\mathcal{D}_1} \Gamma_3^\mu \frac{i(l + \not{p}_u + m_{q_I})}{\mathcal{D}_2} \Gamma_2 \frac{i(l + m_{\tilde{g}})}{\mathcal{D}_3} \right] \quad (\text{C.146})$$

$$= \frac{ig_s^3}{(4\pi)^2} \frac{T_R}{C_A} T_{\beta\alpha}^a \quad (\text{C.147})$$

$$\int_l \text{Tr} \left[ \frac{(\mathcal{L}'P_L + \mathcal{R}'P_R)(l + \not{p}_u + \not{p}_b + m_{q_I})\gamma^\mu(l + \not{p}_u + m_{q_I})(\mathcal{L}P_L + \mathcal{R}P_R)(l + m_{\tilde{g}})}{\mathcal{D}_1 \mathcal{D}_2 \mathcal{D}_3} \right] \quad (\text{C.148})$$

$$= \frac{ig_s^3}{(4\pi)^2} \frac{T_R}{C_A} T_{\beta\alpha}^a 2((\mathcal{L}'\mathcal{L} + \mathcal{R}'\mathcal{R})m_{q_I}m_{\tilde{g}}(2C^\mu + (2p_u + p_b)^\mu C_0)^\mu + (\mathcal{L}'\mathcal{R} + \mathcal{R}'\mathcal{L}) \quad (\text{C.149})$$

$$(C^{\sigma\sigma\mu} + C^{\sigma\sigma}(2p_u + p_b)^\mu + C^\sigma(p_b^\sigma p_u^\mu + p_u^\sigma(2p_u + p_b)^\mu) + C^\mu(m_{\tilde{g}}^2 - p_u \cdot p_b)) \quad (\text{C.150})$$

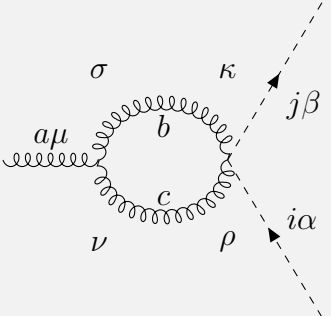
Giving us the same vertex correction as in appendix C.2.2 only with a different colour factor and swapped masses  $m_{\tilde{g}} \leftrightarrow m_{q_I}$ .

To get the counterterm we consider only the UV divergent part  $\overline{\mathbf{UV}}$  by looking at table 11:

$$\overline{\mathbf{UV}}[\Lambda] = \frac{ig_s^3}{(4\pi)^2} \frac{T_R}{C_A} 2 \frac{1}{2} (-2) T_{\beta\alpha}^a (2p_u + p_b)^\mu (4) \left(\frac{1}{4} \Delta\right) \quad (\text{C.151})$$

$$= -\frac{ig_s^3}{(4\pi)^2} \frac{T_R}{C_A} 2 T_{\beta\alpha}^a (2p_u + p_b)^\mu \Delta \quad (\text{C.152})$$

### Gluon gluon loop



$$\Gamma_1^\mu = -ig_s f^{cba} \Gamma^{\mu\sigma\nu}$$

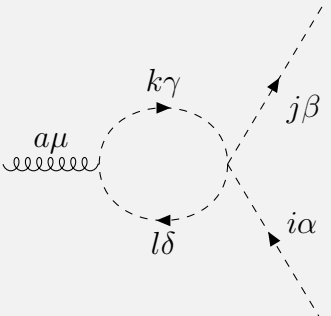
$$\Gamma_2^\nu \sigma = ig_s^2 g^{\rho\kappa} (T^c T^b + T^b T^c)_{\beta\alpha} \delta_{ji}$$

$$\Lambda_{\beta\alpha}^{\mu a}(0, 0, 0) \quad (\text{C.153})$$

$$= 0 \quad (\text{C.154})$$

Since  $f^{cba}(T^c T^b + T^b T^c) = 0$  due to the antisymmetry and also from the fact that the gluon is on-shell.

### Squark squark loop



$$\Gamma_1^\mu = ig_s (2l + p_b)^\mu T_{\gamma\delta}^a$$

$$\Gamma_2 = -i(X_{ijkl} \delta_{\beta\alpha} \delta_{\gamma\delta} + Y_{ijkl} \delta_{\alpha\delta} \delta_{\beta\gamma})$$

$$\Lambda_{\beta\alpha}^{\mu a}(0, m_{\tilde{q}_k}^2, m_{\tilde{q}_k}^2) \quad (\text{C.155})$$

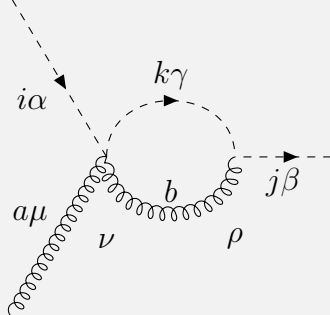
$$= \mu^{4-D} \int \frac{d^D l}{(2\pi)^D} \Gamma_1^\mu \frac{i}{\mathcal{D}_1} \Gamma_2 \frac{i}{\mathcal{D}_2} \quad (\text{C.156})$$

$$= - \frac{ig_s}{(4\pi)^2} Y_{ijkk} T_{\beta\alpha}^a \int_l \frac{(2l + p_b)^\mu}{\mathcal{D}_1 \mathcal{D}_2} \quad (\text{C.157})$$

$$= - \frac{ig_s}{(4\pi)^2} Y_{ijkk} T_{\beta\alpha}^a p_b^\mu (2B_1 + B_0) \quad (\text{C.158})$$

$$= 0 \quad (\text{C.159})$$

### Gluon squark loop



$$\begin{aligned} \Gamma_1^{\mu\nu} &= ig_s^2 g^{\mu\nu} (T^a T^b + T^b T^a)_{\gamma\alpha} \delta_{ki} \\ \Gamma_2^\rho &= -ig_s (-l + p_1)^\rho T_{\beta\gamma}^b \delta_{jk} \end{aligned}$$

$$\Lambda_{\beta\alpha}^{\mu a}(p_1^2 = m_{\tilde{q}_i}^2, m_{\tilde{q}_i}^2, 0) \quad (\text{C.160})$$

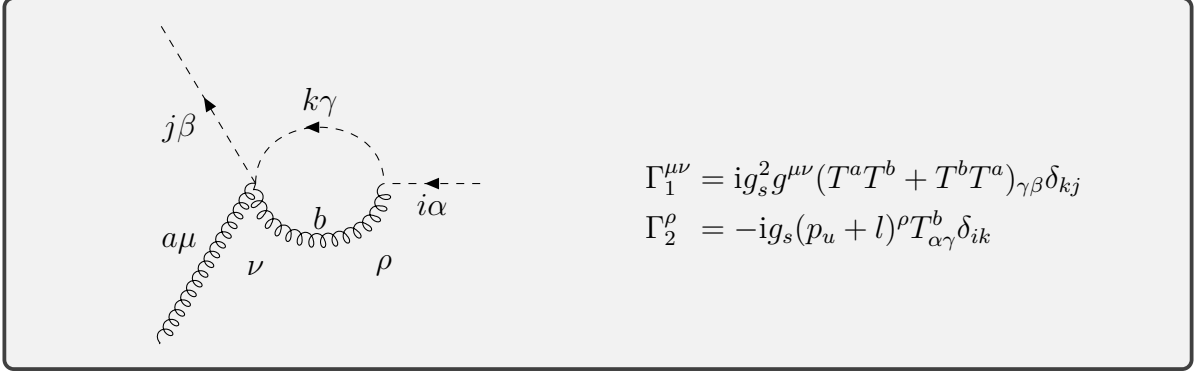
$$= \mu^{4-D} \int \frac{d^D l}{(2\pi)^D} \Gamma_1^{\mu\nu} \frac{i}{\mathcal{D}_1} \Gamma_2^\rho \frac{-ig^{\rho\nu}}{\mathcal{D}_2} \quad (\text{C.161})$$

$$= \frac{ig_s^3}{(4\pi)^2} T_{\beta\alpha}^a (C_F - \frac{1}{2C_A}) \int_l \frac{(-l + p_1)^\mu}{\mathcal{D}_1 \mathcal{D}_2} \quad (\text{C.162})$$

$$= \frac{ig_s^3}{(4\pi)^2} T_{\beta\alpha}^a (C_F - \frac{1}{2C_A}) (-B^\mu + B_0 p_1^\mu) \quad (\text{C.163})$$

$$= \frac{ig_s^3}{(4\pi)^2} T_{\beta\alpha}^a (C_F - \frac{1}{2C_A}) (B_0 - B_1) p_1^\mu \quad (\text{C.164})$$

Next up, the corresponding crossing is  $p_1 \rightarrow -p_u$  and we get a factor of  $(-1)$  from the inverions of the charge flow:



$$\Lambda_{\beta\alpha}^{\mu a}(p_u^2, m_{\tilde{q}_i}^2, 0) \quad (\text{C.165})$$

$$= \frac{ig_s^3}{(4\pi)^2} T_{\beta\alpha}^a (C_F - \frac{1}{2C_A}) (B_0 - B_1) p_u^\mu \quad (\text{C.166})$$

To get the counterterm for both diagrams we consider only the UV divergent part  $\overline{\text{UV}}$  by looking at table 11:

$$\overline{\text{UV}}[\Lambda] = \frac{ig_s^3}{(4\pi)^2} T_{\beta\alpha}^a (C_F - \frac{1}{2C_A}) (1 + \frac{1}{2}) \Delta(2p_u + p_b)^\mu \quad (\text{C.167})$$

$$= -\frac{ig_s^3}{(4\pi)^2} T_{\beta\alpha}^a \frac{7}{4} \Delta(2p_u + p_b)^\mu \quad (\text{C.168})$$

### C.2.3. Quark-squark-gaugino vertex

We compute the loop corrections to the  $q\tilde{q}\tilde{\chi}$ -vertex using the parametrization displayed in fig. 24. This vertex appears in both the s-channel and u-channel.

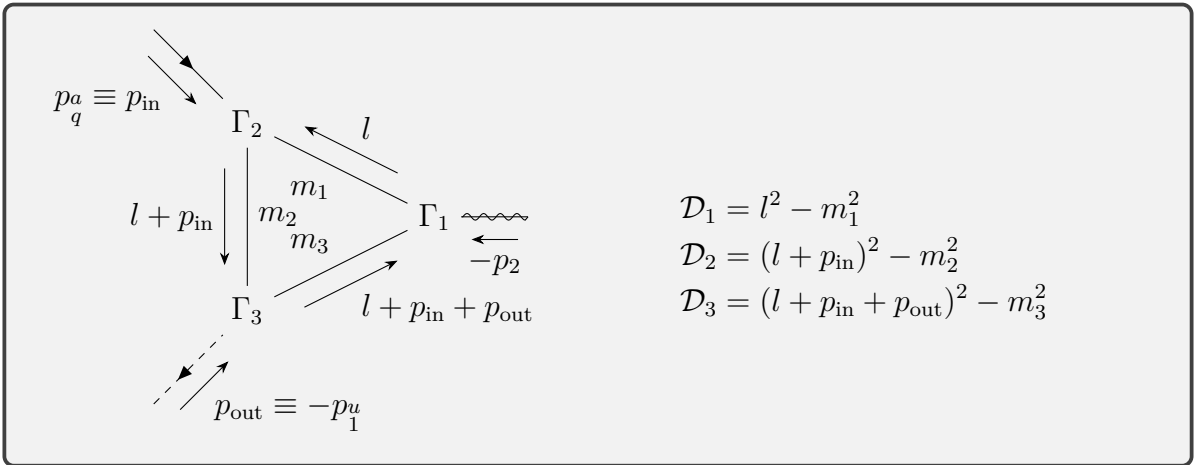
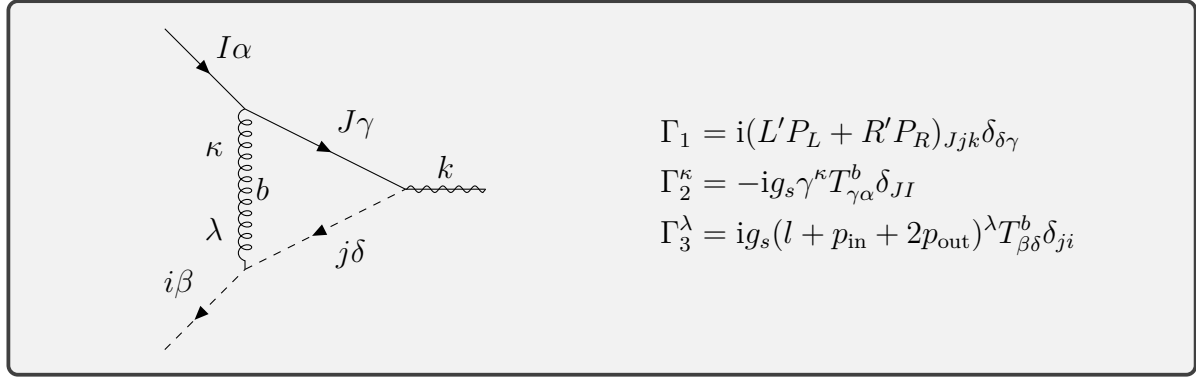


Figure 24: Parametrization of the  $q\tilde{q}\tilde{\chi}$ -vertex



### Quark-gluon-squark loop



$$\Lambda_{\beta\alpha}(p_{\text{in}}^2, p_{\text{out}}^2, m_{\tilde{\chi}}^2, 0, 0, m_{\tilde{q}}^2) \quad (\text{C.169})$$

$$= \mu^{4-D} \int \frac{d^D l}{(2\pi)^D} \Gamma_1 \frac{-i\not{l}}{\mathcal{D}_1} \Gamma_2^\kappa \frac{-ig^{\kappa\lambda}}{\mathcal{D}_2} \Gamma_3^\lambda \frac{i}{\mathcal{D}_3} \quad (\text{C.170})$$

$$= \frac{ig_s^3}{(4\pi)^2} C_F \delta_{\beta\alpha} (L'P_L + R'P_R) \int_l \frac{\not{l}(\not{l} + \not{p}_{\text{in}} + 2\not{p}_{\text{out}})}{\mathcal{D}_1 \mathcal{D}_2 \mathcal{D}_3} \quad (\text{C.171})$$

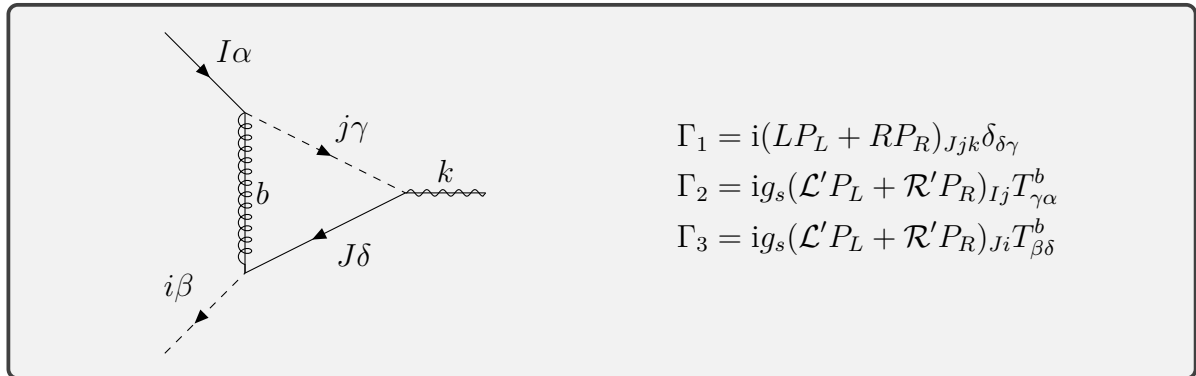
$$= \frac{ig_s^3}{(4\pi)^2} C_F \delta_{\beta\alpha} (L'P_L + R'P_R)_{Ii} (C^{\mu\mu} + \gamma^\mu C^\mu (\not{p}_{\text{in}} + 2\not{p}_{\text{out}})) \quad (\text{C.172})$$

$$(\text{C.173})$$

To get the counterterm we consider only the UV divergent part  $\overline{\mathbf{UV}}$  by looking at table 11:

$$\delta \bar{Z}_g \Gamma = \frac{ig_s^3}{(4\pi)^2} C_F \delta_{\beta\alpha} (L'P_L + R'P_R) 4\left(\frac{1}{4}\Delta\right) \quad (\text{C.174})$$

### Squark-gluino-quark loop



$$\Lambda_{\beta\alpha}(p_{\text{in}}^2, p_{\text{out}}^2, m_{\tilde{\chi}}^2, m_{\tilde{q}_J}^2, m_{\tilde{g}}, m_{q_J}^2) \quad (\text{C.175})$$

$$= \mu^{4-D} \int \frac{d^D l}{(2\pi)^D} \Gamma_1 \frac{i(l + \not{p}_{\text{in}} + \not{p}_{\text{out}} + m_{q_J})}{\mathcal{D}_3} \Gamma_3 \frac{i(l + \not{p}_{\text{in}} + m_{\tilde{g}})}{\mathcal{D}_2} \Gamma_2 \frac{i}{\mathcal{D}_1} \quad (\text{C.176})$$

$$= -\frac{ig_s^3}{(4\pi)^2} C_F \delta_{\beta\alpha} (LP_L + RP_R) \quad (\text{C.177})$$

$$\int_l \frac{(l + \not{p}_{\text{in}} + \not{p}_{\text{out}} + m_{q_J})(\mathcal{L}'P_L + \mathcal{R}'P_R)(l + \not{p}_{\text{in}} + m_{\tilde{g}})(\mathcal{L}'P_L + \mathcal{R}'P_R)}{\mathcal{D}_1 \mathcal{D}_2 \mathcal{D}_3} \quad (\text{C.178})$$

$$= -\frac{ig_s^3}{(4\pi)^2} C_F \delta_{\beta\alpha} \quad (\text{C.179})$$

$$\left( (L\mathcal{L}'\mathcal{R}'P_L + R\mathcal{R}'\mathcal{L}'P_R) \left( C^{\mu\mu} + C_0(\not{p}_{\text{in}} + \not{p}_{\text{out}})(\not{p}_{\text{in}} + m_{\tilde{g}}) + C^\mu \gamma^\mu (2\not{p}_{\text{in}} + \not{p}_{\text{out}} + m_{\tilde{g}}) \right) \right) \quad (\text{C.180})$$

$$(L\mathcal{L}'\mathcal{L}'P_L + R\mathcal{R}'\mathcal{R}'P_R) m_{q_J} (C^\mu \gamma^\mu + C_0(\not{p}_{\text{in}} + m_{\tilde{g}})) \quad (\text{C.181})$$

To get the counterterm we consider only the UV divergent part  $\overline{\text{UV}}$  by looking at table 11. Due to the coupling

$$\delta \bar{Z}_g \Gamma = 0. \quad (\text{C.182})$$

#### C.2.4. Gluino-gaugino-gluon vertex

We compute the loop corrections to the  $\tilde{g}\tilde{\chi}g$ -vertex using the parametrization displayed in fig. 25. This vertex appears in neither the s-channel nor the u-channel. The diagram containing this vertex correction is shown in fig. 26 and gets combined with the conjugated s-channel and u-channel.

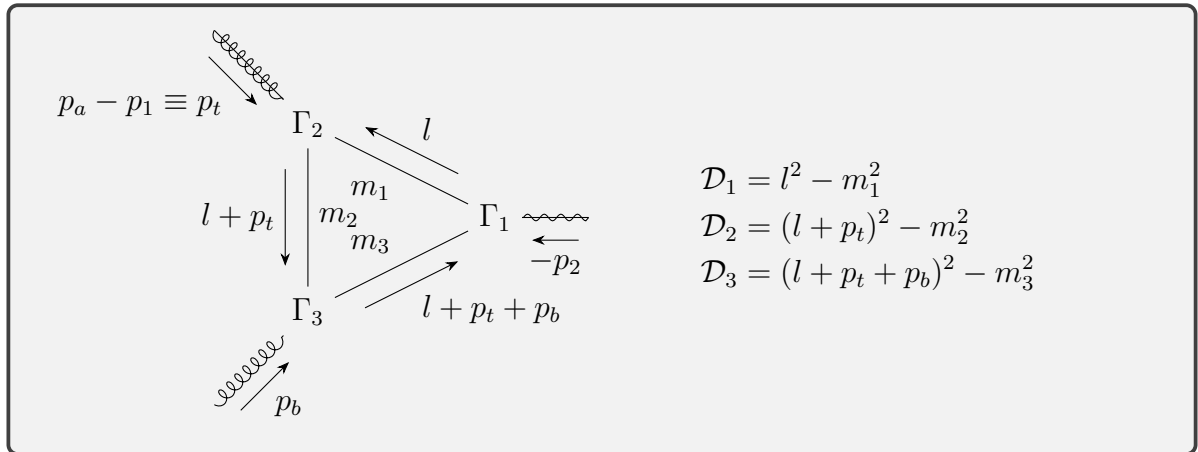


Figure 25: Parametrization of the  $\tilde{g}\tilde{\chi}g$ -vertex

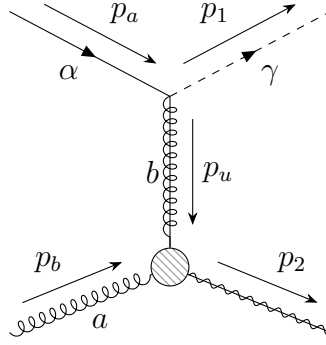
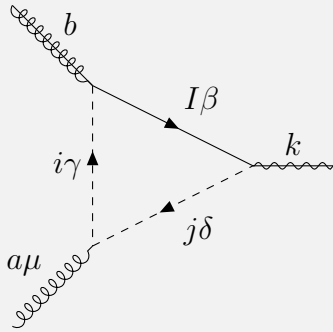


Figure 26: Loosely identified t-channel diagram.

### Quark-squark-squark loop



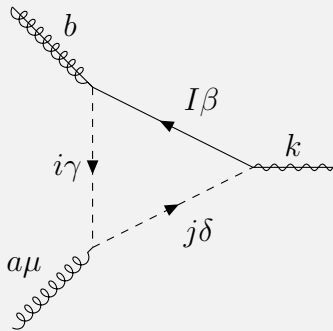
$$\begin{aligned}\Gamma_1 &= i(P_L L'_{Ijk} + P_R R'_{Ijk})\delta_{\gamma\delta} \\ \Gamma_2 &= ig_s(P_L \mathcal{L}_{Ii} + P_R \mathcal{R}_{Ii})T_{\beta\gamma}^b \\ \Gamma_3^\mu &= ig_s(2l + 2p_t + p_b)^\mu T_{\gamma\delta}^a \delta_{ij}\end{aligned}$$

$$\Lambda^{\mu ab}(p_t^2, 0, m_{\tilde{\chi}_k}^2, m_{q_I}^2, m_{\tilde{q}_i}^2, m_{\tilde{q}_i}^2) \quad (\text{C.183})$$

$$= \mu^{4-D} \int \frac{d^D l}{(2\pi)^D} \Gamma_1 \frac{-i \not{l}}{\mathcal{D}_1} \Gamma_2 \frac{i}{\mathcal{D}_2} \Gamma_3^\mu \frac{i}{\mathcal{D}_3} \quad (\text{C.184})$$

$$= -\frac{g_s^2}{(4\pi)^2} (P_L L' \mathcal{R} + P_R R' \mathcal{L}) \int_l \frac{l(2l + 2p_t + p_b)^\mu}{\mathcal{D}_1 \mathcal{D}_2 \mathcal{D}_3} T_{\beta\gamma}^b T_{\gamma\beta}^a \quad (\text{C.185})$$

$$= -\frac{g_s^2}{(4\pi)^2} T_R \delta^{ab} (P_L L'_{Iik} \mathcal{R}_{Ii} + P_R R'_{Iik} \mathcal{L}_{Ii}) \gamma_\nu (2C^{\nu\mu} + C^\nu (2p_t + p_b)^\mu) \quad (\text{C.186})$$



$$\begin{aligned}\Gamma_1 &= i(P_L L_{Ijk} + P_R R_{Ijk})\delta_{\gamma\delta} \\ \Gamma_2 &= ig_s(P_L \mathcal{L}'_{Ii} + P_R \mathcal{R}'_{Ii})T_{\gamma\beta}^b \\ \Gamma_3^\mu &= ig_s(2l + 2p_t + p_b)^\mu T_{\delta\gamma}^a \delta_{ij}\end{aligned}$$

The inversion in the charge flow gives the same result with

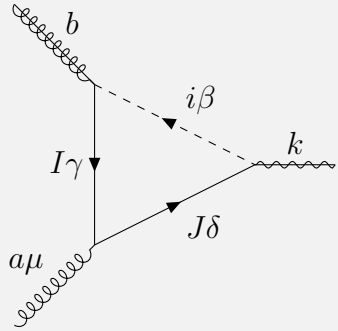
$$L \leftrightarrow L' \quad (C.187)$$

$$R \leftrightarrow R' \quad (C.188)$$

$$\mathcal{L} \leftrightarrow \mathcal{L}' \quad (C.189)$$

$$\mathcal{R} \leftrightarrow \mathcal{R}' . \quad (C.190)$$

### Squark-quark-quark loop



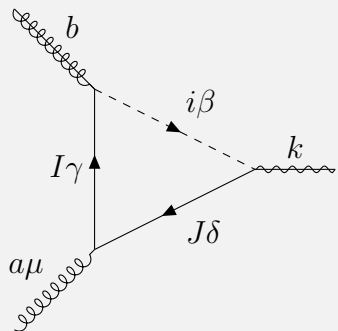
$$\begin{aligned} \Gamma_1 &= i(P_L L'_{Jik} + P_R R'_{Jik}) \delta_{\gamma\delta} \\ \Gamma_2 &= ig_s (P_L \mathcal{L}_{Ii} + P_R \mathcal{R}_{Ii}) T_{\beta\gamma}^b \\ \Gamma_3^\mu &= -ig_s \gamma^\mu T_{\gamma\delta}^a \delta_{IJ} \end{aligned}$$

$$\Lambda^{\mu ab}(p_t^2, 0, m_{\tilde{\chi}_k}^2, m_{\tilde{q}_i}^2, m_{q_I}^2, m_{q_I}^2) \quad (C.191)$$

$$= \mu^{4-D} \int \frac{d^D l}{(2\pi)^D} \Gamma_1 \frac{i(\not{l} + \not{p}_t + \not{p}_b)}{\mathcal{D}_3} \Gamma_3^\mu \frac{i(\not{l} + \not{p}_t)}{\mathcal{D}_2} \Gamma_2 \frac{i}{\mathcal{D}_1} \quad (C.192)$$

$$= -\frac{g_s^2}{(4\pi)^2} (P_L L' \mathcal{R} + P_R R' \mathcal{L}) \int_l \frac{(\not{l} + \not{p}_t + \not{p}_b) \gamma^\mu (\not{l} + \not{p}_t)}{\mathcal{D}_1 \mathcal{D}_2 \mathcal{D}_3} T_{\gamma\beta}^a T_{\beta\gamma}^b \quad (C.193)$$

$$\begin{aligned} &= -\frac{g_s^2}{(4\pi)^2} T_R \delta^{ab} (P_L L'_{Iik} \mathcal{R}_{Ii} + P_R R'_{Iik} \mathcal{L}_{Ii}) (2C^{\nu\mu} \gamma_\nu + C^{\nu\nu} \gamma^\mu \\ &\quad + C^\nu (\gamma_\nu \gamma^\mu \not{p}_t + (\not{p}_t + \not{p}_b) \gamma^\mu \gamma_\nu) + C_0 (\not{p}_t + \not{p}_b) \gamma^\mu \not{p}_t) \end{aligned} \quad (C.194)$$



$$\begin{aligned} \Gamma_1 &= i(P_L L'_{Jik} + P_R R'_{Jik}) \delta_{\gamma\delta} \\ \Gamma_2 &= ig_s (P_L \mathcal{L}_{Ii} + P_R \mathcal{R}_{Ii}) T_{\beta\gamma}^b \\ \Gamma_3^\mu &= -ig_s \gamma^\mu T_{\gamma\delta}^a \delta_{IJ} \end{aligned}$$

The inversion in the charge flow gives the same result with

$$L \leftrightarrow L' \tag{C.195}$$

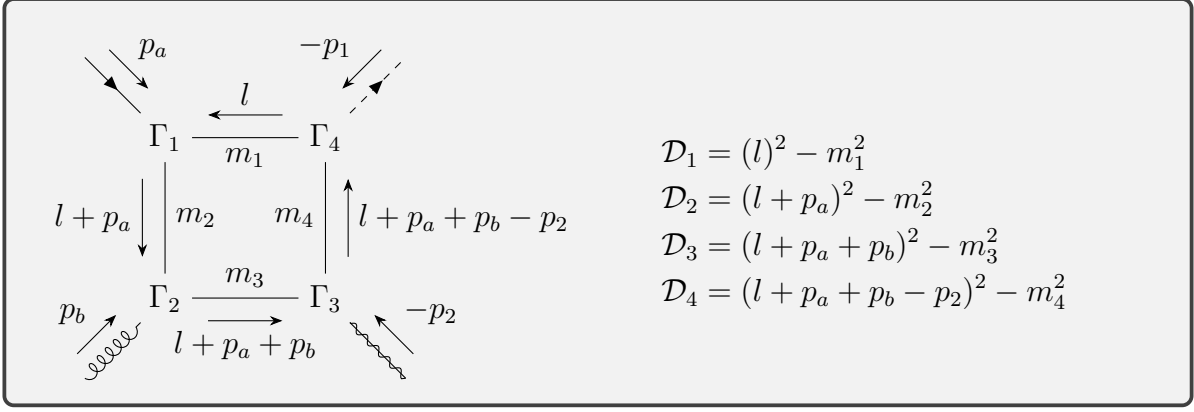
$$R \leftrightarrow R' \tag{C.196}$$

$$\mathcal{L} \leftrightarrow \mathcal{L}' \tag{C.197}$$

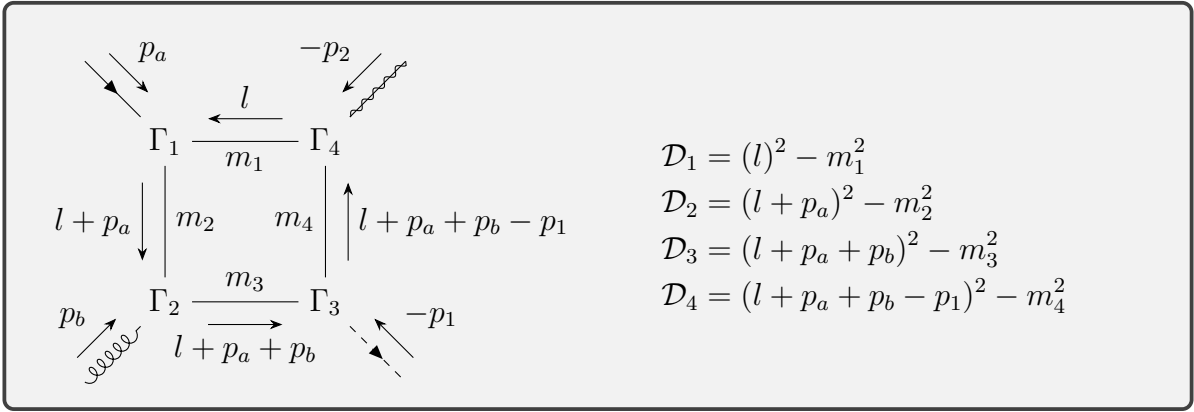
$$\mathcal{R} \leftrightarrow \mathcal{R}' . \tag{C.198}$$

### C.3. Boxes

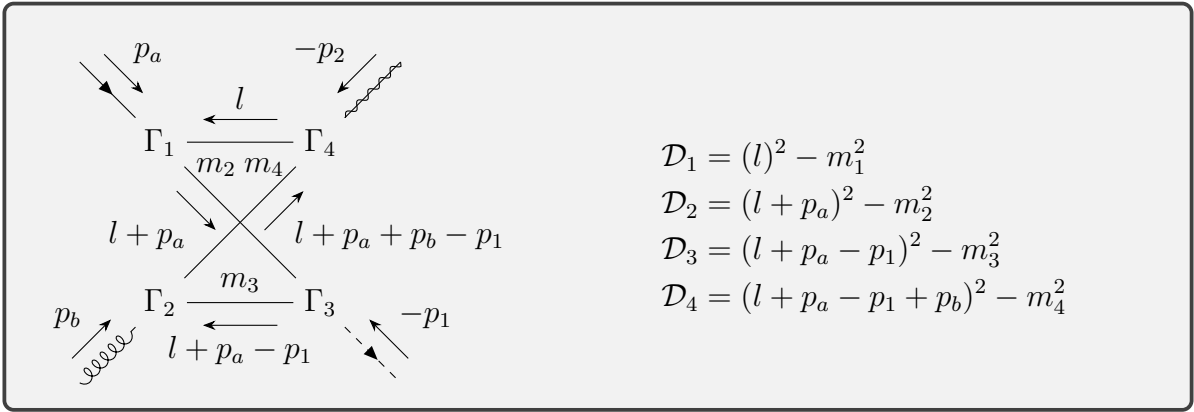
We compute the loop corrections to the Boxes using the parametrization displayed in fig. 27. Since the results get quite big, we only give the first steps and the remaining calculation can be done with e.g. `FeynCalc` in `Mathematica`.



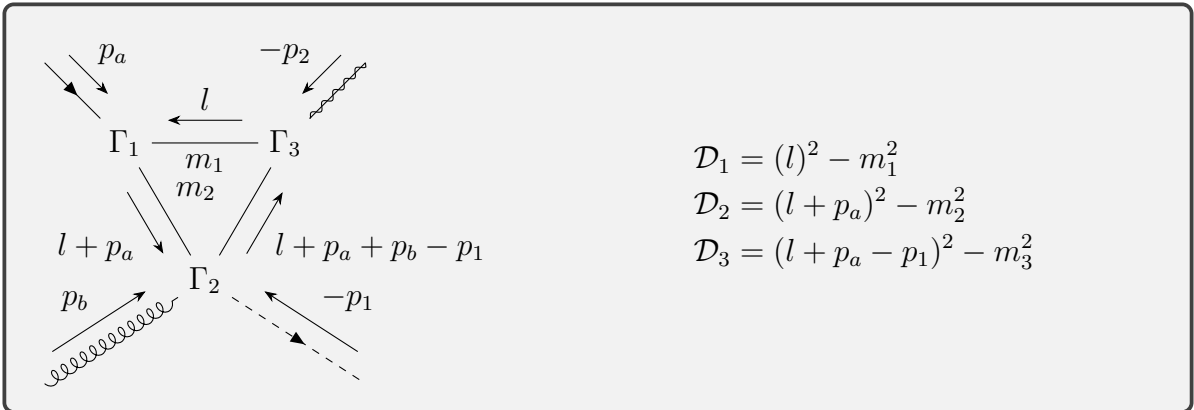
(i)



(ii)



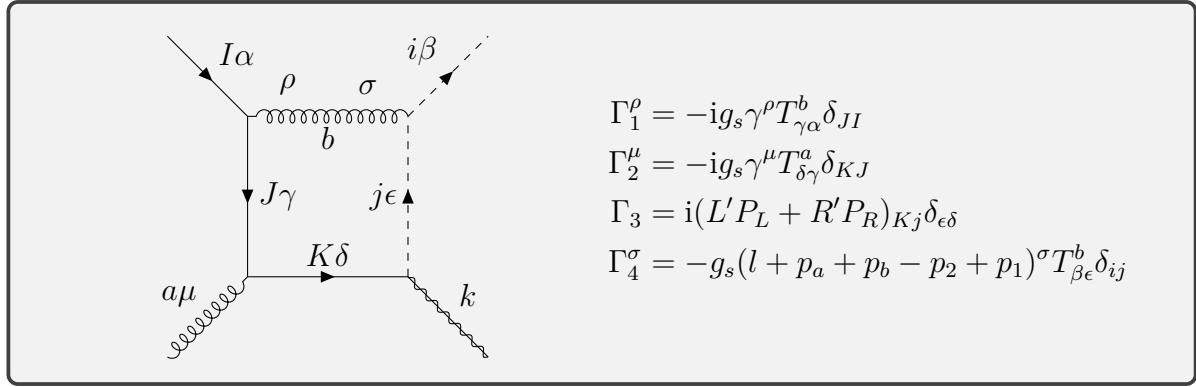
(iii)



(iv)

Figure 27: Parametrization of the Boxes

## C.3.1. Gluon-quark-quark-squark box

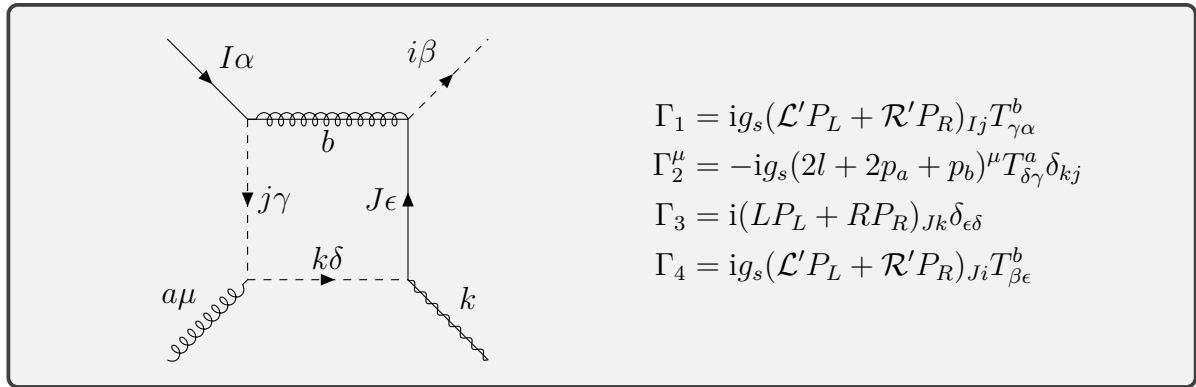


$$B_{\beta\alpha}^{\mu a}(0, 0, m_{\tilde{\chi}_k}^2, m_{\tilde{q}_i}^2, s, t, 0, 0, 0, m_{\tilde{q}_i}^2) \quad (C.199)$$

$$= \mu^{4-D} \int \frac{d^D l}{(2\pi)^D} \Gamma_4^\sigma \frac{i}{\mathcal{D}_4} \Gamma_3 \frac{i(l + \not{p}_a + \not{p}_b)}{\mathcal{D}_2} \Gamma_2^\mu \frac{i(l + \not{p}_a)}{\mathcal{D}_3} \Gamma_1^\rho \frac{-ig_{\sigma\rho}}{\mathcal{D}_1} \quad (C.200)$$

$$\begin{aligned}&= \frac{ig_s^3}{(4\pi)^2} (L'P_L + R'P_R)_{Ii} \int_l \frac{(l + \not{p}_a + \not{p}_b) \gamma^\mu (l + \not{p}_a) (l + 2\not{p}_a + 2\not{p}_b - 2\not{p}_2)}{\mathcal{D}_1 \mathcal{D}_2 \mathcal{D}_3 \mathcal{D}_4} \\ &\quad T_{\beta\epsilon}^b T_{\epsilon\gamma}^a T_{\gamma\alpha}^b \quad (C.201)\end{aligned}$$

## C.3.2. Gluino-squark-squark-quark box



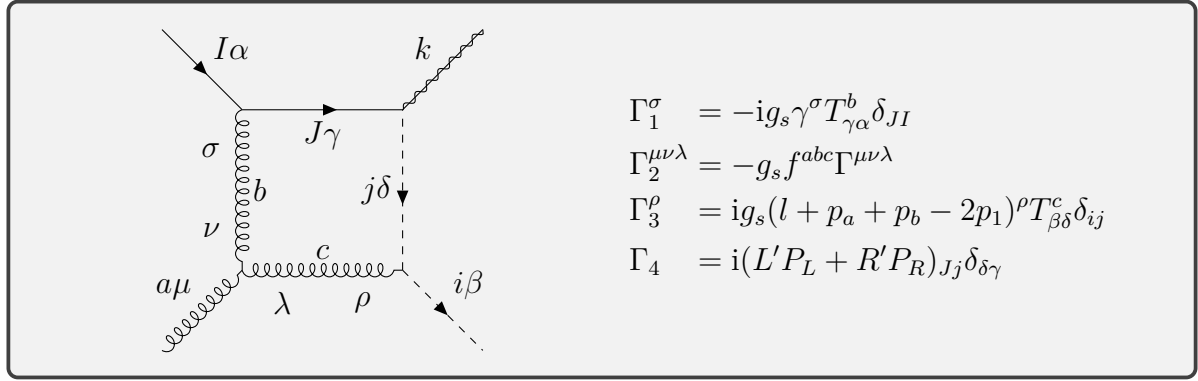
$$B_{\beta\alpha}^{\mu a}(0, 0, m_{\tilde{\chi}_k}^2, m_{\tilde{q}_i}^2, s, t, m_{\tilde{g}}^2, m_{\tilde{q}_j}^2, m_{\tilde{q}_j}^2, m_{\tilde{q}_j}^2) \quad (C.202)$$

$$= \mu^{4-D} \int \frac{d^D l}{(2\pi)^D} \Gamma_3 \frac{-i(l + \not{p}_a + \not{p}_b - \not{p}_2 - m_{q_J})}{\mathcal{D}_4} \Gamma_4 \frac{i(l + m_{\tilde{g}})}{\mathcal{D}_1} \Gamma_1 \frac{i}{\mathcal{D}_2} \Gamma_2^\mu \frac{i}{\mathcal{D}_3} \quad (C.203)$$

$$= \frac{ig_s^3}{(4\pi)^2} T_{\beta\epsilon}^b T_{\epsilon\gamma}^a T_{\gamma\alpha}^b \int_l (2l + 2p_a + p_b)^\mu$$

$$\begin{aligned}
& \left( -(L_{Jj}\mathcal{L}'\mathcal{L}'P_L + R_{Jj}\mathcal{R}'\mathcal{R}'P_R) \frac{m_{qJ}m_{\tilde{g}}}{\mathcal{D}_1\mathcal{D}_2\mathcal{D}_3\mathcal{D}_4} \right. \\
& + (L_{Jj}\mathcal{R}'\mathcal{R}'P_L + R_{Jj}\mathcal{L}'\mathcal{L}'P_R) \frac{(l + \not{p}_a + \not{p}_b - \not{p}_2)m_{\tilde{g}}}{\mathcal{D}_1\mathcal{D}_2\mathcal{D}_3\mathcal{D}_4} \\
& - (L_{Jj}\mathcal{L}'\mathcal{R}'P_L + R_{Jj}\mathcal{R}'\mathcal{L}'P_R) \frac{m_{qJ}l}{\mathcal{D}_1\mathcal{D}_2\mathcal{D}_3\mathcal{D}_4} \\
& \left. + (L_{Jj}\mathcal{R}'\mathcal{L}'P_L + R_{Jj}\mathcal{L}'\mathcal{R}'P_R) \frac{(l + \not{p}_a + \not{p}_b - \not{p}_2)l}{\mathcal{D}_1\mathcal{D}_2\mathcal{D}_3\mathcal{D}_4} \right)
\end{aligned} \tag{C.204}$$

### C.3.3. Quark-gluon-gluon-squark box



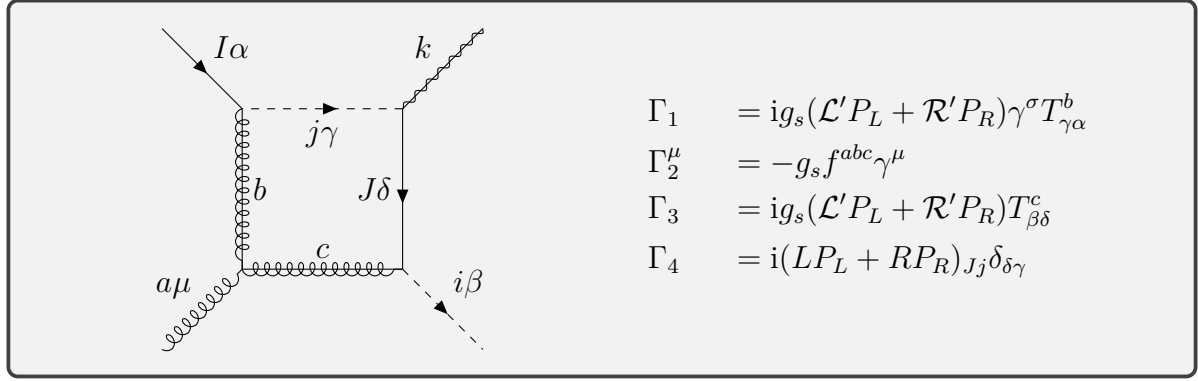
$$B_{\beta\alpha}^{\mu a}(0, 0, m_{\tilde{q}_i}^2, m_{\tilde{\chi}_k}^2, s, u, 0, 0, 0, m_{\tilde{q}_i}^2) \tag{C.205}$$

$$= \mu^{4-D} \int \frac{d^D l}{(2\pi)^D} \Gamma_4 \frac{-i\not{l}}{\mathcal{D}_1} \Gamma_1^\sigma \frac{-ig_{\sigma\nu}}{\mathcal{D}_2} \Gamma_2^{\mu\nu\lambda} \frac{-ig_{\lambda\rho}}{\mathcal{D}_3} \Gamma_3^\rho \frac{i}{\mathcal{D}_4} \tag{C.206}$$

$$\begin{aligned}
&= \frac{ig_s^3}{(4\pi)^2} (L'P_L + R'P_R)_{Ii} \int_l \frac{l^\sigma \gamma^\sigma \Gamma^{\mu\sigma\rho} (l + p_a + p_b - 2p_1)^\rho}{\mathcal{D}_1\mathcal{D}_2\mathcal{D}_3\mathcal{D}_4} \\
&\quad T_{\beta\delta}^c T_{\delta\alpha}^b f^{abc}
\end{aligned} \tag{C.207}$$



## C.3.4. Squark-gluino-gluino-quark box



$$B_{\beta\alpha}^{\mu a}(0, 0, m_{\tilde{q}_i}^2, m_{\tilde{\chi}_k}^2, s, u, m_{\tilde{q}_j}^2, m_{\tilde{g}}^2, m_{\tilde{g}}^2, m_{q_J}^2) \quad (\text{C.208})$$

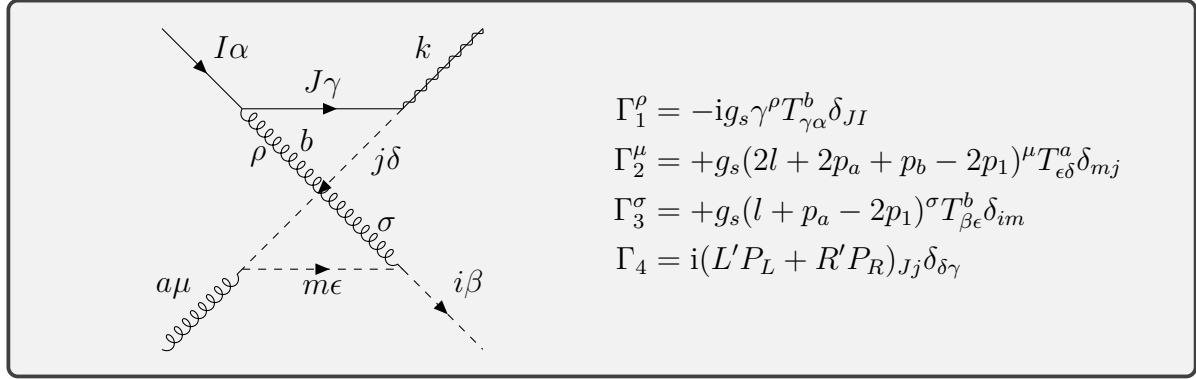
$$= \mu^{4-D} \int \frac{d^D l}{(2\pi)^D} \Gamma_4 \frac{i(l + \not{p}_a + \not{p}_b + \not{p}_1 - m_{q_J})}{\mathcal{D}_4} \Gamma_3 \frac{i(l + \not{p}_a + \not{p}_b + m_{\tilde{g}})}{\mathcal{D}_3} \quad (\text{C.209})$$

$$\Gamma_2^\mu \frac{i(l + \not{p}_a + m_{\tilde{g}})}{\mathcal{D}_2} \Gamma_1 \frac{i}{\mathcal{D}_1} \quad (\text{C.210})$$

$$= \frac{ig_s^3}{(4\pi)^2} T_{\beta\delta}^c T_{\delta\alpha}^b f^{abc} \int_l \quad (\text{C.211})$$

$$\begin{aligned} & \left( (L_{Jj} \mathcal{L}' \mathcal{L}' P_L + R_{Jj} \mathcal{R}' \mathcal{R}' P_R) \frac{m_{q_J} ((l + \not{p}_a + \not{p}_b) \gamma^\mu m_{\tilde{g}} + m_{\tilde{g}} \gamma^\mu (l + \not{p}_a))}{\mathcal{D}_1 \mathcal{D}_2 \mathcal{D}_3 \mathcal{D}_4} \right. \\ & + (L_{Jj} \mathcal{R}' \mathcal{R}' P_L + R_{Jj} \mathcal{L}' \mathcal{L}' P_R) \frac{((l + \not{p}_a + \not{p}_b - \not{p}_1) ((l + \not{p}_a + \not{p}_b) \gamma^\mu m_{\tilde{g}} + m_{\tilde{g}} \gamma^\mu (l + \not{p}_a))}{\mathcal{D}_1 \mathcal{D}_2 \mathcal{D}_3 \mathcal{D}_4} \\ & + (L_{Jj} \mathcal{L}' \mathcal{R}' P_L + R_{Jj} \mathcal{R}' \mathcal{L}' P_R) \frac{m_{q_J} (\gamma^\mu m_{\tilde{g}}^2 + (l + \not{p}_a + \not{p}_b) \gamma^\mu (l + \not{p}_a))}{\mathcal{D}_1 \mathcal{D}_2 \mathcal{D}_3 \mathcal{D}_4} \\ & \left. + (L_{Jj} \mathcal{R}' \mathcal{L}' P_L + R_{Jj} \mathcal{L}' \mathcal{R}' P_R) \frac{((l + \not{p}_a + \not{p}_b - \not{p}_1) (\gamma^\mu m_{\tilde{g}}^2 + (l + \not{p}_a + \not{p}_b) \gamma^\mu (l + \not{p}_a)))}{\mathcal{D}_1 \mathcal{D}_2 \mathcal{D}_3 \mathcal{D}_4} \right) \quad (\text{C.212}) \end{aligned}$$

## C.3.5. Quark-gluon-squark-squark box

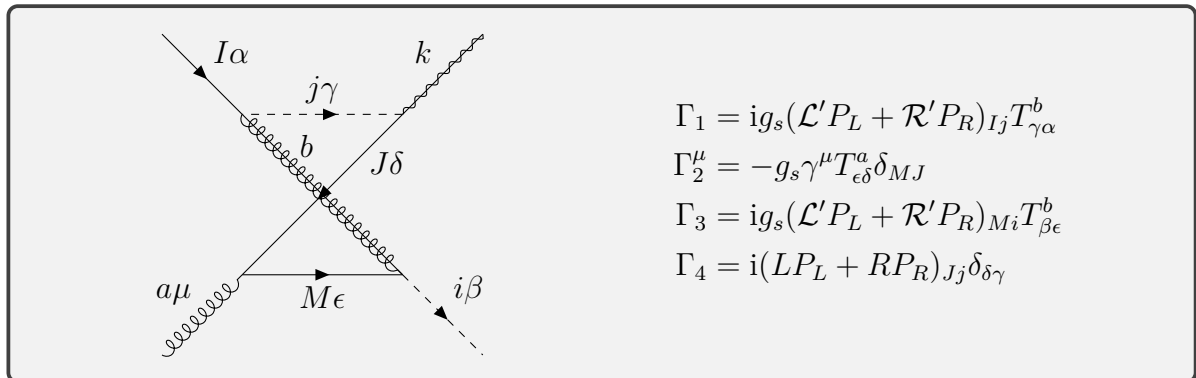


$$B_{\beta\alpha}^{\mu a}(0, m_{\tilde{q}_i}^2, 0, m_{\tilde{\chi}_k}^2, t, u, 0, 0, m_{\tilde{q}_i}^2, m_{\tilde{q}_i}^2) \quad (\text{C.213})$$

$$= \mu^{4-D} \int \frac{d^D l}{(2\pi)^D} \Gamma_4 \frac{-i \not{l}}{\mathcal{D}_1} \Gamma_1^\rho \frac{-i g_{\sigma\rho}}{\mathcal{D}_2} \Gamma_3^\sigma \frac{i}{\mathcal{D}_3} \Gamma_2^\mu \frac{i}{\mathcal{D}_4} \quad (\text{C.214})$$

$$= -\frac{ig_s^3}{(4\pi)^2} (L'P_L + R'P_R)_{Ii} \int_l \frac{l(l + \not{p}_a - 2\not{p}_1)(2l + 2p_a + p_b - 2p_1)^\mu}{\mathcal{D}_1 \mathcal{D}_2 \mathcal{D}_3 \mathcal{D}_4} T_{\beta\epsilon}^b T_{\epsilon\gamma}^a T_{\gamma\alpha}^b \quad (\text{C.215})$$

## C.3.6. Squark-gluino-quark-quark box



$$B_{\beta\alpha}^{\mu a}(0, m_{\tilde{q}_i}^2, 0, m_{\tilde{\chi}_k}^2, t, u, m_{\tilde{q}_j}^2, m_{\tilde{g}}^2, m_{q_j}^2, m_{q_j}^2) \quad (\text{C.216})$$

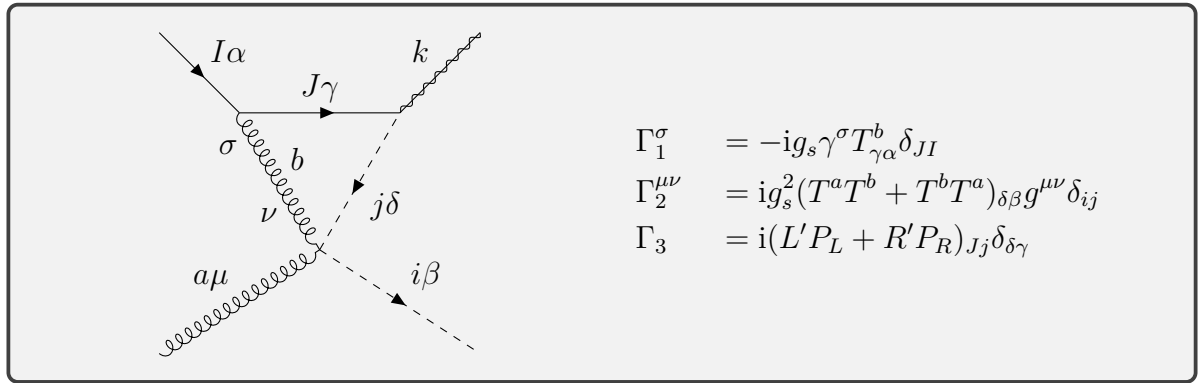
$$= \mu^{4-D} \int \frac{d^D l}{(2\pi)^D} \Gamma_4 \frac{i(l + \not{p}_a - \not{p}_1 + \not{p}_b + m_{q_J})}{\mathcal{D}_1} \Gamma_2^\mu \frac{i(l + \not{p}_a - \not{p}_1 + m_{q_J})}{\mathcal{D}_2} \quad (\text{C.217})$$

$$\Gamma_3 \frac{i(l + \not{p}_a + m_{\tilde{g}})}{\mathcal{D}_3} \Gamma_1 \frac{i}{\mathcal{D}_4} \quad (\text{C.218})$$

$$= -\frac{ig_s^3}{(4\pi)^2} T_{\beta\epsilon}^b T_{\epsilon\gamma}^a T_{\gamma\alpha}^b \int_l \quad (C.219)$$

$$\begin{aligned} & \left( (L_{Jj} \mathcal{L}' \mathcal{L}' P_L + R_{Jj} \mathcal{R}' \mathcal{R}' P_R) \frac{m_{\tilde{g}} m_{qJ} ((l + \not{p}_a - \not{p}_1 + \not{p}_b) \gamma^\mu + \gamma^\mu l + \not{p}_a - \not{p}_1)}{\mathcal{D}_1 \mathcal{D}_2 \mathcal{D}_3 \mathcal{D}_4} \right. \\ & + (L_{Jj} \mathcal{R}' \mathcal{R}' P_L + R_{Jj} \mathcal{L}' \mathcal{L}' P_R) \frac{m_{\tilde{g}} (\gamma^\mu m_{qJ}^2 + (l + \not{p}_a - \not{p}_1 + \not{p}_b) \gamma^\mu (l + \not{p}_a - \not{p}_1))}{\mathcal{D}_1 \mathcal{D}_2 \mathcal{D}_3 \mathcal{D}_4} \\ & + (L_{Jj} \mathcal{L}' \mathcal{R}' P_L + R_{Jj} \mathcal{R}' \mathcal{L}' P_R) \frac{m_{qJ} (l + \not{p}_a) ((l + \not{p}_a - \not{p}_1 + \not{p}_b) \gamma^\mu + \gamma^\mu l + \not{p}_a - \not{p}_1)}{\mathcal{D}_1 \mathcal{D}_2 \mathcal{D}_3 \mathcal{D}_4} \\ & \left. + (L_{Jj} \mathcal{R}' \mathcal{L}' P_L + R_{Jj} \mathcal{L}' \mathcal{R}' P_R) \frac{(l + \not{p}_a) (\gamma^\mu m_{qJ}^2 + (l + \not{p}_a - \not{p}_1 + \not{p}_b) \gamma^\mu (l + \not{p}_a - \not{p}_1))}{\mathcal{D}_1 \mathcal{D}_2 \mathcal{D}_3 \mathcal{D}_4} \right) \end{aligned} \quad (C.220)$$

### C.3.7. Quark-gluon-squark box



$$B_{\beta\alpha}^{\mu a}(0, 0, m_{\tilde{q}_i}^2, m_{\tilde{\chi}_k}^2, s, u, 0, 0, 0, m_{\tilde{q}_i}^2) \quad (C.221)$$

$$= \mu^{4-D} \int \frac{d^D l}{(2\pi)^D} \Gamma_3 \frac{-i \not{l}}{\mathcal{D}_1} \Gamma_1^\sigma \frac{-ig_{\sigma\nu}}{\mathcal{D}_2} \Gamma_2^{\mu\nu} \frac{i}{\mathcal{D}_3} \Gamma_3 \quad (C.222)$$

$$\begin{aligned} &= \frac{ig_s^3}{(4\pi)^2} (L' P_L + R' P_R)_{Ii} \int_l \frac{l \gamma^\mu}{\mathcal{D}_1 \mathcal{D}_2 \mathcal{D}_3} \\ & \quad (T_{\beta\epsilon}^a T_{\epsilon\delta}^b + T_{\beta\epsilon}^b T_{\epsilon\delta}^a) T_{\delta\alpha}^b \end{aligned} \quad (C.223)$$

## C.4. FeynCalc implementation

For completeness, we present the code used for automatically computing the virtuals. The dependencies of the code are `FeynCalc`[34] and `Colormath`[68].

```
In[1]:= (* Dependencies *)
Needs['FeynCalc`']
Get['ColorMath1.0.m`']
```

```

In[2]:= (* polarization sum of the external gluon *)
Polsum [mu_, nu_] := -MT[mu, nu] \
+ AXG*(((FV[q, mu]*FV[pb, nu]+FV[q, nu]*FV[pb, mu])/SP[q, pb] \
- SP[q, q]*FV[pb, mu]*FV[pb, nu]/SP[q, pb]/SP[q, pb]))/.{q→pa+pb}

suchannel[LOOP_] := (
  PR=ChiralityProjector[+1];
  PL=ChiralityProjector[-1];

  (* evaluate the loop in D dimensions *)
  OK = Simplify[TID[DiracSimplify[LOOP], 1, UsePaVeBasis→True]];
  PVL=Simplify[DiracSimplify[TID[OK, 1, ToPaVe→True]]];

  (* s channel amplitude combined with s channel *)
  (* where the uug vertex is replaced by the loop*)
  AMPS=SS*2*Polsum[mu, nu]/96/16/Pi^4*
    (I*(Lp*PL+Rp*PR)).
    (I*GS[pa+pb]/SP[q, q]) .
    ChangeDimension[PVL, 4].
    GS[pa].
    (I*gs*GA[nu]).t[{Ga}, Qa, Qb].
    (-I*GS[pa+pb]/SP[q, q]) .
    (-I*(L*PL+R*PR)).
    (GS[p2]+MX);
  (* u channel amplitude combined with s channel *)
  (* where the uug vertex is replaced by the loop *)
  AMPU=UU*2*Polsum[mu, nu]/96/16/Pi^4*
    (I*(Lp*PL+Rp*PR)).
    (I*GS[pa+pb]/SP[q, q]) .
    ChangeDimension[PVL, 4].
    GS[pa].
    (-I*(L*PL+R*PR)).
    (GS[p2]+MX).
    ((-I)/(u-MU^2)).
    (I*gs*FV[pa-p2+p1, nu]).t[{Ga}, Qa, Qb];

  (* final simplification and epsilon expansion *)
  MMMM = Simplify[CSimplify[Tr[(AMPS+AMPU)/.
    {p1→ pa+pb-p2}]]]/.{u→-t-s+MXs+MUs};
  epsser = Series[MMMM/. {D→4-2*eps}, {eps, 0, 2}];
)

In[3]:= (* exemplary quark-quark-gluon loop *)
uug=-gs^3*t[{Gb}, Qb, Qbp].t[{Ga}, Qbp, Qap].t[{Gb}, Qap, Qa].
GAD[nu].GSD[1+pa+pb].GAD[mu].GSD[1+pa].GAD[nu].
FAD[{1, 0}, {1+pa+pb, 0}, {1+pa, 0}]

```

`suchannel[uug];`

In above code we omitted **ScalarProduct** which simplifies momenta. **CForm** and **FeynCalc2FORM** come in handy to export the code in compatible formats. If we do not want to compute in the 't Hooft Veltman scheme we could use **ChangeDimension** to get an overall D dimensional expression (CDR).

If one intends to cancel UV and IR divergence separately extra care is needed since **FeynCalc** seems to simplify expressions where UV and IR divergence cancel, e.g.  $B_0(0, 0, 0) = 0$  or  $C_0^{\mu\mu}(0, 0, q^2, 0, 0, 0) = 0$ .

## D. Real corrections

### D.1. Polarized dipole kinematics and connection matrix

The subtraction of the dipoles from the real corrections involves helicity correlations of the external gluon. The following explicit calculations are not very interesting, however we list them here anyway since the process of squark-gaugino production is the first implementation of such correlated dipoles into **Resummino**. As in the computation of the polarized born cross section we use formatting closely related to the implementation, where this contributes to better understanding. <sup>4</sup>

#### D.1.1. Initial state emitter and final state spectator

First we define several kinematic quantities

$$s_1 = 2p_a p_b - 2p_3 p_a - 2p_3 p_b = m_1^2 + m_2^2 + 2p_1 p_2 = s - 2p_3 q \quad (D.1)$$

$$\text{K1P1} \rightarrow p_1 p_b = \text{K1Q-K1P1} \quad (D.2)$$

$$\begin{aligned} \text{K2P1} \rightarrow p_2 p_b &= p_2 (q - p_a) = (q - p_1 - p_3) q - p_a p_2 = (q - p_3) q - p_1 q - p_a p_2 \\ &= \frac{1}{2} (s + s_1) - (p_1 q + p_a p_2) = (\mathbf{s} + \mathbf{s1}) / 2 - (\text{K1Q} + \text{K2P1}) . \end{aligned} \quad (D.3)$$

One notices these quantities are crossed  $p_a \leftrightarrow p_b$  since our gluon is associated with the momentum  $p_b$  in contrast to the equations from the dipole papers [37][38].

We use the phase space transformation from [38, section 5.3.1]

$$\begin{aligned} x_{ij,a} &= \frac{p_a p_i + p_a p_j - p_i p_j}{p_a p_i + p_a p_j} = 1 - \frac{p_i p_j}{p_a p_i + p_a p_j} = 1 - \frac{(q - p_2 - p_1) p_1}{p_a q - p_a p_2} \\ &= 1 - \frac{2(q p_1 - p_2 p_1 - m_1^2) + m_2^2 - m_2^2}{2(p_a q - p_a p_2)} = 1 - \frac{2q p_1 - s_1 + \Delta M^2}{2(p_a q - p_a p_2)} \\ &= 1 - (2 * \text{K1Q} - \mathbf{s1} + \mathbf{dM2o}) / (\mathbf{s} - 2 * \text{K2P1}) \end{aligned} \quad (D.4)$$

$$\tilde{z}_j = \frac{p_a p_j}{p_a p_i + p_a p_j} = 2 * \text{K1P1} / (\mathbf{s} - 2 * \text{K2P1}) . \quad (D.5)$$

<sup>4</sup>The analytic calculations are given in  $p_a p_b \rightarrow p_1 p_2 p_3$  kinematic nomenclature. The implementation expressions however use  $p_1 p_2 \rightarrow k_1 k_2 k_3$ .

For these dipole parameters we already inserted  $i = 3$  and  $j = 1$ .

$$\tilde{p}_{ai} = x_{ij,a} p_a \quad (D.6)$$

$$\tilde{p}_j = p_i + p_j - (1 - x_{ij,a}) p_a \quad (D.7)$$

$$Q^2 = (\tilde{p}_b + \tilde{p}_{ai})^2 = (p_b + \tilde{p}_{ai})^2 = \frac{1}{2} 2p_b p_a x_{ij,a} = x_{ij,a} s \quad (D.8)$$

$$Pt1Kt1 = \tilde{p}_1 p_b = \tilde{p}_j p_b = p_1 p_b + p_3 p_b - \frac{1}{2} (1 - x_{ij,a}) s \quad (D.9)$$

$$\begin{aligned} &= p_1 p_b + p_3 p_b + (p_1 + p_2 + p_3) p_a - p_a p_b \\ &- \frac{1}{2} (1 - x_{ij,a}) s = p_1 (p_a + p_b) + p_2 p_a + p_3 p_b + p_3 p_a - p_a p_b - \frac{1}{2} (1 - x_{ij,a}) s \\ &= p_1 (p_a + p_b) + p_2 p_a - \frac{1}{2} s_1 - \frac{1}{2} (1 - x_{ij,a}) s \\ &= (K1Q+K2P1) - ((1-xija)*s+s1)/2 \end{aligned} \quad (D.10)$$

From above computations we can determine intermediate momenta contractions that will appear in our  $7 \times 4$  dipole connection matrix.

$$P1Ki = p_a p_3 = p_a (q - p_1 - p_2) = s/2 - (K1P1+K2P1) \quad (D.11)$$

$$KiKj = p_3 p_1 = K1Q - (s1-dM2o)/2 \quad (D.12)$$

$$Pt1Pt1 = 0 \quad (D.13)$$

$$Pt1Kj = p_b p_1 = K1Q - K1P1 \quad (D.14)$$

$$Pt1Ki = p_b p_3 = (q - p_a) p_3 = \frac{1}{2} (s - s_1) - p_a p_3 = (s-s1)/2 - P1Ki \quad (D.15)$$

$$Kt1Kt1 = m_1^2 = Mo1**2 \quad (D.16)$$

$$Kt1Kj = \tilde{p}_j p_j = p_i p_j + m_1^2 - (1 - x_{ij,a}) p_a p_j = Mo1**2 + KiKj - (1-xija)*K1P1 \quad (D.17)$$

$$Kt1Ki = \tilde{p}_j p_i = p_i p_j - (1 - x_{ij,a}) p_a p_i = KiKj - (1-xija)*P1Ki \quad (D.18)$$

$$\begin{aligned} QtKj &= (p_b + \tilde{p}_{ai}) p_1 = (p_b + p_a - p_a + x_{ij,a} p_a) p_1 = qp_1 - (1 - x_{ij,a}) p_a p_1 \\ &= K1Q - (1-xija)*K1P1 \end{aligned} \quad (D.19)$$

$$QtKi = (p_b + \tilde{p}_{ai}) p_3 = qp_3 - (1 - x_{ij,a}) p_a p_3 = (s-s1)/2 - (1-xija)*P1Ki \quad (D.20)$$

$$Pt1Qt = p_b (p_b + \tilde{p}_{ai}) = \frac{1}{2} x_{ij,a} s = Pt1Pt1 + (xija*s-Mi1**2-Mi2**2)/2 \quad (D.21)$$

$$\begin{aligned} QtKt1 &= \tilde{p}_j (p_2 + \tilde{p}_j) = m_1^2 + \tilde{p}_j p_2 = m_1^2 + \frac{1}{2} (x_{ij,a} s - m_1^2 - m_2^2) \\ &= Kt1Kt1 + (xija*s-Mo1**2-Mo2**2)/2 \end{aligned} \quad (D.22)$$

Next up we show the final dipole connection matrix of the Lorentz structures from the dipole kernel

$$g^{\mu\nu}, p_j^\mu p_j^\nu, p_i^\mu p_i^\nu, p_j^\mu p_i^\nu + p_i^\nu p_j^\mu \quad (D.23)$$

and the polarized matrix element

$$g^{\mu\nu}, \tilde{p}_a^\mu \tilde{p}_a^\nu, \tilde{q}^\mu \tilde{q}^\nu, \tilde{p}_j^\mu \tilde{p}_j^\nu, \tilde{p}_a^\mu \tilde{q}^\nu + \tilde{p}_a^\nu \tilde{q}^\mu, \tilde{p}_a^\mu \tilde{p}_1^\nu + \tilde{p}_a^\nu \tilde{p}_1^\mu, \tilde{p}_1^\mu \tilde{q}^\nu + \tilde{p}_1^\nu \tilde{q}^\mu. \quad (D.24)$$

The following  $7 \cdot 4 = 28$  equations list the elements of our matrix.

$$g^{\mu\nu} g^{\mu\nu} = 4 \quad (D.25)$$

$$g^{\mu\nu} \tilde{p}_a^\mu \tilde{p}_a^\nu = 0 = \text{Pt1Pt1} \quad (D.26)$$

$$g^{\mu\nu} \tilde{q}^\mu \tilde{q}^\nu = x_{ij,a}s \quad (D.27)$$

$$g^{\mu\nu} \tilde{p}_j^\mu \tilde{p}_j^\nu = \text{Kt1Kt1} \quad (D.28)$$

$$g^{\mu\nu} (\tilde{p}_a^\mu \tilde{q}^\nu + \tilde{p}_a^\nu \tilde{q}^\mu) = 2*\text{Pt1Qt} \quad (D.29)$$

$$g^{\mu\nu} (\tilde{p}_a^\mu \tilde{p}_1^\nu + \tilde{p}_a^\nu \tilde{p}_1^\mu) = 2*\text{Pt1Kt1} \quad (D.30)$$

$$g^{\mu\nu} (\tilde{p}_1^\mu \tilde{q}^\nu + \tilde{p}_1^\nu \tilde{q}^\mu) = 2*\text{QtKt1} \quad (D.31)$$

$$g^{\mu\nu} p_j^\mu p_j^\nu = \text{Mo1**2} \quad (D.32)$$

$$\tilde{p}_a^\mu \tilde{p}_a^\nu p_j^\mu p_j^\nu = \text{Pt1Kj**2} \quad (D.33)$$

$$\tilde{q}^\mu \tilde{q}^\nu p_j^\mu p_j^\nu = \text{QtKj**2} \quad (D.34)$$

$$\tilde{p}_j^\mu \tilde{p}_j^\nu p_j^\mu p_j^\nu = \text{Kt1Kj**2} \quad (D.35)$$

$$(\tilde{p}_a^\mu \tilde{q}^\nu + \tilde{p}_a^\nu \tilde{q}^\mu) p_j^\mu p_j^\nu = 2*\text{Pt1Kj*QtKj} \quad (D.36)$$

$$(\tilde{p}_a^\mu \tilde{p}_1^\nu + \tilde{p}_a^\nu \tilde{p}_1^\mu) p_j^\mu p_j^\nu = 2*\text{Pt1Kj*Kt1Kj} \quad (D.37)$$

$$(\tilde{p}_1^\mu \tilde{q}^\nu + \tilde{p}_1^\nu \tilde{q}^\mu) p_j^\mu p_j^\nu = 2*\text{Kt1Kj*QtKj} \quad (D.38)$$

$$g^{\mu\nu} p_i^\mu p_i^\nu = 0 \quad (D.39)$$

$$\tilde{p}_a^\mu \tilde{p}_a^\nu p_i^\mu p_i^\nu = \text{Pt1Ki**2} \quad (D.40)$$

$$\tilde{q}^\mu \tilde{q}^\nu p_i^\mu p_i^\nu = \text{QtKi**2} \quad (D.41)$$

$$\tilde{p}_j^\mu \tilde{p}_j^\nu p_i^\mu p_i^\nu = \text{Kt1Ki**2} \quad (D.42)$$

$$(\tilde{p}_a^\mu \tilde{q}^\nu + \tilde{p}_a^\nu \tilde{q}^\mu) p_i^\mu p_i^\nu = 2*\text{Pt1Ki*QtKi} \quad (D.43)$$

$$(\tilde{p}_a^\mu \tilde{p}_1^\nu + \tilde{p}_a^\nu \tilde{p}_1^\mu) p_i^\mu p_i^\nu = 2*\text{Pt1Ki*Kt1Ki} \quad (D.44)$$

$$(\tilde{p}_1^\mu \tilde{q}^\nu + \tilde{p}_1^\nu \tilde{q}^\mu) p_i^\mu p_i^\nu = 2*\text{Kt1Ki*QtKi} \quad (D.45)$$

$$g^{\mu\nu} (p_i^\mu p_j^\nu + p_i^\nu p_j^\mu) = 2*\text{KiKj} \quad (D.46)$$

$$\tilde{p}_a^\mu \tilde{p}_a^\nu (p_i^\mu p_j^\nu + p_i^\nu p_j^\mu) = 2*\text{Pt1Kj*Pt1Ki} \quad (D.47)$$

$$\tilde{q}^\mu \tilde{q}^\nu (p_i^\mu p_j^\nu + p_i^\nu p_j^\mu) = 2*\text{QtKj*QtKi} \quad (D.48)$$

$$\tilde{p}_j^\mu \tilde{p}_j^\nu (p_i^\mu p_j^\nu + p_i^\nu p_j^\mu) = 2*\text{Kt1Kj*Kt1Ki} \quad (D.49)$$

$$(\tilde{p}_a^\mu \tilde{q}^\nu + \tilde{p}_a^\nu \tilde{q}^\mu) (p_i^\mu p_j^\nu + p_i^\nu p_j^\mu) = 2*\text{Pt1Kj*QtKi} + 2*\text{Pt1Ki*QtKj} \quad (D.50)$$

$$(\tilde{p}_a^\mu \tilde{p}_1^\nu + \tilde{p}_a^\nu \tilde{p}_1^\mu) (p_i^\mu p_j^\nu + p_i^\nu p_j^\mu) = 2*\text{Pt1Kj*Kt1Ki} + 2*\text{Pt1Ki*Kt1Kj} \quad (D.51)$$

$$(\tilde{p}_1^\mu \tilde{q}^\nu + \tilde{p}_1^\nu \tilde{q}^\mu) (p_i^\mu p_j^\nu + p_i^\nu p_j^\mu) = 2*\text{Kt1Kj*QtKi} + 2*\text{Kt1Ki*QtKj} \quad (D.52)$$

### D.1.2. Initial state emitter and final state spectator

Again, as in the previous calculation we start with the same quantities which are crossing  $p_a$  and  $p_b$ .

$$s_1 = 2p_a p_b - 2p_3 p_a - 2p_3 p_b = m_1^2 + m_2^2 + 2p_1 p_2 = s - 2p_3 q \quad (D.53)$$

$$\text{K1P1} \rightarrow p_1 p_b = \text{K1Q-K1P1} \quad (\text{D.54})$$

$$\begin{aligned} \text{K2P1} \rightarrow p_2 p_b &= p_2 (q - p_a) = (q - p_1 - p_3) q - p_a p_2 = (q - p_3) q - p_1 q - p_a p_2 \\ &= \frac{1}{2} (s + s_1) - (p_1 q + p_a p_2) = (\mathbf{s} + \mathbf{s}_1) / 2 - (\text{K1Q} + \text{K2P1}) \end{aligned} \quad (\text{D.55})$$

To evaluate the dipoles we need following parameters from [37, section 5.5]

$$x_{ij,a} = \frac{p_a p_b - p_a p_i - p_i p_b}{p_a p_b} = \frac{s_1}{s} = \mathbf{s}_1 / \mathbf{s} \quad (\text{D.56})$$

$$\tilde{z}_b = \frac{2p_a p_b}{(s + 2p_a p_3)} = \frac{2p_a p_b}{2(s - p_a (q - p_3))} = \frac{s}{2(s - p_a p_1 - p_a p_2)} = \mathbf{s} / (2 * (\mathbf{s} - \text{K1P1} - \text{K2P1})) \quad (\text{D.57})$$

$$\tilde{z}_i = 1 - \tilde{z}_b = \frac{2p_a p_3}{(s + 2p_a p_3)} \quad (\text{D.58})$$

$$\frac{\tilde{z}_b}{\tilde{z}_i} = \frac{p_a p_b}{p_a p_3} \quad (\text{D.59})$$

$$\frac{\tilde{z}_i}{\tilde{z}_b} = \frac{p_a p_3}{p_a p_b}, \quad (\text{D.60})$$

already setting  $i = 3$  and  $j = 1$  for our purposes. We keep computing the outlined quantities to generate a proper Lorentz transformation and thereby  $\tilde{k}_j$ .

$$\tilde{p}_{ai} = x_{i,ab} p_a \quad (\text{D.61})$$

$$\tilde{k}_j = k_j - \frac{2k_j \cdot (K + \tilde{K})}{(K + \tilde{K})^2} (k + \tilde{K}) - \frac{2k_j \cdot K}{K^2} \tilde{K} \quad (\text{D.62})$$

$$\begin{aligned} (K + \tilde{K})^2 &= ((p_a + p_b - p_i) + (\tilde{p}_{ai} + p_b))^2 \\ &= ((1 + x_{i,ab}) p_a + 2p_b - p_i)^2 \\ &= (1 + x_{i,ab}) 4p_a p_b - 4p_b p_i - 2(1 + x_{i,ab}) p_i p_a \\ &= 2s + 2s_1 - 4p_b p_i - 2(1 + x_{i,ab}) p_i p_a = 2s + 2s_1 - 2(s - s_1 - 2p_a p_i) \end{aligned} \quad (\text{D.63})$$

$$\begin{aligned} &- 2(1 + x_{i,ab}) p_i p_a \\ &= 4s_1 + 4p_a p_i - 2(1 + x_{i,ab}) p_i p_a = 4s_1 + 2(1 - x_{i,ab}) ((q - p_1 - p_2) p_a) \\ &= 4s_1 + s - s_1 + 2(1 - x_{i,ab}) ((-p_1 - p_2) p_a) \\ &= \mathbf{s} + 3 * \mathbf{s}_1 - 2 * (1 - \mathbf{x}_{iab}) * (\text{K1P1} + \text{K2P1}) \end{aligned} \quad (\text{D.64})$$

$$k_j \tilde{K} = x_{i,ab} p_a p_1 + p_b p_1 = x_{i,ab} p_a p_1 + (q - p_a) p_1 = \text{K1Q} - (1 - \mathbf{x}_{iab}) * \text{K1P1} \quad (\text{D.65})$$

$$\begin{aligned} k_j K &= p_1 p_a + p_1 p_b - p_1 p_3 = p_1 (p_1 + p_2 + p_3) - p_1 p_3 = p_1 (p_1 + p_2) \\ &= p_1 p_2 + \frac{1}{2} p_1^2 + \frac{1}{2} p_2^2 - \frac{1}{2} p_2^2 + \frac{1}{2} p_1^2 = (\mathbf{s}_1 - \mathbf{dM2o}) / 2 \end{aligned} \quad (\text{D.66})$$

Then we can resolve the contraction of  $k_j$  with various momenta.

$$\tilde{p}_{ai} \tilde{k}_j = x_{i,ab} p_1 p_a - \frac{2k_j \cdot (K + \tilde{K})}{(K + \tilde{K})^2} (x_{i,ab} p_a (K + \tilde{K})) + \frac{2p_1 K}{K^2} x_{i,ab} p_a \tilde{K}$$



$$\begin{aligned}
&= x_{i,ab} p_1 p_a - \frac{2k_j (K + \tilde{K})}{(K + \tilde{K})^2} (x_{i,ab} p_a ((1 + x_{i,ab}) p_a + 2p_b - p_i)) + \frac{2p_1 K}{2s_1} x_{i,ab} s \\
&= x_{i,ab} p_1 p_a - \frac{2k_j (K + \tilde{K})}{(K + \tilde{K})^2} (s_1 - x_{i,ab} p_a p_i) + p_1 K \\
&= x_{i,ab} p_1 p_a - \frac{2k_j (K + \tilde{K})}{(K + \tilde{K})^2} (s_1 - x_{i,ab} p_a (q - p_1 - p_2)) + p_1 K \\
&= x_{i,ab} p_1 p_a - \frac{2k_j (K + \tilde{K})}{(K + \tilde{K})^2} \left( \frac{1}{2} s_1 + x_{i,ab} p_a (p_1 + p_2) \right) + p_1 K \\
&= \text{xiab} * \text{K1P1} - (\text{K1Kt} + \text{K1K}) / \text{KKt2} * (\text{s1} + 2 * \text{xiab} * (\text{K1P1} + \text{K2P1})) + \text{K1K} \quad (\text{D.67})
\end{aligned}$$

$$p_b \tilde{k}_j = p_1 q - p_1 p_a - \frac{2k_j (K + \tilde{K})}{(K + \tilde{K})^2} (p_b ((1 + x_{i,ab}) p_a + 2p_b - p_i)) + \frac{2p_1 K}{K^2} p_b \tilde{K} \quad (\text{D.68})$$

$$p_b \tilde{k}_j = p_1 q - p_1 p_a - \frac{k_j (K + \tilde{K})}{(K + \tilde{K})^2} ((1 + x_{i,ab}) s - 2p_b p_i) + p_1 K \quad (\text{D.69})$$

$$p_b \tilde{k}_j = p_1 q - p_1 p_a - \frac{k_j (K + \tilde{K})}{(K + \tilde{K})^2} (s + s_1 + s_1 - s + 2p_a p_i) + p_1 K \quad (\text{D.70})$$

$$p_b \tilde{k}_j = p_1 q - p_1 p_a - \frac{k_j (K + \tilde{K})}{(K + \tilde{K})^2} (2s_1 + s - 2p_a (p_1 + p_2)) + p_1 K \quad (\text{D.71})$$

$$= \text{K1Q} - \text{K1P1} - (\text{K1Kt} + \text{K1K}) / \text{KKt2} * (\text{s} + 2 * \text{s1} - 2 * (\text{K1P1} + \text{K2P1})) + \text{K1K} \quad (\text{D.72})$$

$$\tilde{p}_{ai} k_i = \tilde{p}_{ai} p_i = x_{i,ab} p_a (q - p_1 - p_2) = \frac{1}{2} s_1 - x_{i,ab} p_a (p_1 + p_2) = \text{s1}/2 - \text{xiab} * (\text{K1P1} + \text{K2P1}) \quad (\text{D.73})$$

$$p_b k_i = \frac{1}{2} (s - s_1) - p_a p_i = \frac{1}{2} (-s_1) + p_a (p_1 + p_2) = \text{K1P1} + \text{K2P1} - \text{s1}/2 \quad (\text{D.74})$$

$$\tilde{Q} k_i = \tilde{K} k_i = \tilde{p}_{ai} k_i + p_b k_i = \text{PtaKi} + \text{PbKi} \quad (\text{D.75})$$

$$Q2 = (\tilde{p}_b + \tilde{p}_{ai})^2 = (p_b + \tilde{p}_{ai})^2 = \frac{1}{2} 2p_b p_a x_{ij,a} = x_{ij,a} s = s_1 \quad (\text{D.76})$$

$$\text{PbKt1} = \tilde{p}_1 p_b = p_b \tilde{k}_j \quad (\text{D.77})$$

$$\text{Pt1Pb} = 0 \quad (\text{D.78})$$

$$\text{Pt1Ki} = \text{PbKi} \quad (\text{D.79})$$

$$(\text{D.80})$$

$$\text{Kt1Ki} = p_3 p_1 - \frac{2k_j (K + \tilde{K})}{(K + \tilde{K})^2} (p_3 ((1 + x_{i,ab}) p_a + 2p_b - p_i)) + \frac{2p_1 K}{K^2} p_3 \tilde{K}$$

$$\begin{aligned}
&= p_1 q - K p_1 - \frac{2k_j (K + \tilde{K})}{(K + \tilde{K})^2} \left( \tilde{Q} k_i + p_3 (p_a + p_b) \right) + \frac{2p_1 K}{s_1} p_3 \tilde{K} \\
&= p_1 q - K p_1 - \frac{2k_j (K + \tilde{K})}{(K + \tilde{K})^2} \left( \tilde{Q} k_i + \frac{1}{2} (-s_1 + s) \right) + \frac{2p_1 K}{s_1} p_3 \tilde{K} \\
&= \text{K1Q-K1K-(K1Kt+K1K)/KKt2*(s-s1+2*QtKi)+2*K1K*QtKi/s1} \quad (\text{D.81})
\end{aligned}$$

$$\text{QtPb} = \frac{1}{2} s_1 \quad (\text{D.82})$$

$$\text{QtKt1} = (\tilde{k}_1 + \tilde{k}_2) \tilde{k}_1 \stackrel{\text{Loren.Traf.}}{=} (k_1 + k_2) k_1 = k_1 K = \text{K1K} \quad (\text{D.83})$$

Finally, we show the dipole connection matrix of the Lorentz structures from the dipole kernel

$$g^{\mu\nu}, p_b^\mu p_b^\nu, p_i^\mu p_i^\nu, p_b^\mu p_i^\nu + p_i^\nu p_b^\mu \quad (\text{D.84})$$

and the polarized matrix element

$$g^{\mu\nu}, \tilde{p}_a^\mu \tilde{p}_a^\nu, \tilde{q}^\mu \tilde{q}^\nu, \tilde{p}_j^\mu \tilde{p}_j^\nu, \tilde{p}_a^\mu \tilde{q}^\nu + \tilde{p}_a^\nu \tilde{q}^\mu, \tilde{p}_a^\mu \tilde{p}_1^\nu + \tilde{p}_a^\nu \tilde{p}_1^\mu, \tilde{p}_1^\mu \tilde{q}^\nu + \tilde{p}_1^\nu \tilde{q}^\mu \quad (\text{D.85})$$

The following  $7 \cdot 4 = 28$  equations list the elements of our matrix.

$$g^{\mu\nu} g^{\mu\nu} = 4 \quad (\text{D.86})$$

$$g^{\mu\nu} \tilde{p}_a^\mu \tilde{p}_a^\nu = 0 = \text{Pt1Pt1} \quad (\text{D.87})$$

$$g^{\mu\nu} \tilde{q}^\mu \tilde{q}^\nu = x_{ij,a} s = s_1 \quad (\text{D.88})$$

$$g^{\mu\nu} \tilde{p}_j^\mu \tilde{p}_j^\nu = \text{Kt1Kt1} = m_1^2 \quad (\text{D.89})$$

$$g^{\mu\nu} (\tilde{p}_a^\mu \tilde{q}^\nu + \tilde{p}_a^\nu \tilde{q}^\mu) = 2 * \text{Pt1Qt} = s_1 \quad (\text{D.90})$$

$$g^{\mu\nu} (\tilde{p}_a^\mu \tilde{p}_1^\nu + \tilde{p}_a^\nu \tilde{p}_1^\mu) = 2 * \text{Pt1Kt1} \quad (\text{D.91})$$

$$g^{\mu\nu} (\tilde{p}_1^\mu \tilde{q}^\nu + \tilde{p}_1^\nu \tilde{q}^\mu) = 2 * \text{QtKt1} \quad (\text{D.92})$$

$$g^{\mu\nu} p_b^\mu p_b^\nu = 0 \quad (\text{D.93})$$

$$\tilde{p}_a^\mu \tilde{p}_a^\nu p_b^\mu p_b^\nu = \text{Pt1Pb**2} \quad (\text{D.94})$$

$$\tilde{q}^\mu \tilde{q}^\nu p_b^\mu p_b^\nu = \text{QtPb**2} \quad (\text{D.95})$$

$$\tilde{p}_j^\mu \tilde{p}_j^\nu p_b^\mu p_b^\nu = \text{PbKt1**2} \quad (\text{D.96})$$

$$(\tilde{p}_a^\mu \tilde{q}^\nu + \tilde{p}_a^\nu \tilde{q}^\mu) p_b^\mu p_b^\nu = 2 * \text{Pt1Pb*QtPb} \quad (\text{D.97})$$

$$(\tilde{p}_a^\mu \tilde{p}_1^\nu + \tilde{p}_a^\nu \tilde{p}_1^\mu) p_b^\mu p_b^\nu = 2 * \text{Pt1Pb*PbKt1} \quad (\text{D.98})$$

$$(\tilde{p}_1^\mu \tilde{q}^\nu + \tilde{p}_1^\nu \tilde{q}^\mu) p_b^\mu p_b^\nu = 2 * \text{PbKt1*QtPb} \quad (\text{D.99})$$

$$g^{\mu\nu} p_i^\mu p_i^\nu = 0 \quad (\text{D.100})$$

$$\tilde{p}_a^\mu \tilde{p}_a^\nu p_i^\mu p_i^\nu = \text{Pt1Ki**2} \quad (\text{D.101})$$

$$\tilde{q}^\mu \tilde{q}^\nu p_i^\mu p_i^\nu = \text{QtKi**2} \quad (\text{D.102})$$

$$\tilde{p}_j^\mu \tilde{p}_j^\nu p_i^\mu p_i^\nu = \text{Kt1Ki**2} \quad (\text{D.103})$$

$$(\tilde{p}_a^\mu \tilde{q}^\nu + \tilde{p}_a^\nu \tilde{q}^\mu) p_i^\mu p_i^\nu = 2 * \text{Pt1Ki*QtKi} \quad (\text{D.104})$$

$$(\tilde{p}_a^\mu \tilde{p}_1^\nu + \tilde{p}_a^\nu \tilde{p}_1^\mu) p_i^\mu p_i^\nu = 2 * \text{Pt1Ki} * \text{Kt1Ki} \quad (\text{D.105})$$

$$(\tilde{p}_1^\mu \tilde{q}^\nu + \tilde{p}_1^\nu \tilde{q}^\mu) p_i^\mu p_i^\nu = 2 * \text{Kt1Ki} * \text{QtKi} \quad (\text{D.106})$$

$$g^{\mu\nu} (p_i^\mu p_b^\nu + p_i^\nu p_b^\mu) = 2 * \text{PbKi} \quad (\text{D.107})$$

$$\tilde{p}_a^\mu \tilde{p}_a^\nu (p_i^\mu p_b^\nu + p_i^\nu p_b^\mu) = 2 * \text{Pt1Pb} * \text{Pt1Ki} \quad (\text{D.108})$$

$$\tilde{q}^\mu \tilde{q}^\nu (p_i^\mu p_b^\nu + p_i^\nu p_b^\mu) = 2 * \text{QtPb} * \text{QtKi} \quad (\text{D.109})$$

$$\tilde{p}_j^\mu \tilde{p}_j^\nu (p_i^\mu p_b^\nu + p_i^\nu p_b^\mu) = 2 * \text{PbKt1} * \text{Kt1Ki} \quad (\text{D.110})$$

$$(\tilde{p}_a^\mu \tilde{q}^\nu + \tilde{p}_a^\nu \tilde{q}^\mu) (p_i^\mu p_b^\nu + p_i^\nu p_b^\mu) = 2 * \text{Pt1Pb} * \text{QtKi} + 2 * \text{Pt1Ki} * \text{QtPb} \quad (\text{D.111})$$

$$(\tilde{p}_a^\mu \tilde{p}_1^\nu + \tilde{p}_a^\nu \tilde{p}_1^\mu) (p_i^\mu p_b^\nu + p_i^\nu p_b^\mu) = 2 * \text{Pt1Pb} * \text{Kt1Ki} + 2 * \text{Pt1Ki} * \text{PbKt1} \quad (\text{D.112})$$

$$(\tilde{p}_1^\mu \tilde{q}^\nu + \tilde{p}_1^\nu \tilde{q}^\mu) (p_i^\mu p_b^\nu + p_i^\nu p_b^\mu) = 2 * \text{PbKt1} * \text{QtKi} + 2 * \text{Kt1Ki} * \text{QtPb} \quad (\text{D.113})$$

## E. Relations

A list of useful equations.

### E.1. Colour

These relations are available in most standard text books on quantum field theory and the standard model (e.g. [56]).

#### E.1.1. Definitions

$$T_F = T_R = \frac{1}{2} \quad (\text{E.1})$$

$$C_A = T_a = N_c = N = 3 \quad (\text{E.2})$$

$$C_F = \frac{N^2 - 1}{2N} = \frac{4}{3} \quad (\text{E.3})$$

$$\text{Tr}[T^a T^b] = T_R \delta_{ab} \quad (\text{E.4})$$

#### E.1.2. Fierz identity

$$T_{\alpha\beta}^a T_{\gamma\delta}^a = \frac{1}{2} (\delta_{\alpha\delta} \delta_{\gamma\beta} - \frac{1}{N} \delta_{\alpha\beta} \delta_{\gamma\delta}) \quad (\text{E.5})$$

And consequently

$$T_{\alpha\gamma}^a T_{\gamma\beta}^a = C_F \delta_{\alpha\beta} \quad (\text{E.6})$$

follows. One can also solve

$$f^{abc} T_{\beta\alpha}^c T_{\gamma\beta}^b = i C_A T_R T_{\gamma\alpha}^a \quad (\text{E.7})$$

$$T_{\beta\delta}^b T_{\gamma\alpha}^b T_{\delta\gamma}^a = -\frac{T_R}{C_A} T_{\alpha\beta}^a. \quad (\text{E.8})$$

## E.2. Gamma Matrix

Again, the relations are available in most standard text books on quantum field theory and the standard model (e.g. [56]).

### E.2.1. Gamma trace relations

$$\text{Tr}[\gamma_\mu \gamma_\nu] = 4g_{\mu\nu} \quad (\text{E.9})$$

$$\text{Tr}[\gamma_\mu \gamma_\nu \gamma_\delta] = 0 \quad (\text{E.10})$$

$$\text{Tr}[\gamma_\mu \gamma_\nu \gamma_\delta \gamma_\rho] = 4(g_{\mu\nu}g_{\delta\rho} - g_{\mu\delta}g_{\nu\rho} + g_{\mu\rho}g_{\nu\delta}) \quad (\text{E.11})$$

### E.2.2. $D$ -dimensional Gamma Matrix

$$\gamma^\mu \gamma^\nu \gamma_\mu = (2 - D)\gamma^\nu \quad (\text{E.12})$$

$$\gamma^\mu \gamma^\nu \gamma^\sigma \gamma_\mu = (D - 4)\gamma^\nu \gamma^\sigma + 4g^{\nu\sigma} \quad (\text{E.13})$$

$$\gamma^\mu \gamma^\nu \gamma^\sigma \gamma^\rho \gamma_\mu = -2\gamma^\rho \gamma^\sigma \gamma^\nu - (D - 4)\gamma^\nu \gamma^\sigma \gamma^\rho \quad (\text{E.14})$$

## E.3. Passarino-Veltman

Here we list Passarino-Veltman results extracted from [54].

### E.3.1. Reduction

When no parameters are given to a function, the same parameters as on the left-hand side are used.

**$B$ -tensor**

$$B^\mu = p_1^\mu B_1 \quad (\text{E.15})$$

$$B^{\mu\nu} = g_{\mu\nu} B_{00} + p_1^\mu p_1^\nu B_{11} \quad (\text{E.16})$$

$$B_1(p_1^2, m_1^2, m_2^2) = \frac{1}{2p_1^2} [A_0(m_1^2) - A_0(m_2^2) - (p_1^2 - m_2^2 + m_1^2)B_0] \quad (\text{E.17})$$

$$B_{00}(p_1^2, m_1^2, m_2^2) = \frac{1}{2(D-1)} [A_0(m_2^2) + 2m_1^2 B_0 + (p_1^2 - m_2^2 + m_1^2)B_1] \quad (\text{E.18})$$

$$B_{11}(p_1^2, m_1^2, m_2^2) = \frac{1}{2(D-1)} \frac{1}{p^2} [(D-2)A_0(m_2^2) - 2m_1^2 B_0 - D(p_1^2 - m_2^2 + m_1^2)B_1] \quad (\text{E.19})$$

### E.3.2. Divergences

Table 11: Passarino Veltman Loop integral divergences

Integral	UV divergences	$(D - 4) \times \text{Integral}$
$A_0(m^2)$	$m^2 \Delta$	$-2m^2$
$B_0$	$\Delta$	$-2$
$B_1$	$-\frac{1}{2}\Delta$	$1$
$B_{00}$	$-(\frac{p^2}{12} - \frac{1}{4}(m_0^2 + m_1^2))\Delta$	$(\frac{p^2}{6} - \frac{1}{2}(m_0^2 + m_1^2))$
$C_{00}$	$\frac{1}{4}\Delta$	$-\frac{1}{2}$

## F. Implementation into Resummino

The `Fastor` [69] library was very useful for realizing tensor computations in C++ in the context of couplings as well as handling the  $\epsilon$  poles from the Passarino-Veltman integrals. Unfortunately `Looptools` does not give just UV poles, but we can circumvent this by subtracting the IR poles from the total poles. Further the python library `sympy` [70] is worth mentioning, especially the `cse` function for “Common Subexpression Detection and Collection” is convenient for simplifying large C++ code (though the exponentiation operator `’**` needs to be avoided):

```
from sympy import cse, simplify
from sympy.parsing.sympy_parser import parse_expr

result = cse(simplify(parse_expr("C++ math code here")), order='none')
# convert to cpp expressions
for k,l, in result[0]:
    print("auto " + str(k) + " = " + str(l) + ";")
print(result[1])
```

As outlined in this thesis there are many checks to be performed. Instead of just performing these tests once when the code is implemented a test framework (`Catch2` [71]) was added to `Resummino`. This comes with the advantage of reproducible tests and thus one can prevent regression.

## **Eigenständigkeitserklärung**

Hiermit versichere ich, dass die vorliegende Arbeit über "Resummation predictions for associated production of squarks and electroweakinos at the LHC" selbstständig von mir und ohne fremde Hilfe verfasst worden ist, dass keine anderen Quellen und Hilfsmittel als die angegebenen benutzt worden sind und dass die Stellen der Arbeit, die anderen Werken – auch elektronischen Medien – dem Wortlaut oder Sinn nach entnommen wurden, auf jeden Fall unter Angabe der Quelle als Entlehnung kenntlich gemacht worden sind. Mir ist bekannt, dass es sich bei einem Plagiat um eine Täuschung handelt, die gemäß der Prüfungsordnung sanktioniert werden kann.

Ich erkläre mich mit einem Abgleich der Arbeit mit anderen Texten zwecks Auffindung von Übereinstimmungen sowie mit einer zu diesem Zweck vorzunehmenden Speicherung der Arbeit in einer Datenbank einverstanden.

Ich versichere, dass ich die vorliegende Arbeit oder Teile daraus nicht anderweitig als Prüfungsarbeit eingereicht habe.

---

(Datum, Unterschrift)